PHD

The Role of PKC in Cell Polarity, Mitosis and Cancer

Gresham, Rebecca

Award date:
2010

Awarding institution:
University of Bath

The Role of PKCι in Cell Polarity, Mitosis and Cancer

Rebecca Louise Gresham

A thesis submitted for the degree of Doctor of Philosophy

University of Bath

Department of Biology and Biochemistry

September 2010

Summary

PKCι and PKCζ are members of the atypical protein kinase C family and play a key role in regulating cell polarity. PKCι also acts as an oncogene and high levels of PKCι protein in cancerous tissue is linked to a poor patient prognosis. Identifying substrates of PKCι is important to understand how PKCι controls cell polarity and is acting as an oncogene. This work describes the localisation of PKCι and PKCζ, with PKCι and PKCζ localising to the tight junctions and centrosomes during mitosis. The autophosphorylation and activation of PKCι and PKCζ also increases during mitosis. This suggests that substrates of PKCι could be localised to the centrosomes and tight junctions. A kinase assay was developed to elucidate novel PKCι phosphorylation targets. The polarity and centrosomal phosphorylation candidates; Pals-1, Dlg, GSK3β and LGN were tested, however, none of these were found to be *in vitro* PKCι phosphorylation targets, suggesting that PKCι does not function by phosphorylating these proteins. Interestingly, Dlg was found to increase the autophosphorylation of PKCι indicating that it activates PKCι. Previous studies have shown that PKCι may also be involved in the Hippo pathway, which controls cell proliferation and cell death. PKCι activation inhibits the Hippo pathway as a result of the mislocalisation of the Hippo protein. This work has demonstrated that the transcriptional co-activator proteins Yap and Taz, which function downstream of the Hippo pathway, are phosphorylated by PKCι *in vitro.* In addition, overexpression of Yap and PKCι in MDCK cells causes the nuclear accumulation of Yap, indicating that phosphorylation of Yap by PKCι promotes its nuclear entry and possibly transcription of its target genes. Therefore, these results identify a new way in which PKCι regulates the Hippo pathway and suggests the direct regulation of the Hippo pathway could be involved in the promotion of tumorigenesis by PKCι.

Acknowlegements

The author wishes to thank a number of people for their support and encouragement over the years.

Firstly, to Dr. Andrew Chalmers, who supervised and advised on the work in this thesis. Secondly to our collaborators Dr. Makoto Furutani-Seiki and Dr. Stefan Bagby for help with the Hippo pathway and to Claire Webb for protein expression and purification. Our other collaborators Cancer Research Technologies provided invaluble antibody advice. Thanks should also go to Dr. Paul Whitley for his assistance with the protein expression and purification. Finally, thanks should also go to Dr. Adrian Rogers for help with the confocal imaging.

To the BBSRC for funding and to all those who have contributed time and assistance, whether it was technical expertise or just simply moral support.

Contents

Figures

Tables

Abbreviations

Abbreviation	Full Text
APC	Adenomatous polyposis coli
aPKC	Atypical Protein Kinase C
ATG	Aurothioglucose
ATM	Aurothiomalate
Bcl-XL	B-cell lymphoma extra large
cIAPs	Cellulat inhibitors of apoptosis
CRIB	Cdc42/Rac interacting domain
CTGF	Connective tissue growth factor
DaPKC	Drosophila PKCι/ζ
Dlg	Discs Large
DMSO	Dimethyl sulfoxide
EMT	Epithelial-mesenchyme transition
FCS	Foetal calf serum
FERM	F for 4.1 protein, E for ezrin, R for radixin and M for moesin
GCP5	γ-tubulin complex protein-5
GEF	Guanine nucleotide exchange factor
GSK3β	Glycogen Synthase Kinase 3β
has	heart and soul
hCG	Chorionic gonadotrophin
HPV	Human papillomavirus
HRP	Horse radish peroxidase
hScrib	Human Scribble
IRS-1	Insulin receptor substrate 1
IP	Immunoprecipitation
JAM	Junctiona adhesion molecule
KD	Kinase dead
LAP	LRR and PDZ domain
LB	Luria Bertani
Lgl	Lethal Giant Larvae
LIP	Labmbda-interacting protein
LRR	Leucine rich repeats
MAGUK	Membrane-associated guanylate kinase
MDCK	Madin-Darby Canine Kidney Cells
MMR	Marcs modified ringers
NGF	Nerve growth factor
NSCLC	Non-small cell lung cancer
PBS	Phosphate Buffered Saline
PDZ	Postsynaptic density 95, discs large, ZO-1
PFA	Paraformaldehyde
PKM	Protein Kinase M
PMSG	Pregnant mare serum gonadotrophin
PP2A	Protein phosphatase 2A
PSSM	Position specific scoring matrix
SDM	Site-directed mutagenesis
Src-3	Steroid receptor coactivator-3
Sur1	Sulfonylurea receptor 1
TDCLs	Tumour derived cell lines
TER	Transepithelial electrical resistance

WT	Wild type
ZO-1	Zonula Occludens-1
ZO-2	Zonula Occludens-2

Chapter 1

1. Introduction

1.1 Atypical Protein Kinase C Family

The atypical Protein Kinase C proteins (aPKC) are members of the protein kinase C family, a group of serine/threonine kinases that phosphorylate a wide range of target proteins (Newton, 1995). The eleven member family is comprised of three groups; conventional, novel and atypical protein kinase C. aPKC differs from the conventional and novel forms in that it is not calcium or diacylglycerol sensitive. There are two aPKC proteins; PKCι/λ and PKCζ. PKCι and PKCλ are orthologues, PKCλ is the mouse name for human PKCι. PKCι/λ and PKCζ have 72% total amino acid homology and 86% homology within the kinase domain (Akimoto et al., 1994). PKCζ was first cloned in 1992 (Nakanishi and Exton, 1992) and PKCι/λ in 1993 (Akimoto et al., 1994; Selbie et al., 1993). There are also two other aPKC family members; PKCζII and PKMζ. PKCζII has no kinase activity but can interact with the catalytic domain of PKCι/ζ and with Par-6, possibly acting as a dominant negative, preventing the interaction between PKCι/ζ and Par-6 and inhibiting PKCι/ζ function (Parkinson et al., 2004). RNAi of PKCζII in HCII mouse mammary epithelial cells promotes tight junction formation indicating that PKCζII inhibits tight junction development. PKMζ is the catalytic domain of PKCζ, it has no regulatory domain and is therefore constitutively active (Hernandez et al., 2003) and is only found in the brain. This study will focus on PKCι and PKCζ.

Figure 1.1 A schematic diagram showing the domains of human PKCι and PKCζ
PKCι/ζ have four main domains; a regulatory domain that contains a PB1 domain, a pseudosubstrate domain, a zinc-finger domain and a kinase domain that phosphorylates target proteins.

1.1.1 The Par-aPKC Complex

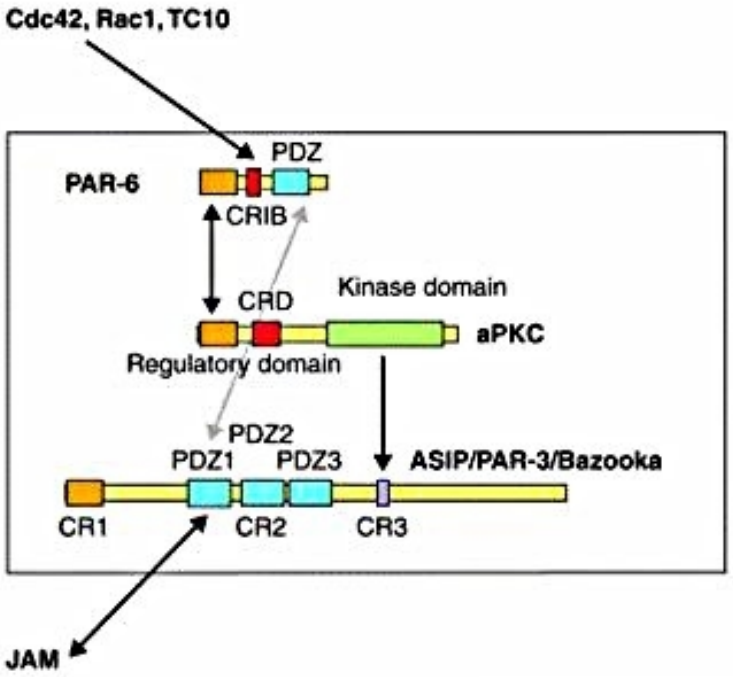

Figure 1.2 The Par-aPKC complex.
PKCι/ζ binds Par-3 and Par-6. CRIB - Cdc42/Rac interacting domain; PDZ - postsynaptic density 95, discs large, zonula occludens-1; CR - conserved region. Adapted from Ohno, (2001).

PKCι/ζ form a conserved complex with Par-6 and Par-3, which is termed the Par-PKC complex (Ohno, 2001). PKCι/ζ binds to Par-6 through the PB1 domain of Par-6 and the regulatory domain of PKCι/ζ (Etienne-Manneville and Hall, 2003b). Par-3 binds to the kinase domain of PKCι/ζ and Par-6 and Par-3 interact with each other through their PDZ domains to complete the complex (figure 1.2).

Par-6 and PKCι/ζ normally colocalise within cells, however Par-3 only joins this complex when the cells polarise and this association has been reported to be transient (Totong et al., 2007). Par-3 seems to act as a scaffolding protein that enlists the Par-6-PKC complex to the apical domain of polarised cells and to areas of tight junction assembly (Denning, 2007). There are other proteins that have been reported to associate with this complex such as lambda-interacting protein (LIP), Rac1 (Jaken and Parker, 2000), members of the 14-3-3 family, Cdc42 (Suzuki and Ohno, 2006) and junctional adhesion molecule (JAM) (Ohno, 2001). These proteins may serve to bring the substrates of PKCι/ζ into close proximity and will be discussed in more detail later.

1.1.2 Differences between PKCι and PKCζ

The phenotypes of the knock-out PKCι (lethal) and PKCζ (viable), which will be discussed later, indicate that they may have functional differences despite their high homology. However, this has not been well studied, especially in the context of cell polarity. Many of the antibodies used bind to both isoforms and dominant negatives usually inhibit both isoforms making the effects of dominant negatives and localisation difficult to distinguish between the two. This has led to some groups referring to aPKC rather than the individual isoform. In contrast knockouts are specific for each isoform and show different phenotypes. Other known differences between the two proteins include the LIP, which is a PKCι specific activator that does not bind PKCζ (Diaz-Meco et al., 1996b). During mouse embryonic development PKCι/λ mRNA is expressed abundantly throughout the embryo. However, PKCζ expression is lower throughout development and is found in fewer tissues. At later stages of development (embryonic day 16.5) PKCι and PKCζ both show high level of mRNA and protein expression in epithelial tissues such as the intestine, kidney and lung (Kovac et al., 2007). This may indicate that in a polarised epithelial tissue the functions of PKCι and PKCζ are redundant. In this report PKCι/ζ will be used when it is not clear which isoform is being researched and PKCι or PKCζ when it is specific.

1.2 Cell Polarity

PKCι/ζ are known regulators of cell polarity (Suzuki and Ohno, 2006). Cell polarity can be defined as the asymmetric distribution of constituents within a single cell that produces an asymmetry of cellular functions. Epithelial cells are one example of polarised cells, they have apical and basolateral domains and each domain carries out different functions. The domains are separated by tight junctions (Farquhar and Palade, 1963) (figure 1.3), which block diffusion across the epithelial sheet and between the apical and basal membrane domains. Tight junctions are composed of the transmembrane proteins; claudin, occludin, JAM and membrane associated proteins; ZO-1, ZO-2 and cingulin. Occludin and claudin are required to maintain the transepithelial electrical resistance (TER) of the cell. They also function as cell-cell adhesion molecules. ZO-1 and ZO-2 are scaffolding proteins that have PDZ, SH3 and an inactive guanylate kinase domain that target other proteins to the tight junctions and bind to actin. Cingulin may also be a scaffolding protein responsible for actin organisation at the tight junction (Balda and Matter, 1998; Mitic and Anderson, 1998). Below the tight junctions are adherens junctions,

which are cadherin-based cell-cell adhesion sites composed of cadherin, β-catenin, α-catenin, vinculin, α-actinin, ZO-1, actin, nectin and LIN-7, with other proteins localising in the area that may be connected to the adherens junction (Nagafuchi, 2001). Adherens junctions are responsible for cell-cell adhesion. Desmosomes are composed of the desmosomal cadherins; desmogliens and desmocollins to which the proteins plakoglobin, plakophilin and desmoplakin associate (Green and Jones, 1996). Hemidesmosomes are composed of α and β-integrins, laminin-5, BP180 and plactin. The desmosomes and hemidesmosomes provide a cell surface attachment site to bind intermediate filaments to help maintain tissue integrity.

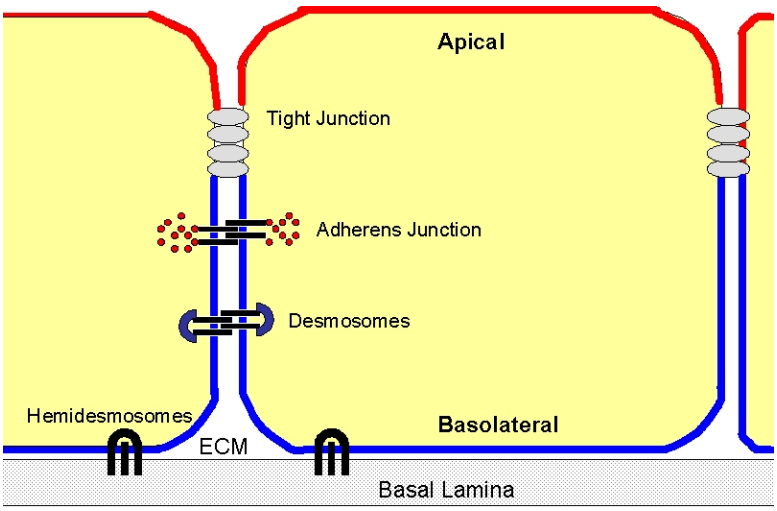

Figure 1.3 A Polarised Epithelial Cell. (courtesy of V. Sherwood)
Polarised epithelial cells have apical and basal domains which are separated by tight junctions. Below the tight junctions are adherens junctions and desmosomes, which provide sites of cell-cell adhesion. Connecting an epithelial sheet to the basal lamina are hemidesmosomes.

Another example of cell polarity occurs in developing embryonic cells, which are often polarised and cell fate determinants are asymmetrically distributed, so that during asymmetric division, each daughter cell receives a different set of cell fate determinants (Knoblich, 2008). This generates cell fate diversity, allowing a complex multicellular organism to arise from a single cell. Other examples of polarised cells are migrating cells, neurones and cells involved in wound healing. Cell polarity is often disrupted in cancer; cells lose polarity and this contributes to tumour formation, which is covered in section 1.7, so cell polarity is important for a diverse range of biological processes and cancer progression.

1.3 The Control of Epithelial Cell Polarity.

There are four main polarity complexes that are required to maintain polarity: the apical PKCι/ζ/Par-3/Par-6 complex, the apical Crumbs/Pals-1/PATJ complex, the basolateral Lethal giant larvae (Lgl)/Discs Large (Dlg)/Scribbles group and the lateral Yurt, Coracle, Neurexin IV and Na^+, K^+-ATPase group, as well as the basolateral protein Par-1. These complexes are evolutionarily conserved (Hurd et al., 2003; Izumi et al., 1998; Joberty et al., 2000; Laprise et al., 2009; Lin et al., 2000; Plant et al., 2003; Yamanaka et al., 2003) and are required to establish and maintain epithelial polarity.

1.4 The Par-aPKC complex

The Par-aPKC complex, as discussed above, is an apical complex that consists of PKCι/ζ, Par-6 and Par-3. The three proteins colocalise at tight junctions (Izumi et al., 1998; Suzuki et al., 2001).

1.4.1 Function of PKCι/ζ

In C. *elegans*, the homologue of PKCι/ζ is called PKC-3. The one cell C. *elegans* embryo is highly polarised and PKC-3 localises to the anterior of the embryo with Par-3 and Par-6 (St Johnston and Ahringer, 2010). The Par-PKC complex is required to establish polarity once the C. *elegans* egg has been fertilised and enters the first mitotic division (Cowan and Hyman, 2007) and loss of these proteins results in a loss of polarity.

Drosophila PKCι/ζ (DaPKC) zygotic null mutants are normal at the embryonic stage, due to maternal DaPKC contribution, but the mutants are lethal at the larval stage (Rolls et al., 2003). The mutants have abnormal neuroblast polarity, indicated by mislocalised Lgl and Par-6. The DaPKC mutants also have defects in epithelial cell polarity and a loss of monolayer morphology. Expression of DaPKC mutants that cannot bind Par-6 or lack kinase activity cause a loss of apico-basal polarity in the embryonic ectoderm and neuroblasts, however the follicular epithelium is grossly normal (Kim et al., 2009). This indicates that the kinase activity of DaPKC is required for many epithelia but may be dispensable in some *Drosophila* epithelial cell types.

PKCι is called heart and soul (has) in Zebrafish. Embryonic has mutants affect the morphogenesis of embryonic polarised epithelia. The adherens junctions are not maintained in has mutants, resulting in multiple lumens in the intestine and disorganised retina (Horne-Badovinac et al., 2001). In the developing *Xenopus* embryo, dominant

negative PKCι/ζ causes a loss of apical identity. There is an expansion of the basolateral domain into the apical domain, as indicated by staining for the basolateral markers, β-1 integrin and occludin. There is also a loss of tight junctions, as indicated by a loss of cingulin staining (Chalmers et al., 2005). During *Xenopus* gastrulation it has been shown that XGAP is phosphorylated by PKCι/ζ, which allows XGAP to bind Par-5. XGAP controls convergent extension in *Xenopus* by cooperating with Par proteins to control cell polarity (Hyodo-Miura et al., 2006).

Aberrant localisation of PKCι/ζ in the chick neuroepithelium results in a disruption of neuronal polarity (Ghosh et al., 2008). Expression of myristoylated PKCι/ζ localises to the entire cell membrane and causes adherens junctions disruption and a loss of neuroepithelial architecture. Inhibition of PKCι/ζ using an inhibitor prevents neurones from gaining polarity (Shi et al., 2003).

PKCζ deficient mice are viable and grossly normal. They have small changes in the spleen and β-cell maturation is slow, NFκB activation is also slowed, indicating that PKCζ is involved in the immune system (Leitges et al., 2001). This may indicate that PKCζ has no role in polarity or that it is functionally redundant and can be replaced with PKCι/λ in polarity. PKCι/λ knock-out mice are embryonic lethal, they die at embryonic day 9 and are highly morphologically abnormal (Soloff et al., 2004). The embryos appear to have no morphological organisation at all, which is consistent with a role for PKCι/λ in cell polarity. A conditional knock-out of PKCι/λ in photoreceptors within the mouse retina results in a lack of cell polarisation, but does not affect receptor differentiation (Koike et al., 2005). When PKCι/λ is conditionally knocked-out in the mouse neocortex there is a loss of adherens junctions and polarity (Imai et al., 2006). There is a disruption of neuroepithelial tissue architecture and the mice die within one month and display hydrocephalus. In a PKCι/λ conditional knock-out in the mouse lens, there is reduced proliferation during development caused by premature withdrawal from the cell cycle (Sugiyama et al., 2009). The lens cells also go through epithelial-mesenchyme transition (EMT), therefore, in the lens PKCι/λ is required for proliferation and to suppress EMT. In summary PKCλ knock-out in different tissues causes a general loss of cell polarity which supports a role for PKCι/λ in cell polarity.

PKCι/ζ are also involved in tight junction regulation in mammalian cell lines. Par-3 binds to the tight junction protein JAM, tethering the Par-PKC complex to the tight junction (Ebnet et al., 2004). PKCι/ζ is the last tight junction protein to be recruited to the

tight junction; however, the kinase activity of PKCι/ζ is required for junctional maturation as in the mouse mammary epithelial MTD1-A cells, expression of a dominant negative PKCλ prevents junctional maturation (Suzuki et al., 2002). ZO-2 is also phosphorylated by PKCι/ζ and associates with PKCι/ζ *in vivo* (Avila-Flores et al., 2001). This phosphorylation occurs during tight junction assembly; however, the purpose of this phosphorylation remains unclear as no studies were carried out with a non-phosphorylatable ZO-2. PKCι/ζ phosphorylates claudin-4 during tight junction formation and prevention of this phosphorylation using a claudin-4 mutant that cannot be phosphorylated prevents tight junction formation (Aono and Hirai, 2008). A dominant negative mutant of PKCι/ζ interferes with tight junction development in MDCK cells, where it has been shown that there is mislocalisation of Par-3, ZO-1, occludin and claudin-1 (Suzuki et al., 2001). In 3D MDCK cysts, dominant negative PKCι/ζ results in multiple lumen cysts (Horikoshi et al., 2009). Therefore, PKCι/ζ is essential for tight junction development.

All of these reports from diverse systems ranging from C. *elegans* to mammals indicate that PKCι/ζ has a crucial role in cell polarity and the establishment and/or maintenance of epithelial cell junctions.

1.4.2 Regulation of PKCι/ζ

One mode of PKCι/ζ activation is through Par-6 and Cdc42. Par-6 links Cdc42 to PKCι/ζ, by binding to Cdc42 through its CRIB domain and binding the regulatory domain of PKCι/ζ. The binding of Par-6 to the regulatory domain of PKCι/ζ is inhibitory, but the binding of Cdc42 to Par-6 relieves the inhibition of Par-6 on PKCι/ζ (Qiu et al., 2000; Yamanaka et al., 2001) allowing PKCι/ζ to autophosphorylate (Akimoto et al., 1994). Loss of Cdc42 phenocopies mutations in Par-6 and PKCι/ζ in the *Drosophila* notum (Georgiou et al., 2008). Cdc42 also targets the Par-PKC complex to the apical cortex (Martin-Belmonte et al., 2007). The association of Cdc42 with the Par-aPKC complex and therefore the activation of PKCι/ζ is thought to be mediated by ceramide which binds directly to the complex (Krishnamurthy et al., 2007). Ceramide depletion results in no association of Cdc42 and the Par-PKC complex and therefore no PKCι/ζ activation, however, this has only been shown in mouse embroid bodies. A Cdc42 activator and therefore activator of PKCι/ζ is Tuba, a guanine nucleotide exchange factor (GEF) specific

for Cdc42 (Qin et al., 2010). Cdc42 is apically enriched in MDCK cysts; however, this enrichment is abolished upon Tuba depletion, as is PKCι/ζ autophosphorylation and therefore activation. So Tuba activates Cdc42 which in turn activates PKCι/ζ through Par-6.

Another PKCι specific activator is LIP which binds to the zinc-finger region of PKCι/λ, but not PKCζ and activates PKCι/λ *in vivo* (Diaz-Meco et al., 1996b), however, this method of PKCι/ζ activation has not been linked to polarity. Dap160 (related to mammalian Intersectin) is also an activator of PKCι/ζ was been found in *Drosophila* neuroblasts. Dap160 colocalises with DaPKC at the apical cortex *in vivo*. *In vitro* Dap160 interacts with DaPKC and stimulates the activity of DaPKC (Chabu and Doe, 2008). Dap160 mutant neuroblasts have ectopic DaPKC localisation and abnormal polarity, indicating that DaPKC is not active. This work needs to be repeated in mammalian epithelial cells to discover whether this is also a PKCι/ζ regulation method in mammals (via Intersectin) or is specific to *Drosophila*.

Par-4 is a PKCι/ζ inhibitor; it binds to the zinc finger and regulatory domain of PKCι/ζ and inhibits its activity *in vivo*. Overexpression of Par-4 induces apoptosis in NIH-3T3 cells, through inhibition of PKCι/ζ (Diaz-Meco et al., 1996a), therefore PKCι/ζ is involved in cell survival which is supported by its role in cancer formation (see section 1.11.). Protein phosphatase 2A (PP2A) is another negative regulator of PKCι/ζ. PP2A is a serine/threonine phosphatase that interacts with tight junctions and colocalises with PKCι/ζ in MDCK cells (Nunbhakdi-Craig et al., 2002). PP2A regulates tight junction assembly by dephosphorylating tight junction proteins phosphorylated by PKCι/ζ such as ZO-2 and occludin.

1.4.3 Par-3

In the C. *elegans* embryo, Par-3 localises to the anterior cortex and is required for cell polarity (Etemad-Moghadam et al., 1995), Par-3 mutants display disrupted actin distribution and a lack of asymmetric division. In *Drosophila*, Par-3 is termed Bazooka. *Drosophila* mutants for Bazooka fail to establish cell polarity after cellularisation (Muller and Wieschaus, 1996). In *Drosophila* neuroblasts, Bazooka is also required for cell polarity. Bazooka binds to Inscuteable and aids the rotation of the mitotic spindle and the subsequent localisation of cell fate determinants (Wodarz et al., 1999). In Bazooka mutant neuroblasts, there is no apical-basal polarity and random spindle orientation. In border cells

of the *Drosophila* ovary, Bazooka loss results in impaired migration (Pinheiro and Montell, 2004).

The mammalian Par-3 was first identified as a binding partner of B-type ephrins (Lin et al., 1999). There are three splice variants of Par-3 of 180kD, 150kD and 100kD. The 180kD and 150kD splice variants are widely expressed during development, however the 100kD variant is limited to the heart and kidney and does not contain a PKCι/ζ binding domain. The 100kD Par-3 strongly binds to Par-6 *in vivo* and is phosphorylated by PKCι/ζ *in vitro,* despite not having a PKCι/ζ binding domain (Lin et al., 2000). The other splica variants are also phosphorylated by PKCι/ζ. Nagai-Tamai and colleagues demonstrated that it is serine 827 (S827) of Par-3 that is phosphorylated by PKCι/ζ *in vivo* in MDCK cells and that this phosphorylation of Par-3 reduces the affinity of PKCι/ζ for Par-3 (Nagai-Tamai et al., 2002). They also showed that expression of a S827 to alanine mutant of Par-3 caused defective polarity and tight junctions after a calcium switch, indicating that Par-3 phosphorylation by PKCι/ζ is necessary for polarity establishment. Overexpression of Par-3 (but not Par-3 lacking the PKC binding region) promotes tight junction formation (Hirose et al., 2002). However, in MDCK cells RNAi of Par-3, followed by a calcium switch does not block tight junction formation, it only slows it down (Chen and Macara, 2005), indicating that Par-3 is not totally necessary for tight junction formation. Par-3 knock-down in 3D MDCK cysts results in impaired apical development and intercellular lumen formation (Horikoshi et al., 2009). The polarity is partly established in single cells, but not as a group of cells. This is also seen with the knock-down of PKCι/ζ, therefore the Par-3-PKCι/ζ interaction is required for proper lumen formation. In mice, Par-3 knock-down is embryonic lethal and the embryos display disrupted epithelia (Hirose et al., 2006).

In *Drosophila*, Par-1 phosphorylates Par-3 causing it to interact with 14-3-3 proteins and restricts Par-3 to the apical domain, but this does not allow Par-3 to bind the Par-aPKC complex (Benton and St Johnston, 2003). However, in mice it has been shown that protein phosphatase 1α dephosphorylates Par-3 bound to 14-3-3, allowing Par-3 to bind the Par-aPKC complex (Traweger et al., 2008). Unfortunately these two events have not been shown in the same species.

1.4.4 Par-6

In C. *elegans*, Par-6 is required for embryonic polarity and loss of Par-6 phenocopies the loss of Par-3 including defective polarity and asymmetric division (Watts

et al., 1996). In *Drosophila* neuroblasts, Par-6 localises apically and is required for Par-3/Bazooka localisation (Petronczki and Knoblich, 2001). In Par-6 mutant neuroblasts asymmetric divisions are misorientated and cell fate determinants are mislocalised. In *Drosophila* Par-6 mutant epithelia, apico-basal polarity is lost. As with Par-3, Par-6 is also required for border cell migration in the *Drosophila* ovary and RNAi of Par-6 results in impaired cell migration (Pinheiro and Montell, 2004). There are three human homologues of Par-6; α, β and γ. They all have PDZ and CRIB domains and all interact with Cdc42 and PKCι/ζ *in vivo* (Noda et al., 2001). Par-6 phosphorylation by PKCι/ζ could not be detected in an *in vitro* kinase assay (Lin et al., 2000), so it is likely that it is not phosphorylated by PKCι/ζ. Par-6 localises to the apical domain of epithelial cells with PKCι/ζ. Par-6 in *Drosophila* is required to localise Patj apically (Hutterer et al., 2004). The amino terminal domain of Par-6 binds the regulatory domain of PKCι/ζ and inhibits PKCι/ζ unless Cdc42 binds to Par-6 (Yamanaka et al., 2001). Overexpression of mutant Par-6 in MDCK cells, followed by a calcium switch, suppresses TER development and the accumulation of the tight junction markers ZO-1, claudin and occludin at the tight junctions is incorrect. This is similar to the effects seen with PKCι/ζ kinase null in MDCK cells (Suzuki et al., 2001) and supports the role of Par-6 in PKCι/ζ activation.

1.5 The Scribble, Lgl, Dlg Complex

Scribble, Lgl and Dlg are all tumour suppressor genes in *Drosophila* that act in a common pathway (Wodarz, 2000). In *Drosophila* the phenotypes of each mutant are indistinguishable. The mutants have abnormal cell polarity, loss of zonula adherens junctions and exhibit tissue overgrowth; therefore they are required for cell polarity and correct tissue architecture. Single zygotic mutants of any of the genes are viable until late larval stages, when tissue overgrowth begins. However, double zygotic mutants for any of the genes are embryonic lethal (Bilder et al., 2000). This indicates that the genes cooperate to generate cell polarity and regulate proliferation.

1.5.1 Lgl

Drosophila Lgl has been shown to be phosphorylated by PKCι/ζ in an *in vitro* kinase assay and little phosphorylation of Lgl is seen in S2 cells depleted of PKCι/ζ (Betschinger et al., 2003). It was demonstrated that phosphorylation of Lgl by PKCι/ζ releases Lgl from the Par-PKCι/ζ complex, it was speculated that this phosphorylation of

Lgl by PKCι/ζ inactivates Lgl at the apical end of *Drosophila* neuroblasts. Lgl is also required to be active at the basal end of the neuroblasts to recruit the cell fate determinant Miranda (Peng et al., 2000) which is only found at the basal end of the cells. So PKCι/ζ inactivates Lgl at the apical end of the cell preventing Lgl activation and Miranda recruitment.

In *Xenopus*, Lgl is inhibited by PKCι/ζ (Chalmers et al., 2005). The two proteins mutually inhibit each other, overexpression of either protein results in the mislocalisation of the other. Each protein can also rescue the effects of the overexpression of the other.

There are two mammalian homologues of *Drosophila* Lgl; Lgl1 and Lgl2. The expression pattern of Lgl1 in the mouse embryo is broad whereas Lgl2 is only found in the liver, kidney and stomach. Lgl1 knockout mice show defects in the brain, with tissue overgrowth and a loss of cell polarity (Klezovitch et al., 2004). In MDCK cells Lgl1 and Lgl2 localise to the lateral membrane as cells become polarised (Musch et al., 2002). Lgl binds Par-6 and PKCι/ζ transiently as polarity is being established, it competes with Par-3 for incorporation into the complex. Lgl is phosphorylated by PKCι/ζ *in vivo* and this causes Lgl to dissociate from the Par-6/PKC complex and Par-3 to bind to the complex (Yamanaka et al., 2003). The phosphorylation by PKCι/ζ inhibits Lgl function in the apical domain. In fibroblast scratch assays, Lgl localises with PKCι/ζ at the leading edge and is phosphorylated. If the five serines phosphorylated by PKCι/ζ are mutated to alanines there is a 19% decrease in fibroblast polarisation, so phosphorylation of Lgl by PKCι/ζ is important for cell polarity (Plant et al., 2003). Little is known about how Lgl functions, but Lgl binds the t-snare, syntaxin 4, indicating a possible role in the regulation of basolateral exocytosis (Musch et al., 2002).

Lgl may act as a tumour suppressor in humans. In colorectal cancer, Lgl is lost in 75% of cases and the less Lgl present the more metastatic the cancer (Schimanski et al., 2005). However, the authors do not speculate on what is causing the loss of Lgl in colorectal cancer or what role the loss of Lgl plays in tumour progression.

1.5.2 Scribble

Human Scribble (hScrib) was first discovered in 2003 as the functional homologue of *Drosophila* Scribble (Dow et al., 2003). It was shown that the human gene can rescue the mutant Scribble phenotype in *Drosophila*. This indicates that as Scribble acts as a tumour suppressor in *Drosophila*, it is possible it has the same role in mammalian cells.

hScrib is a LRR and PDZ domain (LAP) protein with sixteen leucine rich repeats (LRR); LAP proteins interact with transmembrane proteins via the LRRs tethering them to the membrane (Nagasaka et al., 2006). GFP tagged hScrib colocalises with the adherens junction marker E-cadherin in MDCK cells, however, it does not colocalise with ZO-1, indicating it is on the lateral membrane below the tight junctions. Scribble restricts the Par-aPKC complex to the apical membrane (Tanentzapf and Tepass, 2003). shRNA knockdown of scribble results in no loss of apico-basal cell polarity, except when the cells are subjected to a calcium switch, when the cells take longer to regain their polarity. Scribble stabilises the link between α-catenin and E-cadherin to allow adhesive junctions to form (Qin et al., 2005). hScrib has also been linked to the cell cycle, it negatively regulates cell cycle progression inhibiting cell proliferation, therefore it may be a tumour suppressor in humans (Nagasaka et al., 2006).

Loss of scribble also affects cell migration and cell adhesion; cells migrate more, but they lose their cell-cell adhesion (Qin et al., 2005). This was also demonstrated in scratch assays using migrating astrocytes (Osmani et al., 2006). In cells depleted of Scribble there is a lack of cell polarisation and microtubule disorganisation; when Scribble is overexpressed multiple protrusions occur. They also showed that Scribble is found at the leading edge of migrating astrocytes and that it controls Cdc42 recruitment to the leading edge and therefore, PKCι activation.

Murdoch and colleagues demonstrated that a truncated form of Scribble is found in the mouse *circletail* mutant embryos which have massive neural tube defects (Murdoch et al., 2003). There is a failure in neural tube closure, which occurs in the human diseases, spina bifida and anencephaly. This indicates that hScrib may be involved in these human diseases too.

Loss of Scribble in mice mammary glands results in tumours and Scribble is involved in cell death regulation and in the maintenance of cell architecture (Zhan et al., 2008). In human breast cancer samples hScrib is absent in 55% of ductal carcinomas and 81% of lobular carcinomas (Navarro et al., 2005). This indicates that hScrib is important in preventing some types of mammary carcinoma. hScrib is also targeted by the high-risk human papillomavirus (HPV) E6 proteins (Nakagawa and Huibregtse, 2000). HPV has been linked to 90% of uterine carcinomas. The E6 proteins target hScrib for degradation and in MDCK cells, this results in the breakdown of tight junctions damaging the integrity of the tight junctions as seen by a loss of ZO-1 staining. As loss of Scribble in Drosphila

leads to tissue overgrowth, the loss of hScrib in response to HPV infection could result in tumorigenesis.

1.5.3 Dlg

Dlg is a member of the membrane-associated guanylate kinase homologues (MAGUK) (Woods and Bryant, 1994). Dlg has three PDZ domains and an SH3 domain which act as sites of protein-protein interaction. Dlg also has a region which is similar to a guanylate kinase domain, but it has a three amino acid deletion making it kinase inactive. Dlg localises to the septate junctions in *Drosophila* and mutation of Dlg results in a loss of cell polarity and septate junction in imaginal discs. Loss of Dlg also redistributes two proteins of the band 4.1 family, coracle and expanded, from the septate junctions and apical membrane respectively, to the cytoplasm (Woods et al., 1996).

There are five alternatively spliced isoforms of human Dlg (hDlg), 1 to 5. Isoforms; 1, 2, 3 and 5 are found in many tissues, only 1 and 4 are found in the brain and liver, only 1 and 3 at sites of cell-cell contact and only 1 and 2 in the nucleus (McLaughlin et al., 2002). hDlg was first characterised in 1994 and was shown to localise to cell-cell contact regions in polarised MCF-7 cells (Lue et al., 1994). Muller and colleagues also showed that rat Dlg localised to cell-cell contacts in T84 cells and demonstrated that when cells were not in contact, Dlg did not localise to the membrane (Muller et al., 1995). A truncated form of Dlg1 in mice, missing the SH3 and guanylate kinase domains, causes growth retardation and craniofacial abnormalities. The mice also die perinatally, which is probably due to an inability to feed (Caruana and Bernstein, 2001). This indicates that these domains are important for the function of Dlg. However, the authors make no mention of cell polarity within the Dlg mutants, so it is unknown whether the polarity was affected in these mutants.

In HEK293 cells, Dlg1 localisation alters through the cell cycle. In G1 phase it is membrane bound; as cells go through the cell cycle the staining becomes much more cytoplasmic. At metaphase, Dlg1 is found on the mitotic spindle and on the midbody during cytokinesis. Phosphorylation by CDK1 and CDK2 alters the localisation of Dlg1, specifically targeting it into the nucleus (Narayan et al., 2009). Non-phosphorylatable Dlg is excluded from the nucleus. Overexpression of Dlg1 in 3T3 fibroblasts inhibits cell cycle progression by impairing G1-S-phase progression (Ishidate et al., 2000).

Dlg is a target for some human viral oncoproteins including 9ORF1, HTLV-1 Tax and HPV-18 E6 oncoprotein (Lee et al., 1997). It was shown that the oncoproteins bind the

same region of Dlg that binds adenomatous polyposis coli (APC). APC is mutated in many colorectal tumours and is involved in Wnt signalling. Dlg forms a complex with APC and this complex may block cell cycle progression (Matsumine et al., 1996). By binding Dlg the oncoproteins may disrupt the Dlg-APC complex leading to unregulated cell proliferation (Lee et al., 1997). hDlg is also degraded in HPV-positive cervical tumours. In normal epithelial cells hDlg is stabilised at cell-cell contact regions with APC, resulting in no proliferation. Any hDlg not found at the sites of cell-cell contact is degraded, the cells become polarised and Dlg is stabilised. Therefore, if Dlg is degraded and misregulated and not at cell-cell contacts with APC, proliferation can occur, possibly adding to the tumour growth (Mantovani et al., 2001). This idea is supported by the fact that loss of Dlg in *Drosophila* leads to massive tissue overgrowth.

In astrocytes, the cortical recruitment of Dlg to the leading edge of scratch assays is prevented by inhibiting PKCζ; therefore PKCζ controls the recruitment of Dlg to the leading edge (Etienne-Manneville et al., 2005). The authors go on to show that the Dlg-APC interaction at the leading edge is required for microtubule polarisation, centrosome reorientation and cell migration.

The interactions of PKCι/ζ with the Scribble, Lgl, Dlg complex are depicted in figure 1.4.

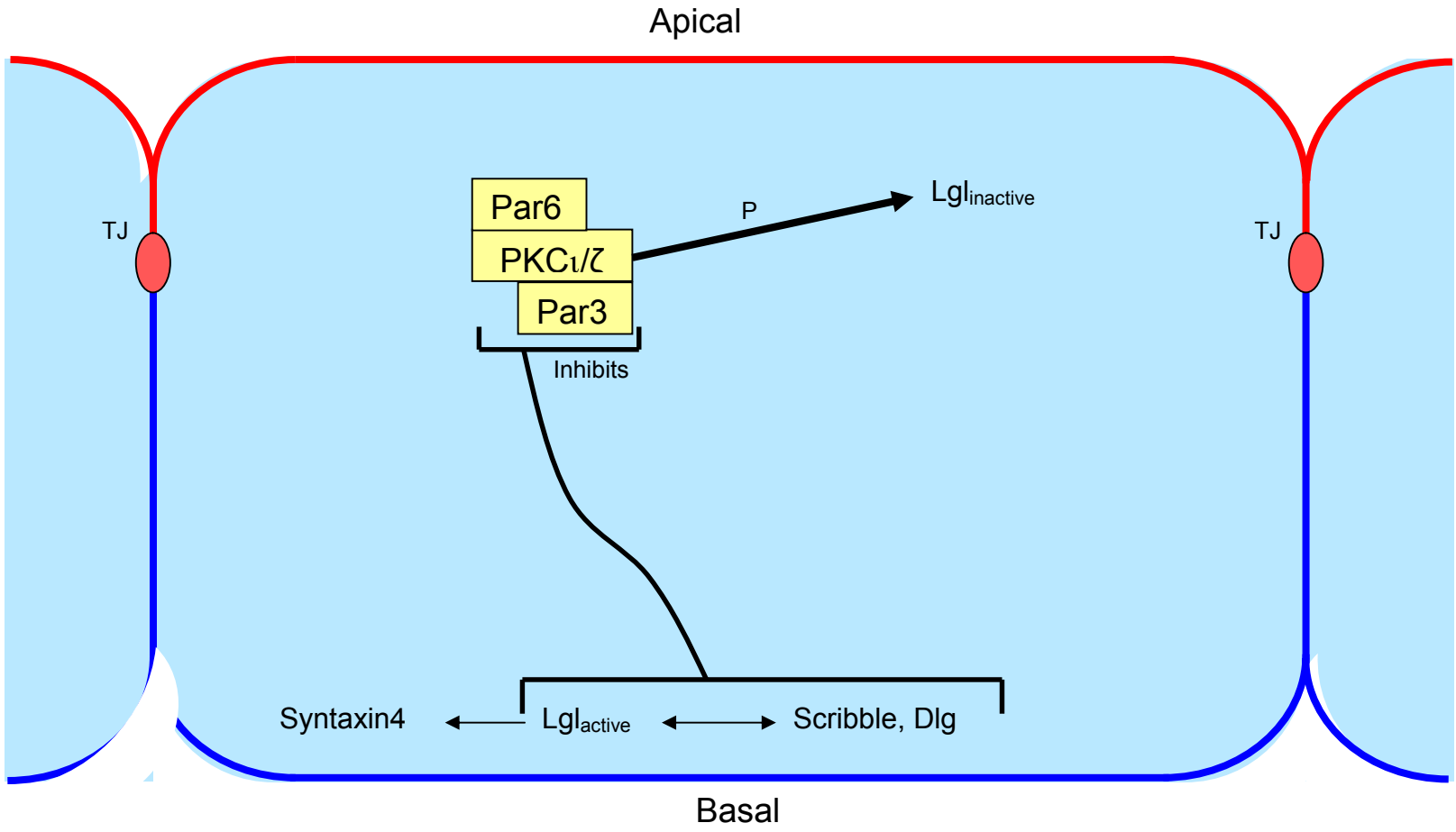

Figure 1.4 PKCι/ζ and the Scribble, Lgl, Dlg complex
A schematic diagram depicting the interactions between PKCι/ζ and the Scribble, Lgl, Dlg complex

1.6 The Crumbs/Pals-1/Patj Complex

The third polarity complex is composed of Crumbs3, Pals-1 and Patj (Lemmers et al., 2002; Makarova et al., 2003; Roh et al., 2002).

1.6.1 Crumbs

Crumbs is A Type 1 membrane protein with a short cytoplasmic tail (Wodarz et al., 1995). In *Drosophila* epithelial cells, Crumbs is localised to the entire apical membrane and concentrates at the zonula adherens (Tepass, 1996; Wodarz et al., 1995). Crumbs overexpression results in the expansion of the apical domain and loss of Crumbs leads to a loss of cell polarity and a failure of zonula adherens junction formation (Grawe et al., 1996; Tepass, 1996). In *Drosophila,* DaPKC binds crumbs at the apical membrane. The authors showed that the human PKCζ phosphorylates a GST-Crumbs fusion protein at threonines 6 and 9 (Sotillos et al., 2004). However this has not been shown in mammalian cells or *in vivo* in *Drosophila*. Overexpression of a non-phosphorylatable form of Crumbs, in the *Drosophila* wing, results in loss of Crumbs and Patj from the apical membrane and aberrant Scribble localisation indicating that phosphorylation by DaPKC is important for cell polarity.

There are three mammalian crumbs genes. CRB1 was the first to be discovered as a mutated gene in retinitis pigmentosa group 12 (RP12), a retinal degeneration disease (den Hollander et al., 1999). Crumbs1 is expressed in the brain and retina, not epithelial cells (den Hollander et al., 2002). Crumbs2 and Crumbs3 were identified shortly after Crumbs1, they have 67% and 54% homology with *Drosophila* Crumbs (Lemmers et al., 2002). Crumbs3 mRNA is expressed in a wide variety of epithelial tissues, skeletal muscle and the brain, but not in other tissues (Lemmers et al., 2004). Crumbs3 localises to the apical membrane in epithelial cells. Overexpression of Crumbs3 in MDCK cells does not alter cell polarity on its own, but when the cells are subjected to a calcium switch there is a delay in tight junction establishment in cells overexpressing Crumbs3 (Lemmers et al., 2004). Crumbs3 also localises to the leading edge of migrating cells (Shin et al., 2005).

Crumbs3 is downregulated in tumour derived cell lines (TDCLs) from nude mice injected with immortal baby mouse kidney epithelial cells (Karp et al., 2008). These cell lines grow beyond contact inhibition resulting in a multilayered phenotype instead of the monolayer seen in cell lines from tissue not derived from tumours, also tight junctions are lost. Re-expression of Crumbs3 in the TDCLs restores the wild type phenotype; therefore, Crumbs3 is responsible for the multilayered, loss of junction phenotype. This indicates that

Crumbs plays an important role in maintaining polarity and loss of Crumbs may contribute to tumour progression.

1.6.2 Patj

Patj is the mammalian homolog of the *Drosophila* protein Discs lost. Discs lost localises at the apical membrane with Crumbs (Bhat et al., 1999). In *Drosophila* epithelia, Discs lost is vital for polarity and loss of Discs lost leads to a loss of the apical localisation of Crumbs and a loss of polarity.

Patj contains eight PDZ domains and localises to the tight junctions and apical domain in epithelial cells and binds Crumbs and Pals-1 (Lemmers et al., 2002). During monolayer MDCK cell polarisation, Patj is targeted to the apical domain and then the tight junction later on in polarisation. In Patj knockdown cells subjected to a calcium switch, there is a delay in tight junction formation. In Patj knockdown MDCK cells grown in 3D culture, no central lumen forms unlike in control cells, so Patj plays an important role in the cell polarity of MDCK cells (Shin et al., 2005). Patj targets Pals-1 to the tight junctions (Roh et al., 2002). It has been shown that Patj is required for the apical localisation of Crumbs and Pals-1 and the lateral localisation of occludin and ZO-3, hence Michel and colleagues hypothesised that Patj may act as a determinant between the apical and lateral border (Michel et al., 2005).

In migrating MDCKII cells, Patj localises to the leading edge and is required for wound healing (Shin et al., 2007). PKCι/ζ and Par-3 also localise to the leading edge of migrating MDCKII cells and in the absence of Patj they are mislocalised, so Patj may be needed for the recruitment of the Par-aPKC complex to the leading edge.

Patj, like Scribble and Dlg, is a target of the HPV E6 proteins. The E6 proteins cause Patj degradation (Storrs and Silverstein, 2007), as Patj is involved in epithelial cell polarity and regulates tight junction formation (Shin et al., 2005), the degradation of Patj may aid the progression of HPV mediated cervical cancer.

1.6.3 Pals-1

Pals-1 is the mammalian homologue of the *Drosophila* protein Stardust. Stardust binds to the cytoplasmic tail of Crumbs (Bachmann et al., 2001) and is required for epithelial polarity in *Drosophila* embryos and loss of Stardust has a phenotype similar to loss of Crumbs (Tepass and Knust, 1993), Stardust mutants also have abberant Crumbs

localisation, indicating that Stardust may localise Crumbs. However, Stardust is downstream of Crumbs and is activated by Crumbs. Interestingly, although Stardust and Crumbs are required for *Drosophila* epithelial polarity, they are not required for neuroblast polarity (Hong et al., 2001).

In mammalian epithelial cells, Pals-1 is targeted to the tight junction via its L27 domain that binds Patj (Roh et al., 2002). Pals-1 also binds the C-terminal region of Crumbs3 (Makarova et al., 2003) and the PDZ domain of Par-6 (Hurd et al., 2003). The binding of Par-6 to Pals-1 is inhibitory to the binding of Patj to Pals-1 (Wang et al., 2004), which may inhibit the function of Pals-1, or the activation of the Crumbs complex.

Partial siRNA knockdown of Pals-1, followed by a calcium switch in MDCKII cells results in a delay in tight junction formation, a loss of Patj expression and a loss of PKCι/ζ at the tight junctions. In 3D culture Pals-1 siRNA results in a disrupted polarity and a failure to form a central lumen (Straight et al., 2004). Total siRNA of Pals-1 in MDCKII cells, followed by a calcium switch, results in no reformation of tight junctions and a lack of E-cadherin at adherens junctions. The E-cadherin is found intracellularly and not trafficked to the cell surface, so Pals-1 is required for the targeting or the fusion of E-cadherin containing vesicles to the membrane (Wang et al., 2007) and for the establishment of polarity.

The interactions of PKCι/ζ with the Crumbs, Pals-1, Patj complex are depicted in figure 1.5.

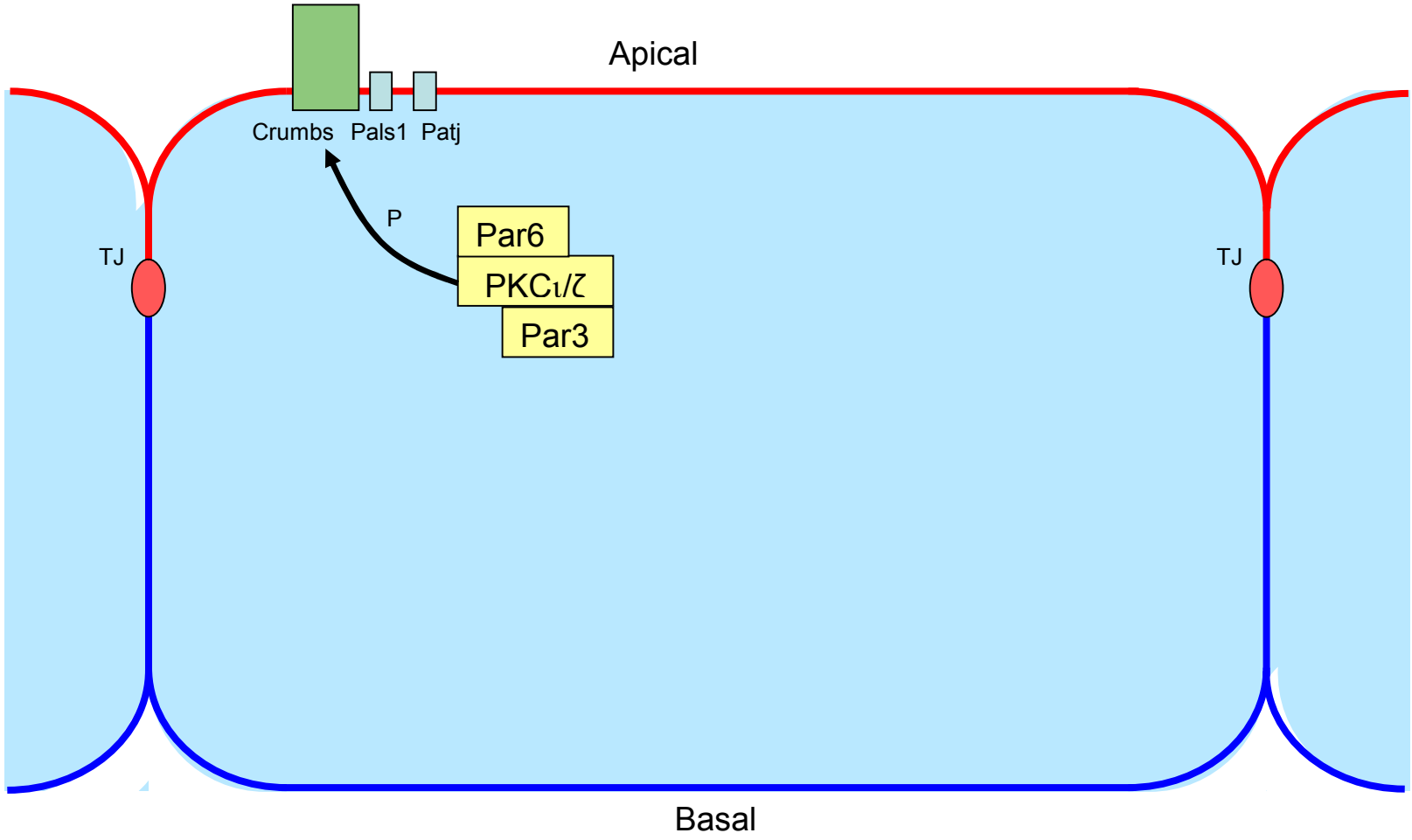

Figure 1.5 PKCι/ζ and the Crumbs, Pals-1, Patj complex
A schematic diagram depicting the interactions between PKCι/ζ and the Crumbs, Pals-1, Patj complex

1.7 The Yurt, Coracle, Neurexin IV and Na^+, K^+-ATPase Group

A new polarity complex that has recently been identified is the Yurt, Coracle, Neurexin IV and Na^+, K^+-ATPase group (Laprise et al., 2009). As a whole, the group promotes the basolateral identity of epithelial cells.

Yurt is a FERM (F for 4.1 protein, E for ezrin, R for radixin and M for moesin) domain containing protein. FERM domains are thought to link cytoplasmic proteins to the plasma membrane (Chishti et al., 1998). *Drosophila* Yurt mutants have an enlarged apical membrane and Crumbs is mislocalised indicating that Yurt is required for Crumbs localisation. In *Drosophila*, Yurt colocalises transiently with Crumbs at the adherens junctions and does not expand any further apically than this. There are also low levels of Yurt found at the basolateral membrane of epithelial cells. So only a small portion of Yurt localises apically with Crumbs. In the developing *Drosophila* embryo, Yurt only interacts with Crumbs later in development; the authors suggest that this change in interaction may be mediated by the phosphorylation of Yurt. They also suggest that Yurt may play a role in suppressing Crumbs to maintain apical-basal polarity (Laprise et al., 2006). Likewise, it has been shown that Yurt negatively regulates Crumbs function. However, Crumbs is responsible for recruiting Yurt to the apical membrane as loss of Crumbs results in Yurt localising totally to the basolateral membrane (Laprise et al., 2009).

The situation in vertebrates is not as clear as in *Drosophila*. In Zebrafish Yurt (also called mosaic eyes) localises apically with Crumbs (Hsu et al., 2006) which it does not in *Drosophila*. In Zebrafish, morpholino knockdown of Yurt phenocopies Crumbs knockdown and the mutants are lethal 5-6 days post fertilisation. It has also been shown by the same authors that Yurt forms a complex with Crumbs and PKCι/ζ in Zebrafish *in vivo*. Although the localisation data for *Drosophila* and Zebrafish do not entirely match, the data indicates that Yurt is critical for epithelial cell polarity.

Yurt and Crumbs also interact in mammals. There are two mammalian Yurt orthologs, EHM2 and EPB41L5 (renamed YMO1). Yurt localises to the lateral membrane in mammalian cells. Immunoprecipitation experiments in HEK293 cells indicate that Crumbs and Yurt interact and point mutants revealed that the FERM binding domain of Crumbs and the FERM domain of Yurt is essential for this interaction (Laprise et al., 2006). Similar interactions between Crumbs and EHM2 have been seen in the mouse retina. RNAi of YMO1 and EHM2 in MDCK cells results in a loss of the lateral membrane

and an increase in the apical and basal membrane. The authors conclude that Yurt is required for basolateral identity in mammals (Laprise et al., 2009).

More recently, Yurt has been shown to act with Coracle. Coracle is a member of the Protein 4.1 superfamily (Lamb et al., 1998). Coracle forms part of the *Drosophila* septate junction and Coracle null mutants are embryonic lethal. The reason for this is probably due to the role of Coracle in transepithelial barrier maintenance being lost. Yurt/Coracle double mutants in *Drosophila* show cell apicalisation (Laprise et al., 2009), similar to that seen in PKCι/ζ overexpression in *Xenopus* (Chalmers et al., 2005). Coracle also functions in a second pathway with Neurexin IV and Na^+, K^+-ATPase, which are also components of the *Drosophila* septate junction. This pathway is independent of Yurt as double mutants for Yurt and Neurexin IV or Na^+, K^+-ATPase enhance the Yurt phenotype. The two complexes have similar functions but do not operate in the same pathway.

The Yurt, Coracle, Neurexin IV and Na^+, K^+-ATPase pathways are an exciting new development in the understanding of how cell polarity is established and maintained in epithelial cells. Further work is now required to determine if these proteins interact with any other polarity proteins. One avenue to explore is Yurt phosphorylation as Yurt shows varying levels of phosphorylation in *Drosophila* (Laprise et al., 2006). It is possible that PKCι/ζ or Par-1 could phosphorylate Yurt leading to the promotion or suppression of Crumbs interaction.

The interactions of PKCι/ζ with the Yurt, Coracle, Neurexin IV and Na^+, K^+-ATPase pathways are depicted in figure 1.6.

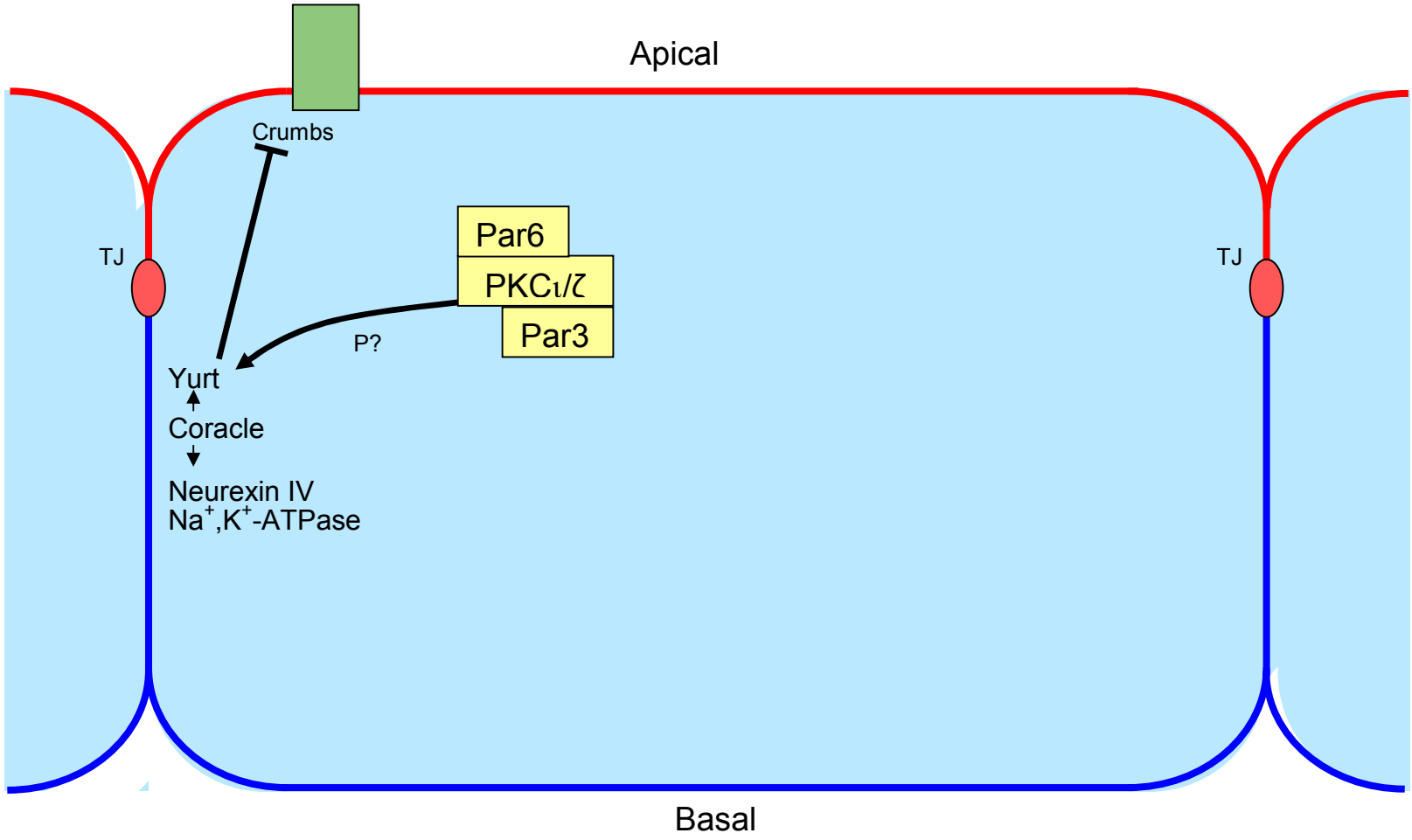

Figure 1.6 PKCι/ζ and the Yurt, Coracle, Neurexin IV and Na^+, K^+-ATPase pathways
A schematic diagram depicting the interactions between PKCι/ζ and the Yurt, Coracle, Neurexin IV and Na^+, K^+-ATPase pathways

1.8 Par-1

Par-1 is a serine/threonine kinase that was first identified in C. *elegans* (Guo and Kemphues, 1995). Par-1 is crucial for the establishment of asymmetry during the first cell cycle in C. *elegans* and its kinase activity is required.

In *Drosophila*, Par-1 is also a crucial player in cell polarity. Par-1 serves to inhibit the Par-PKCι/ζ complex by phosphorylating Bazooka/Par-3 (Benton and St Johnston, 2003), loss of Par-1 results in ectopic lateral localisation of the Par-PKCι/ζ complex. Phosphorylation of Par-3 by Par-1 causes Par-3 to bind to 14-3-3 proteins, preventing it from binding to PKCι/ζ. The phosphorylation of Par-3 by Par-1 therefore prevents ectopic localisation and activation of the Par-PKCι/ζ complex and limits the apical domain. Par-1 has also been linked to microtubule organisation in *Drosophila* (Cox et al., 2001; Doerflinger et al., 2003).

In mammalian cells, Par-1 is a regulator of cell polarity and apical surface formation (Cohen and Musch, 2003). During the development of polarity in MDCK cells overexpression of kinase null Par-1 is deleterious to polarity formation and apical surface formation. In 3D MDCK cell cultures, Par-1 knock-down prevents apical lumen formation (Cohen et al., 2004) and it is suggested that this is due to a role of Par-1 in microtubule and cytoskeletal organisation. Par-1 has also been described in tumour suppression (Elbert et al., 2006) and is thought to antagonise the Wnt signalling inducer Dishevelled, preventing cell transformation.

Par-1 has also been shown to be a substrate of PKCι/ζ (Hurov et al., 2004). The phosphorylation of Par-1 regulates the kinase activity of Par-1, with the phosphorylation reducing the kinase activity. The phosphorylation also regulates the subcellular localisation of Par-1. Phosphorylation of Par-1 causes Par-1 to move into the cytoplasm and intracellular compartments, away from the membrane. If a non-phosphorylatable version of Par-1 is overexpressed in HeLa cells with PKCζ, the Par-1 remains at the membrane. This gives another level of complexity to the control of cell polarity, in which PKCι/ζ can inactivate Par-1, but equally Par-1 can inhibit the formation of the Par-PKCι/ζ complex.

The interactions between PKCι/ζ and Par-1 are depicted in figure 1.7.

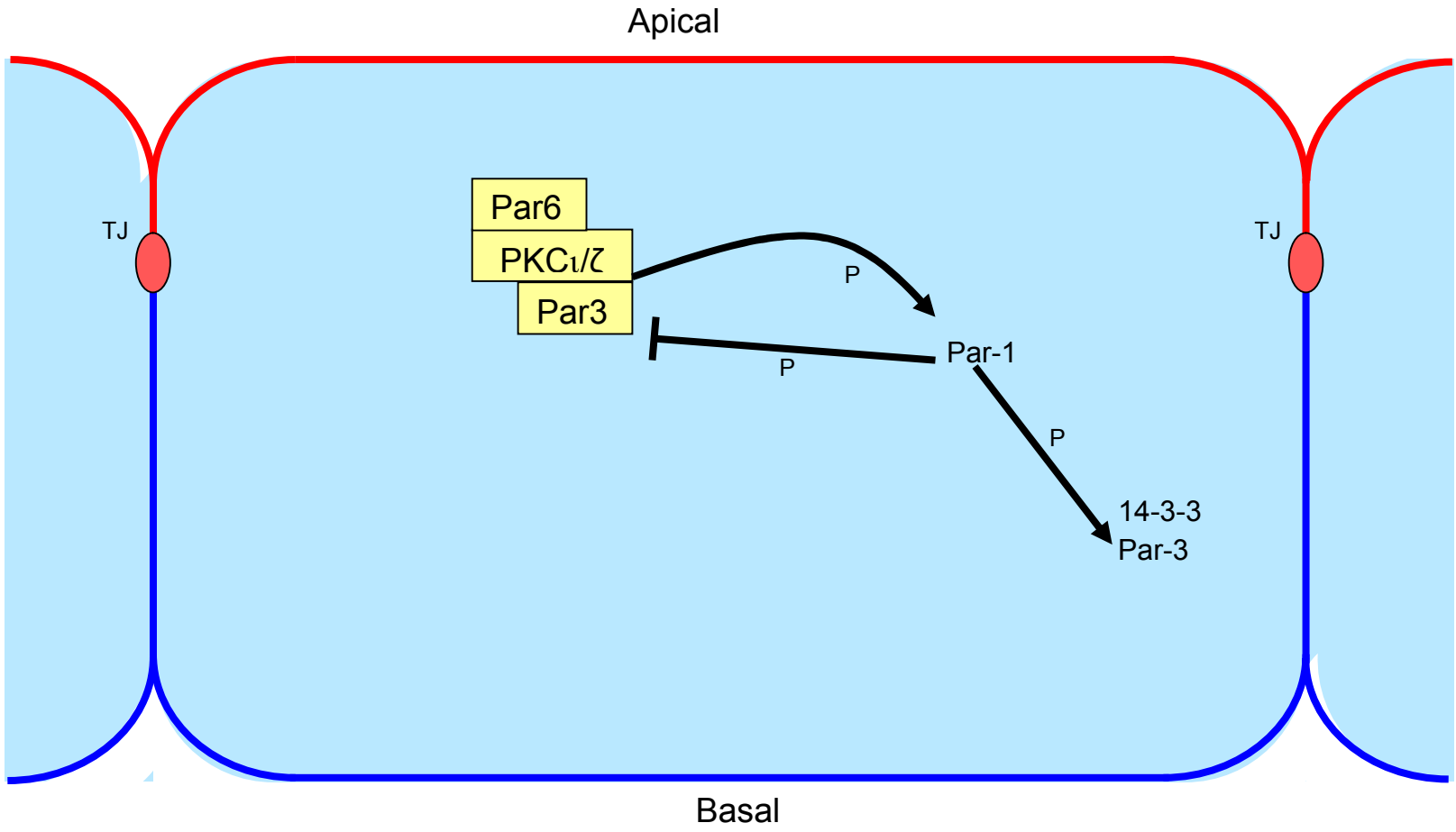

Figure 1.7 PKCι/ζ and Par-1
A schematic diagram depicting the interactions between PKCι/ζ and Par-1

1.9 Polarity Summary

There are four main polarity complexes that are required to maintain polarity: the apical PKCι/ζ/Par-3/Par-6 and Crumbs/Pals-1/Patj complex, the basolateral Lgl/Dlg/Scribbles group and the Yurt, Coracle, Neurexin IV and Na^+, K^+-ATPase group, as well as the basolateral protein Par-1.

The Par-PKCι/ζ complex is a crucial player in cell polarity, possibly interacting with nearly every polarity complex, as shown in figure 1.8. The Par-PKCι/ζ complex inhibits the Lgl/Scribble/Dlg group as a whole, although how or if PKCι/ζ directly inhibits Scribble or Dlg has yet to be investigated. In turn the Lgl/Scribble/Dlg group inhibits the effects of the Par-PKCι/ζ complex. Par-1 phosphorylates Par-3, inhibiting the formation of the Par-PKCι/ζ complex basal to the tight junctions.

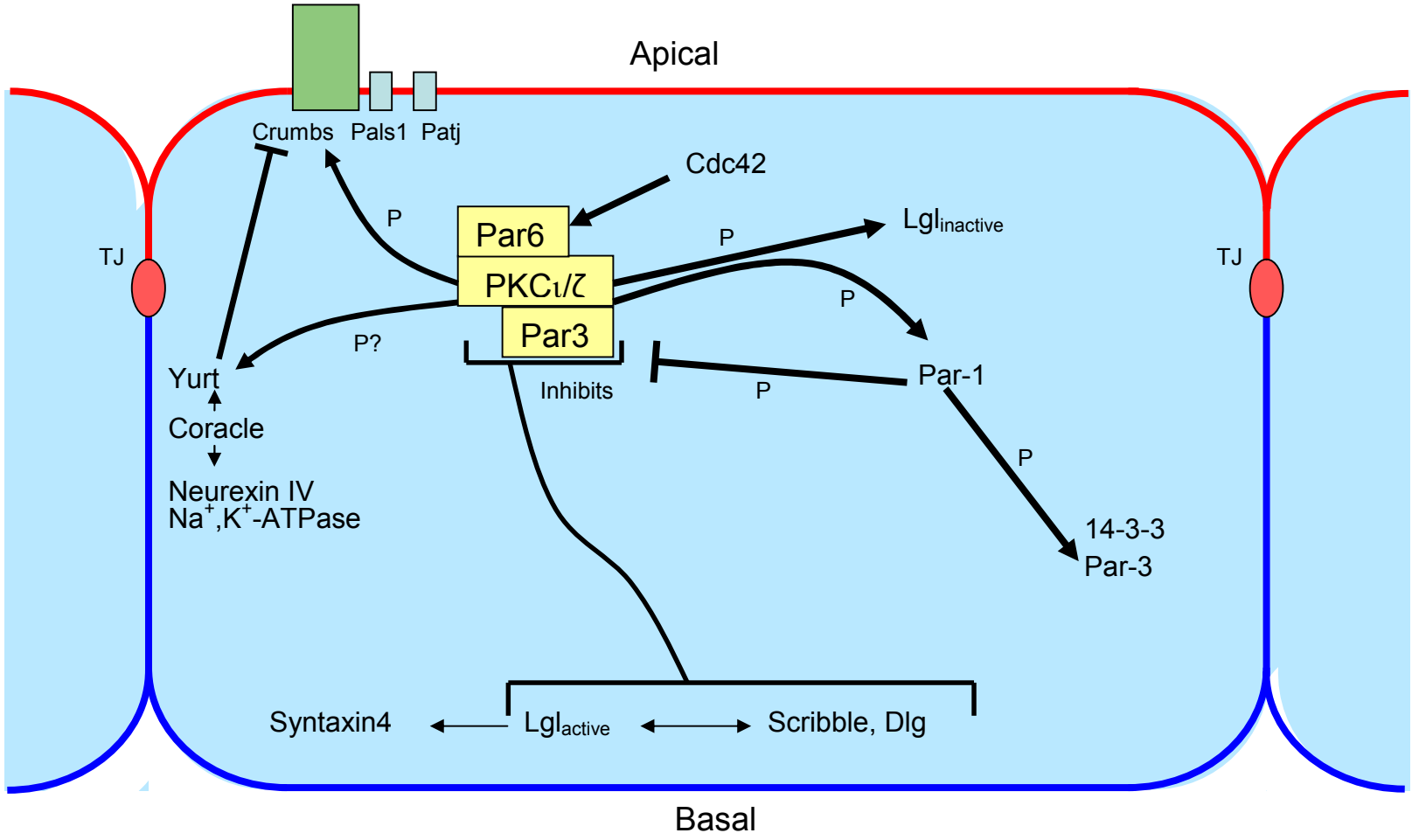

Figure 1.8 Epithelial Cell Polarity and PKCι/ζ Targets
A schematic diagram depicting all of the interactions between PKCι/ζ and the polarity proteins

In turn PKCι/ζ phosphorylates Par-1, inhibiting it's kinase activity and causing it to delocalise from the membrane, restricting it to the basal domain.

PKCι/ζ can also phosphorylate Crumbs in *Drosophila,* but the purpose of this phosphorylation, or whether it occurs in mammalian cells has yet to be elucidated. Par-6 can bind to Pals-1, preventing its association with Patj and therefore, possibly the activation and localisation of the Crumbs complex.

The Yurt, Coracle, Neurexin IV and Na^+, K^+-ATPase group also plays a key role in polarity and Yurt has been shown to interact with Crumbs, inhibiting its function. Yurt itself is phosphorylated, but the kinase responsible has yet to be found. It is possible that the kinase is PKCι/ζ or Par-1.

Overall lots is known about the establishment and maintenance of polarity, particularly in *Drosophila,* further work is required to see if what has been found in *Drosophila* occurs in mammals and to further understand all of the mechanisms regulating cell polarity. The Par-PKCι/ζ complex clearly plays a key role in cell polarity and its polarity substrates needs to be investigated further.

1.10 PKCι/ζ and Cell Fate

PKCι/ζ has been linked to polarity and asymmetric division. PKCι/ζ itself can also act as a cell fate determinant in *Drosophila* neuroblasts (Lee et al., 2006). Overexpression of PKCι/ζ targeted to the membrane, results in neuroblast self renewal, rather than the production of one differentiating daughter cell and one neuroblasts upon cell division. In agreement with this, loss of PKCι/ζ causes a decrease in neuroblast number.

One aspect of asymmetric division is the restriction of cell fate determinants to specific areas of the cell. PKCι/ζ phosphorylates the cell fate determinant Miranda. This phosphorylation leads to basolateral restriction in *Drosophila* neuroblasts and therefore alters the fate of one daughter cell (Atwood and Prehoda, 2009). PKCι/ζ also phosphorylates the cell fate determinant Numb (Smith et al., 2007). This phosphorylation restricts Numb to the basolateral membrane of sensory organ precursor cells in *Drosophila* and in mammalian cells, where Numb is restricted to the basolateral membrane and a non-phosphorylatable version of Numb localises throughout the cell cortex.

1.11 PKCι/ζ and Cancer

Epithelial tissue transformation involves the loss of cell polarity and alteration in the expression of polarity regulators is thought to be responsible (Dow and Humbert, 2007; Huang and Muthuswamy, 2010). The loss of apical-basal polarity can result in EMT which increases invasiveness and is a hallmark of malignant tumours (Thiery, 2002).

1.11.1 Evidence for PKCι Oncogenesis

PKCι is an oncogene in non-small cell lung cancer (NSCLC). There is overexpression of PKCι, mRNA and protein, but not PKCζ in NSCLC and the expression of PKCι is associated with poor patient survival (Regala et al., 2005b). PKCι/ζ is needed for the chemotaxis of NSCLC cells, as inhibition or downregulation of PKCι/ζ results in less chemotaxis of the NSCLC cell line A549 (Liu et al., 2009). Aurothioglucose (ATG) and Aurothiomalate (ATM) are inhibitors of PKCι-Par-6 interactions. They stop PKCι-Rac1 signalling and inhibit tumour growth in nude mice (Stallings-Mann et al., 2006) and inhibit anchorage-independent growth of lung cancer cells (Regala et al., 2008). These drugs are therefore potential treatments for NSCLC and ATM is currently in Phase1 clinical trails (Fields and Regala, 2007).

PKCι is upregulated in human prostate cancer. The mRNA for PKCι is more highly expressed in cancer tissue samples than controls. Also the higher the PKCι expression, the higher the prostate specific antigen failure, a marker used in prostate cancer diagnosis, which is associated with patient death (Ishiguro et al., 2009). However, the exact mechanism by which PKCι promotes prostate cancer cell growth remains unclear as IL-6 signalling, IKKβ phosphorylation and NFκB activation and the phosphorylation of Cdk7 and Cdk2 leading to cell cycle progression have all been implicated (Ishiguro et al., 2009; Win and Acevedo-Duncan, 2008; Win and Acevedo-Duncan, 2009). Further work is required to elucidate the exact mechanism(s) of PKCι during prostate cancer initiation and progression.

PKCι is upregulated in ovarian cancer and its upregulation is linked to poor prognosis (Eder et al., 2005; Zhang et al., 2006). The apical localisation of active PKCι is lost in ovarian cancer, with active PKCι accumulating in the cytoplasm, indicating a loss of apical-basal polarity (Grifoni et al., 2007). Therefore, PKCι is important in ovarian cancer and could be a therapeutic target.

PKCι/ζ is upregulated and mislocalised to the cytoplasm in human breast cancer cells and this is linked to the pathological type of the cancer. The more PKCι/ζ, the more severe the cancer (Kojima et al., 2008). In human breast cancer cells in culture, a PKCζ pseudosubstrate blocks the chemotaxis of the cells (Sun et al., 2005). Therefore, PKCι/ζ may be an effective therapeutic target in breast cancer, especially in preventing metastasis.

Upregulation of PKCι also occurs in human gastric and oesophageal cancers and is associated with metastasis and poor prognosis (Takagawa et al., 2010; Yang et al., 2008). PKCι mRNA is also elevated in human colon carcinomas (Murray et al., 2004). In bile duct and pancreatic carcinoma, high PKCι expression correlates with poor patient survival and metastasis (Li et al., 2008; Scotti et al., 2010). PKCι expression is also high and correlates with increased cyclin E expression in hepatocellular carcinoma (Wang et al., 2009). In normal brain tissue, PKCι staining is weak. However, in human glioma cells PKCι levels are elevated and may play a role in glioma cell proliferation (Patel et al., 2008).

PKCι/ζ and Par-6 regulate cell death in 3D MDCK cell cysts. Inhibition or siRNA of PKCι leads to an increase in apoptosis. The effect of PKCι-Par-6 on apoptosis is mediated through the phosphorylation of GSK3β by PKCι. When PKCι is lost, GSK3β is not phosphorylated and active, and causes caspase dependent cell death (Kim et al., 2007).

1.11.2 Mechanisms of PKCι Oncogenesis

PKCι is thought to be a human oncogene (Regala et al., 2005b). Loss of polarity could be involved in oncogenesis as loss of polarity is associated with cancer progression. PKCι is required for Ras-mediated oncogenic signalling and PKCι and PKCζ can be activated by Ras, through the binding of Ras to the regulatory domain of PKCι (Diaz-Meco et al., 1994). This activation then activates two pathways involving PKCι, the NFκB and Rac1 pathways (Fields and Regala, 2007; Lu et al., 2001). NFκB activation by PKCι increases cell survival via cellular inhibitors of apoptosis (cIAPs) and B-cell lymphoma extra large (Bcl-XL). Rac1 links PKCι to the Pak1-MEK-ERK pathway, increasing tumour growth (Fields et al., 2007). PKCι-Rac1 signalling is crucial for NSCLC tumorigenicity *in vivo* (Regala et al., 2005a). So PKCι links oncogenic Ras to its downstream effectors.

Steroid receptor coactivator-3 (Src-3) is overexpressed in many cancers. PKCι/ζ phosphorylates Src-3 protecting it from proteosome-mediated degradation resulting in

increased cell growth and proliferation (Garabedian and Logan, 2008; Yi et al., 2008). PKCι is also required for the migration and invasion of Src transformed 3T3 cells in culture (Rodriguez et al., 2009).

PKCι regulation by Bcr-Abl, an oncogenic fusion protein, via transcriptional activation has also been described. In chronic myelogenous leukaemia, PKCι is required for the Bcr-Abl mediated resistance to Taxol-induced apoptosis. The PKCι upregulation causes NFκB activation and cell survival (Gustafson et al., 2004). Abl also phosphorylates PKCι leading to PKCι activation (Grunicke et al., 2003). The authors suggest that this phosphorylation covalently modifies PKCι, causing constitutive activation, but the mechanism surrounding the modification remains unclear.

PKCι also phosphorylates Bad in NSCLC, preventing its interaction with Bcl-XL. This stops Bad acting as a proapoptotic kinase, leading to cell survival (Jin et al., 2005).

1.12 Other Roles of PKCι/ζ

In addition to cell polarity and tumour progression PKCι/ζ has been linked to a number of other cellular processes.

1.12.1 Insulin Signalling

PKCι/λ is involved in glucose induced insulin secretion in mice. A pancreatic PKCλ knockout has abnormal glucose tolerance when glucose load is increased (Hashimoto et al., 2005). More insulin is released basally but less in response to glucose, leading to an impaired glucose tolerance. The effects of PKCλ come from modulation of gene expression, the mRNA for Glut2 and HNF3β is decreased in PKCλ knockout pancreatic β-cells. Glut2 is a glucose transporter. HNF3β is a transcription factor responsible for the transcription of sulfonylurea receptor 1 (Sur1) and Kir6.2. Sur1 senses intercellular ATP concentrations and aids potassium channel opening, Kir6.2 aids potassium channel opening.

It has also been shown that insulin sensitivity is increased in PKCλ liver specific knockout mice (Matsumoto et al., 2003). The concentration of insulin in plasma is reduced in the knockout mice in response to glucose and more glucose is absorbed. There is also a marked reduction in mRNA levels for SREBP-1, a transcription factor that regulates the gene expression of triglyceride synthesis genes and fatty acid synthase. Consequently there is a decrease in the hepatic lipid content in PKCλ liver-specific knockout mice. The authors

propose that the increase in insulin sensitivity is due to an inhibition of the TNFα-PKCλ-IKKβ-NFκB pathway as inhibition of IKKβ increases insulin sensitivity.

Muscle-specific knockout of PKCλ results in an obesity and diabetes phenotype and glucose transport is impaired (Farese et al., 2007). PKCι/ζ is also involved in insulin signalling and phosphorylates insulin receptor substrate 1 (IRS-1) and Akt1 providing negative feedback in insulin signalling and may be linked to insulin resistance (Weyrich et al., 2007). The glucose transporter GLUT4 does not get translocated to the membrane, therefore, PKCλ is involved in the glucose response in response to insulin in skeletal muscle. In PKCλ knockout adipocytes in culture, insulin-stimulated glucose transport is impaired (Bandyopadhyay et al., 2004), which is measured by deoxyglucose uptake. This affect can be rescued by the expression of wild-type PKCλ. The authors suggest that insulin activates PKCλ, increasing glucose uptake.

PKCζ has also been shown to phosphorylate the IRS-1 in hepatotoma Fao cells (Liu et al., 2001). PKCι/λ was not investigated. The phosphorylation of IRS-1 by PKCζ causes IRS-1 to dissociate from the insulin receptor. This causes the insulin signal to be terminated indicating that PKCζ is involved in a nedative feedback loop. PKCζ can transmit and terminate the insulin signal. Overall these studies indicate that PKCι/ζ plays a crucial role in insulin signalling that may be separate to its role in polarity.

1.12.2 Endocytosis

The Par-PKCι/ζ complex may have a role in endocytic trafficking. Specifically, in cells treated with a dominant negative Par-6 or Cdc42, uptake of MHC1 occurs normally, but its recycling is impaired, so Par-6/Cdc42 and by implication the Par-PKCι/ζ complex is responsible for the recycling of clathrin independent cargo (Balklava et al., 2007). In contrast, the uptake of clathrin-dependent cargo is impaired in dominant negative Par-6 or Cdc42 treated cells. Transferrin uptake is reduced by 30% in these cells. However, the mechanism by which the Par-PKCι/ζ complex controls endocytosis has not been completely elucidated.

One method could be that the Par-PKCι/ζ complex controls endocytosis via actomysin contractility as in C. *elegans* actomysin contractility is stimulated by Par-3 and Cdc42 (Wissler and Labouesse, 2007). Another method of endocytic control could be mediated by the known PKCι/ζ phosphorylation target Numb (Nishimura and Kaibuchi,

2007). Expression of phosphomimetic Numb inhibits integrin endocytosis in cell migration in HeLa cells.

Overall these reports indicate that the Par-PKCι/ζ complex may play a crucial role in endocytosis that needs to be investigated further.

1.12.3 RNA Transciption

Nucleolin is phosphorylated by PKCι/ζ *in vivo* (Zhou et al., 1997). Nucleolin is involved in chromatin organisation, DNA transcription and ribosome assembly. The authors suggest that a possible role for PKCι/ζ phosphorylation of nucleolin is to modulate nucleolin-RNA interactions.

1.13 Summary

PKCι/ζ plays a role in a diverse range of cellular functions including; polarity, tumour formation, cell fate, endocytosis and insulin signalling. Due to these wide effects and the increase of PKCι in cancer, the function of PKCι needs to be investigated further.

The aim of this thesis is to discover novel PKCι phosphorylation substrates with the goal of understanding the effects of PKCι in cancer.

1.14 Aims

The central aim of this thesis is to discover novel phosphorylation targets of PKCι and begin to understand the effects that phosphorylation by PKCι has on these novel targets. This will hopefully aid our understanding of how PKCι mediates its effects within a normal cell setting and within a cancerous one.

Chapter 2

2.1 Materials

All chemicals were obtained from Sigma unless otherwise stated.

Buffer/Solution	Components
2.5% cysteine	2.5g/100mls dH_2O, ~7 pellets NaOH, adjust to pH 7.8-8.1
10% Blocking Buffer	500ml PBS, 50g milk powder (dried skimmed milk with non milk fat), 500µl Tween 20
4x Sample Buffer 10ml	2.5ml 1M Tris pH 6.8, 4.0ml 20% SDS, 400µl 100% glycerol, 0.008g bromophenol blue
10x Electrophoresis Buffer	2M glycine, 0.25M Tris, 1% SDS
10x MMR	2M NaCl, 0.04M KCl, 20mM $MgCl_2.6H_2O$, 4omM $CaCl_2.2H_2O$, 2mM EDTA disodium salt, 1M Hepes
Bacterial Protease Inhibitors	Protease inhibitors were dissolved in DMSO and H_2O according to the manufacturer's instructions.
Benzocaine	480mls ethanol, 20mls water, 50g benzocaine (10%)
Blotting Buffer 1L	750ml distilled water, 200ml MeOH, 10x electrophoresis buffer
Coomassie Stain	60% dH_2O, 30% Methanol, 10% Acetic Acid (Fisher), 0.2% Coomassie brilliant blue (Fluka).
Destain	60% dH_2O, 30% Methanol, 10% Acetic Acid (Fisher)
Freezing media	FCS containing 10% DMSO
Injection Buffer	1% Ficoll in 1x MMR
IP Buffer	50mM Tris, 0.15M NaCl, 1% triton, 0.5% sodium deoxycholic acid, 0.1% SDS, 1mM EDTA
Kinase Assay Buffer	4mM MOPS, 4mM $MgCl_2$, 1 mM EGTA, 0.4mM EDTA, 50µM DTT, pH 7.2
LB Agar 1L	LB Broth, 15g Agar
LB Broth 1L	10g Tryptone, 5g Yeast extract, 10g NaCl
Mowiol®	Mowiol® (Calbiochem) was reconstituted according to the manufacturer's instructions.
PBS	1 PBS tablet (Oxoid) per 100ml dH_2O
PBS Lysis Buffer	20ml PBS, 1ml Bacterial protease inhibitors, 1% Triton
PBST	PBS, 0.1% Tween 20
PBS with protease inhibitors	20ml PBS, 1ml Bacterial protease inhibitors
TBST	0.1M KCl, 0.02M Tris base, 0.1% Tween 20 to pH 7.4

Table 2.1 Solution Composition

Construct	Linearisation Enzyme
GFP	Not1
PKCι	Not1
Lgl-GFP	Not1
Par-1-GFP	Sal1

Table 2.2 Constructs and Linearisation Enzymes

Antibody Specificity	Species	Supplier	Dilution (unless otherwise stated)
GFP	Goat	Abcam	1:20,000
GFP	Rabbit	Abcam	1:10,000
Phosphoserine	Mouse	Sigma	1:10,000
Phosphothreonine	Rabbit	Abcam	1:250
C20 PKC	Rabbit	Santa cruz	1:200
Phospho-PKC	Rabbit	Santa cruz	1:200
PKCι	Mouse	BD Transduction	1:500
PKCξ	Mouse	Santa Cruz	1:5000
α-Tubulin	Mouse	Sigma	1:5000
Phospho Par-1	Rabbit	Abcam	1:500
GST	Mouse	Sigma	1:1000
Goat IgG		Invitrogen	1:40,000
Mouse IgG		Sigma	1:5000
Rabbit IgG		Sigma	1:10,000

Table 2.3 Antibodies used in Western Blotting and Immunoprecipitation

Name	Species	Tag	Vector	Resistance	Origin
GFP			pCSGFP3	Ampicillin	
LgL	*X Laevis*	GFP	pCSGFP	Ampicillin	
PKC	*X Laevis*		pCS2	Ampicillin	
PKC A120E	Human	His	pCDNA3.1	Ampicillin	P. Salas (Wald et al., 2008)
Scribble	Human	GFP	pEGFP-C1	Kanamycin	I. Macara (Qin et al., 2005)
Pals1	Mouse	YFP	pEYFP-C1	Kanamycin	B. Margolis (Kamberov et al., 2000)
Pals1	Mouse	GST	pDest15	Ampicillin	
Dlg	Rat	HA	pCDNA3	Ampicillin	L. Banks (Massimi et al., 2006)
Dlg	Rat	GST	pDest15	Ampicillin	
Par-1b	Human	GST	pGEX	Ampicillin	H. Piwinica-Worms (Hurov et al., 2004)
mLgl	Mouse	GST	pGEX	Ampicillin	T. Pawson (Plant et al., 2003)
Patj	Human	Myc	pIRES	Ampicillin	A Le Bivic (Lemmers et al., 2002)
Yap	Medaka	His	pSV281	Kanamycin	S. Bagby (unpublished)
Taz	Medaka	His	pSV281	Kanamycin	S. Bagby (unpublished)
Yap	Human	Flag	pCS2+	Ampicillin	M. Furutani-Seiki (unpublished)
LGN	Mouse	GST	pGEX	Ampicillin	V. Slepak (Nair et al., 2005)
GSK3β	Human	GST	pGEX-6P-2	Ampicillin	HK Paudel (Sun et al., 2002)

Table 2.4 Plasmids

Primer	Sequence
Dlg TOPO Forward	CACC ATG AGC GGG GCA GGG CGG CGG ACA
Dlg TOPO Reverse	TAA TTT TTC TTT TGC TGG GAC CCA GAT GT
Scribbles TOPO Forward	CACC ATG CTC AAG TGC ATC CCG
Scribbles TOPO Reverse	GGA GGG CAC AGG GCC CAG GCC
Patj TOPO Forward	CAC CAT GCC TGA AAA TCC TGC
Patj TOPO Reverse	TTA CCG TTT CCC AAC GAT GC
Pals-1 TOPO Forward	CAC CAT GAC AAC ATC ATA TAT GAA TGG
Pals-1 TOPO Reverse	TCA CCT TAG CCA GGT GGA TGG
Yap S54A Forward	CATGAGGATGAGGAAGCTGCCGGACGCATTCTTCAAGCC CCCGGAGCCCAAGTC
Yap S54A Reverse	GACTTGGGCTCCGGGGGCTTGAAGAATGCGTCCGGCAGC TTCCTCATCCTCATG
Taz S45A Forward	CATGAGGATGAGGAAGCTGCCGGACGCATTCTTCAAGCC CCCGGAGCCCAAGTC
Taz S45A Reverse	GACTTGGGCTCCGGGGGCTTGAAGAATGCGTCCGGCAGC TTCCTCATCCTCATG
Dlg S472A Forward	CTT CAT CGT GGC GCA ACG GGA CTT GGT TTC
Dlg S472A Reverse	GAA ACC AAG TCC CGT TGC GCC ACG ATG AAG
Dlg Sequencing primer	GCC TTA AAG AAT ACA TCT G
GST Sequencing Primer	GGG CTG GCA AGC CAC GTT TGG TG

Table 2.5 Primers used for TOPO® Cloning, SDM and Sequencing

Construct	Annealing Temperature °C	Extension Time (minutes)
Patj	52.3	4.5
Scribble	59.0	5
Pals-1	52.3	2
Dlg	57.4	2.7

Table 2.6 PCR Conditions

Gene	Species	Accession Number
Lgl	Mouse	NM_145438
Scribble	Human	NM_182706
Pals-1	Mouse	AF_199008
Dlg	Rat	NM_021265
Par1b	Human	NM_017490
Patj	Human	NM_176877
GSK3β	Human	NM_002093
Yap	Medaka	
Taz	Medaka	
Yap	Human	NM_001130145
Taz	Human	NM_000116

Table 2.7 Accession Numbers for Genes used for the Phosphorylation Prediction Tools

Cell Type	Media
MDCK	DMEM (Lonza), 10% FCS, 2mM L-glutamine (Cambrex), pen/strep (100U/ml penicillin, 100µg/ml streptomycin - Cambrex)
Caco-2	DMEM, 20% FCS, 2mM L-glutamine, 1x Non-essential amino acids, pen/strep
A549	DMEM, 10% FCS, 2mM L-Glutamine, pen/strep
HeLa	DMEM, 10% FCS, 2mM L-glutamine, pen/strep
OVCAR-3	RPMI-1640, 20% FCS, 0.01mg/ml bovine insulin, pen/strep

Table 2.8 Tissue Culture Media for Different Cell Types

Antibody Specificity	Species	Supplier	Cat. No.	Starting Dilution	Dilution (unless otherwise stated)
C20 PKC	Rabbit	Santa cruz	SC-21C	200µg/ml	1:100
Phospho-PKC	Rabbit	Santa cruz	SC-12894-R	200µg/ml	1:150
PKCι	Mouse	BD Transduction	610176	250µg/ml	1:100
PKCζ	Mouse	Santa Cruz	SC-17781	200µg/ml	1:100
γ-tubulin	Mouse	Abcam	Ab-11316	28mg/ml	1:1000
Pericentrin	Rabbit	Covance	PRB-432C	0.2mg/ml	1:500
ZO-1	Mouse	Zymed	339100	0.5µg/µl	1:25
α-tubulin	Rat	Abcam	Ab-6160	1mg/ml	1:100
Flag Tag	Mouse	Sigma	F-1804	1mg/ml	1:300
Anti-Rabbit 488		Invitrogen	A11008	2mg/ml	1:500
Anti-Rabbit 568		Invitrogen	A11011	2mg/ml	1:300
Anti-Mouse 488		Invitrogen	A11001	2mg/ml	1:500
Anti-Mouse 568		Invitrogen	A11004	2mg/ml	1:500
Anti-Rat 488		Molecular probes	A11006	2mg/ml	1:300

Table 2.9 Antibodies used in Immunofluorescence

2.2 Methods

2.2.1 RNA Manufacture

The plasmid DNA template was linearised using the appropriate enzyme in the correct buffer according to the guidelines set out by Roche (see table 2.2 for the list of enzymes). RNA was made using this template and the mMessage Machine kit according to the manufacturer's instructions (Ambion). This kit utilises an RNA polymerase (Sp6 or T7) to make the RNA. RNA was quantified using a Genequant machine (GE Healthcare) and also run out on a 1% agarose gel in a Mupid-EXu electrophoresis tank, to check the integrity of the RNA.

2.2.2 Fertilisation of *Xenopus laevis* Eggs

Male *X. laevis (Xenopus)* were killed by a schedule 1 method using benzocaine. Testes were harvested from the freshly killed male and used immediately, or stored for up to 5 days in L-15 medium (Sigma) at 4°C. Female *Xenopus* were injected with 50units of Pregnant Mare Serum Gonadotrophin (PMSG - Intervet®) 3 days prior to egg collection and with 500units of chorionic gonadotrophin (hCG - Intervet®) 12 hours prior to egg collection. The female *Xenopus* were put into 1x MMR (Marcs Modified Ringers) to maintain the ability of the laid eggs to be fertilised and eggs were collected from this medium. The collected eggs were washed once with 0.1x MMR and fertilised with the harvested testes, in this procedure, a small piece of the testes, approximately 5mm wide was cut from a testis. It was placed into the dish containing the *Xenopus* eggs and then torn apart and wiped over the eggs. This was to release all of the sperm allowing fertilisation. The fertilised eggs were dejellied approximately 40mins post fertilisation, 2.5% (w/v) cysteine was added to the fertilised eggs and left for 2-3mins until the jelly could be seen to have been removed. The eggs were then washed 4 times with 0.1x MMR.

2.2.3 Microinjection of RNA and Protein Extraction

Glass capillary tubes (0.53" width, Drummond Scientific) were pulled using a Sutter P-97 needle puller. RNA microinjection was carried out using a Drummond micro-injector, RNA volume and concentration as stated. Embryos were injected into one cell at the 2-cell stage and then incubated at 14°C overnight until they reached approximately stage 9. Embryos were staged by cell number or as described previously (Nieuwkoop and Faber, 1967). The embryos were examined using a Leica M26 (Deerfieled, Illinois) and

any dead embryos removed. The remaining embryos were snap frozen, in batches of 50, on dry ice.

The frozen embryos were resuspended in 500µl of 1xPBS, then 500µl of Freon 1,1,2-trichlorotrifluoroethane (Riedel-de Haën) was added and the mixture vortexed. The mix was then centrifuged at 13.2K rpm at 4°C for 10 minutes and the supernatant retained. The supernatant was either used immediately in a Western blot or immunoprecipitation or was stored at 4°C for 2-3days or at -20°C for longer than 3 days.

2.2.4 Immunoprecipitation

Dried Protein-A sepharose beads (Amersham) were prepared by immersion in dH_2O followed by two washes in dH_2O and then three washes in IP buffer by low speed centrifugation. The beads were centrifuged, the supernatant removed and discarded. Fresh buffer was then added and the centrifugation repeated. A pre-clearing reaction was set up comprising of 10µl lamb's serum, 50µl beads and the Freon extracted embryo mixture. A coupling reaction was also set up which comprised of 50µl beads, 500µl IP buffer and the primary anti-GFP antibody as stated. Both reactions were incubated at 4°C with rotation for 2hours. After the incubation time for both preparations the coupling reaction was washed three times with IP buffer by low speed centrifugation and resuspension, to remove any unbound antibody. The pre-clearing reaction was centrifuged and the supernatant added to the washed coupling beads. This preparation was incubated overnight at 4°C with rotation. Following the overnight incubation the beads were washed with PBS using low speed centrifugation. See table 2.3 for the antibodies used.

2.2.5 SDS-PAGE and Western Blotting

The Western blotting apparatus was a Bio-Rad Mini-protean II. The SDS-PAGE gels were 10% gels, unless otherwise stated. Prior to loading 4X sample buffer was added to the protein sample and boiled for 5 minutes. Approximately 40µg of protein was added to each well. On each gel a protein ladder (Fermentas) was run in one lane. The gels were run in electrophoresis buffer at 100V until the protein had reached the separating gel and then at 150V until the proteins were separated sufficiently, as determined by the separation of the bands on the protein ladder.

The gel was equilibrated in blotting buffer along with nitrocellulose membrane (Whatman), filter paper and fibre pads. The blotting cassette was assembled and bubbles removed by rolling with a glass tube. The blot was run at 100V for 1 hour. The

nitrocellulose membrane was then removed and Ponceau (Sigma) stained to show the transferred protein. The nitrocellulose membrane was rocked in 10% blocking buffer for 1 hour at room temperature, followed by the primary antibody diluted in 10% blocking buffer and rocked overnight at 4°C. The membrane was washed in 2% blocking buffer in PBS 5 times. The secondary antibody was then added, diluted in 2% blocking buffer in PBS, and rocked for 2 hours at room temperature. The membrane was then washed 5 times in PBS plus Tween 20 (PBST) followed by addition of ECL reagent (Chemiglow® - Alpha Innotech or *ChemiLucent*™ - Millipore) to detect horseradish peroxidase (HRP) conjugated secondary antibodies. The membrane was then exposed to film (Hyperfilm, Amersham) in the dark for 1-10 minutes and developed using a Protec Optimax film processor. The film was scanned with a HP Scanjet G2410 (Hewlett Packard, Berkshire, UK). To create a digital image of the Western blot. See table 2.3 for the antibodies used.

Membrane stripping of the antibodies was carried out using an IgG elution buffer (Pierce) for 2 hours at room temperature or overnight at 4°C. The membrane was washed 5 times with Tris buffered saline plus Tween 20 (TBST) and then blocked as above and the second antibody of interest added, in the same way as the first.

2.2.6 Site-directed Mutagenesis

Site-directed mutagenesis was carried out using the Stratagene QuikChange® mutagenesis kit. Briefly primers were designed to contain the correct mutation (see table 2.5 for further information) PCR was then carried out according to the manufacturer's instructions. The template DNA was digested using the Dpn1 enzyme and transformed into XL1-Blue supercompetent cells and allowed to grow on antibiotic containing LB agar plates overnight at 37°C. one to four colonies were selected, grown up overnight at 37°C with shaking in antibiotic containing LB broth and then mini-prepped the following day and sent for sequencing.

2.2.7 Preparation of Glutathione-S-transferase (GST)-tagged DNA Constructs

GST tagged Par-1, GSK-3β and LGN were kindly donated by H. Piwinica-Worms, HK. Paudel and V. Slepak respectively. Dlg, Pals-1 and Rassf7 GST-tagged constructs were made using the Gateway® Cloning kit (Stratagene). The DNA was amplified using primers specific to the gene of interest (see table 2.6) with CACC added to the forward

primer, the PCR annealing and extension conditions varied between reactions and are listed in table 2.6. The general PCR conditions are listed below.

1. 2 minutes at 95°C
2. 20 Seconds at 95°C
3. 30 Seconds at the annealing temperature
4. X minutes at 72°C depending on the extension time
5. Repeat steps 2- 4, 29 times
6. 10 minutes at 72°C

The integrity of the PCR was checked by running on a DNA gel. The TOPO® Cloning reaction was carried out according to the manufacturers instructions to create the TOPO® entry vector which was transformed into bacteria. A single bacterial colony was picked and grown up in 5ml Luria Bertani (LB) broth overnight at 37°C with shaking. This culture was mini-prepped (Sigma) to harvest the DNA. The amplified DNA was digested with the restriction enzyme BSRG1 attL1 and attL2 sites and there fore will excise the gene and allow conformation that it is present when the mix is run on a gel. The DNA which showed correct excision was sequenced (MWG operon). The TOPO® entry vector containing our gene of interest was then cloned into the destination vector pDEST™15 Vector using the Gateway® LR Clonase™ Enzyme Mix according to the manufacturers instructions. The product was mini-prepped, run on a gel and then sequenced using the GST primer (see table 2.5).

2.2.8 Transformation of E.*coli*

E.*coli* were transformed with the appropriate plasmid using the heat shock method. The bacteria were defrosted on ice; approximately 10ng of plasmid DNA was added and allowed to bind to the outside of the bacteria, whilst on ice, for 30 minutes. The bacteria were then heat shocked at 42°C for 45 seconds and then put onto ice for 2 minutes. Warm LB broth (containing no antibiotic) was added to the mix at this stage and the bacteria are allowed to grow at 37°C and express the plasmid's antibiotic resistance for at least 1 hour. The mix is then spread onto an LB agar plate containing the appropriate antibiotic and allowed to grow at 37°C overnight.

2.2.9 Expression of GST Fusion Proteins

Par-1, Lgl and GSK-3β were in the pGEX-2T vector and were expressed in the BL21 strain of *E.coli* (gift from Dr. Paul Whitley), this strain uses isopropyl-1-thio-β-D-galactopyranoside (IPTG) (Sigma) as the inducing agent. All other constructs were expressed in the BL21-A1 (Invitrogen) strain of *E.coli,* this strain uses L-arabinose (Sigma) as the inducing agent.

Synthesis of the fusion protein was induced in the log phase of the 500ml bacterial cultures with 0.1 mM IPTG or 0.2% L-arabinose, diluted in dH_2O, for three hours with shaking at 37°C. Log phase was determined when the culture had an optical density of 0.5 to 1 by taking a spectrophotometer reading at 600nm on a Helios Spectrophotometer (Unicam, Leeds, UK). 1ml samples were taken before and three hours after addition of the inducing agent. The cells were then pelleted and resuspended in 20ml PBS lysis buffer. The lysate was then sonificated for 3 30second bursts in a 150PW ultrasonic disintegrating (MSE Scientific Instruments, London, UK) and the lysate cleared by centrifugation at 13200rpm for 20 minutes at 4°C. Glutathione-sepharose beads (Amersham) were washed in PBS lysis buffer and added to the supernatant to bind the GST fusion protein. The mixture was incubated with rotation for thirty minutes at 4°C. The beads were then washed 4 times with PBS containing protease inhibitors (Sigma) then poured into a disposable chromatography column (Quiagen). The fusion protein was eluted using cold 50mM Tris pH 8.0 (Fisher) containing 20mM reduced glutathione (Sigma). The reduced glutathione was removed using dialysis against PBS through a 3.5K molecular weight cut off SnakeSkin dialysis tubing (Pierce). The absorbance of the protein was then measured on a spectrophotometer and the concentration determined using the extinction coefficient. The concentration was adjusted to 1mg/ml where possible. The purified protein was stored at 4°C.

The protein expression was analysed by SDS-PAGE followed by staining with Coomassie for one hour and then destaining for sixteen hours. The gel was then scanned.

2.2.10 Kinase Assay

100ng of purified recombinant GST-tagged PKCι (Calbiochem) was mixed with 10μg of the fusion protein in kinase assay buffer along with 10-15μCi of ^{32}P-labelled γ-ATP (Perkin Elmer). The reactions were run at 30°C for 30 minutes and then quenched with 4x sample buffer containing 5mM EDTA.

The reaction products were run on an SDS-PAGE gel (percentage composition varied depending on protein size) and analysed using autoradiography onto Amersham™ Hyperfilm™. The film was developed as before and digitally scanned.

2.2.11 Bioinformatics

DNA sequences were obtained from NCBI and the accession numbers are listed in table 2.7. The domain analysis was carried out using the simple modular architecture research tool (SMART). www.smart.embl-heidelberg.de. The phosphorylation prediction was carried out using scansite, www.scansite.mit.edu/motifscan.seq.phtml, PhosphoELM (http://phospho.elm.eu.org/), NetPhos (http://www.cbs.dtu.dk/services/NetPhos/) and Human protein Reference Database HPRD (http://www.hprd.org/).

2.2.12 Cell Culture

Cells in DMSO freezing media were revived from liquid nitrogen and allowed to grow at 37°C with 5% carbon dioxide in growth media (see table 2.8 for different cell type's growth medium). When cells reached near confluency they were passaged into experimental or maintenance, T25 flasks or 4 well plates (Iwaki). Passaging was carried out using 5ml trypsin (Lonza) to detach the cells from the flask. Cells were passaged at least twice following revival from liquid nitrogen and not more than 20 times for experimental use.

2.2.13 Immunofluorescence

Cells were plated onto coverslips (Fisher) in 4 well plates and left for two nights in growth media to adhere and make junctions. They were then washed twice with warm PBS then fixed using 4% Paraformaldehyde (PFA) and permeabilised using methanol cooled to -20°C. Cells were then blocked with 10% foetal calf serum (FCS - Sigma) diluted in PBS followed by washing with 2% FCS and PBS. Primary antibodies, diluted in 2% FCS were incubated with the cells for at least 2 hours followed by extensive washing with 2% FCS and PBS. Secondary antibodies and the nuclear stain TOPRO-3 were incubated in the same manner except for the timing, which was reduced to at least 30 minutes followed by extensive washing as above. Cells were mounted onto coverslips using Mowiol and allowed to set at room temperature overnight. The antibodies used are listed in table 2.9.

Imaging was carried out using a Zeiss LSM510 confocal microscope and images were processed using the Zeiss LSM image browser software (Thornwood, NY).

2.2.14 Transfection

Transfection of MDCK cells in four well plates, plated 1/8 from confluency the day before, in growth media was carried out using Lipofectamine™ LTX (Invitrogen). 50µl of DMEM with L-glutamine was added to 2µg of DNA in one eppendorf and 50µl of DMEM with L-glutamine was added to 8µl of Lipofectamine™ LTX. The mixtures were incubated for 5 minutes and then combined and incubated for a further 20minutes. The cells were washed and the media changed to antibiotic free media. The mixture was then added to the cells in a drop wise fashion and gently mixed then left for at least 16 hours. The cells were then visualised using IF and the confocal microscope.

2.2.15 Nocodazole Treatment

Cells were plated onto coverslips allowed to stick for 24hrs and then the media was replaced by fresh media. 0.33µM of Nocodazole was diluted in dimethyl sulfoxide (DMSO) and water and then added to the cells in a drop wise fashion. DMSO alone was used as a control. The cells were incubated for 4 hours and then fixed and stained as described previously.

Chapter 3

Subcellular Localisation of Endogenous PKCι and PKCζ

3.1 Introduction

There are a number of commercial PKCι and PKCζ antibodies that can be used to look at the localisation of PKCι and PKCζ. Many of them are raised against the C-terminal region of PKCι/ζ proteins. This region is almost identical in the two proteins (Nakaya et al., 2000), so it is very likely that the antibodies will recognise both isoforms of PKC even if they specify one isoform, for example Santa Cruz produce a C20 PKCι/ζ antibody that recognises both isoforms. There are antibodies available that are specific for each isoform however, for example BD Transduction produce a PKCι antibody and Santa Cruz produce a PKCζ one. Finally there is an antibody available against a phosphorylated form of PKCι/ζ, which is believed to be the active form (Akimoto et al., 1994). Throughout this report PKCι/ζ will be used to describe staining that does not differentiate between the two isoforms and PKCι or PKCζ, specifically when they do.

The range of different antibodies means that although a number of sites of localisation have been described, the literature on PKCι/ζ localisation is complicated and often incomplete. The aim of this chapter is to describe the localisation of PKCι and PKCζ in MDCK cells which are commonly used to study cell polarity.

3.1.1 PKCι and PKCζ Localise Apically in Embryos

The best characterised localisations of PKCι/ζ are apically and at the tight junctions. In C *elegans*, there is only one PKC, PKC-3 and this localises apically in epithelial cells (Totong et al., 2007) including the gut epithelium (Bossinger et al., 2001). In *Drosophila* embryos, DaPKC localises apically in early epithelial development (Harris and Peifer, 2005; Sotillos et al., 2004). In *Drosophila* pupae dorsal thorax, DaPKC localises apically and at cell junctions (Georgiou et al., 2008). DaPKC also localises apically in the *Drosophila* ectodermal epithelium (Kim et al., 2009) and apically in neuroblasts (Atwood and Prehoda, 2009; Chabu and Doe, 2008; Krahn et al., 2010). In the developing Zebrafish embryo, PKCι/ζ localise apically in the oesophagus, intestine and retinal neuroepithelium, but only PKCι localises to the apical membrane in the Zebrafish swimbladder (Horne-Badovinac et al., 2001). In *Xenopus* embryos, PKCι/ζ localises

apically (Chalmers et al., 2005; Chalmers, 2003). In *Xenopus* kidney epithelial A6 cells, PKCι/ζ localises apically with some cytoplasmic staining (Nakaya et al., 2000). In chick embryos, PKCι/ζ and active phospho-PKCι/ζ localise to the apical luminal margin of the neuroepithelium (Ghosh et al., 2008).

In mouse embroid bodies, PKCλ/ζ and active phospho-PKCι/ζ localise to the apical membrane (Krishnamurthy et al., 2007) and in the mouse blastocyst PKCλ/ζ localises to the apical membrane of the epithelial trophectoderm (Eckert et al., 2005) and during preimplantation development, PKCλ/ζ becomes progressively apically and tight junctionally localised (Pauken and Capco, 2000; Plusa et al., 2005). During mouse embryogenesis, PKCλ is also found at the apical edge of the embryonic retina (Koike et al., 2005). PKCλ/ζ is found at the apical junctions of lens epithelial cells in mice; PKCλ/ζ remains apical during elongation of the cells, but is gradually lost as the cells differentiate (Sugiyama et al., 2009). A similar effect is seen during mouse cortical neurogenesis, in which PKCλ/ζ localises strongly at the ventricular zone at E12, however, the intensity of the staining at this region decreases during development (Costa et al., 2008). Therefore, PKCι/ζ has a well documented apical localisation which suggests a role in regulating polarity in the developing embryo.

3.1.2 PKCι and PKCζ Localise Apically in Cultured Cells

Kidney derived MDCK cells show apical and tight junction PKCι/ζ localisation in 2D culture (Izumi et al., 1998; Nunbhakdi-Craig et al., 2002) and in 3D culture (Kim et al., 2007). PKCι/ζ are also found at the leading edge of migrating MDCK cells (Shin et al., 2007) and on the primary cilia of MDCK cells (Fan et al., 2004).

In colon derived, Caco-2 cells, PKCι/ζ are localised apically (Mashukova et al., 2009; Michel et al., 2005; Wald et al., 2008). In mouse epithelial MTD1-A cells PKCι/ζ also localises to the apical membrane and tight junctions (Suzuki et al., 2002), as it does in the human keratinocyte cell line HaCaT (Aono and Hirai, 2008). Therefore PKCι/ζ has apical and tight junctional localisation in cultured epithelial cells, but it is not clear if it is PKCι, PKCζ or both as most of the antibodies used recognise both isoforms.

3.1.3 PKCι and PKCζ Localise to the Nucleus

In addition to the tight junction localisation, PKCζ has been shown to localise to the peri-nuclear and nuclear region of PC12 cells (Neri et al., 1999; Zhou et al., 1997) and to

the nucleus, in 786-O cells growing at a low cell density, (Pal et al., 1998). PKCι/λ also localises to the nucleus and shuttles continuously in and out in HeLa cells (Perander et al., 2001); this was shown by treating the cells with Leptomycin B, a nuclear export inhibitor. When treated with Leptomycin B, there was rapid nuclear accumulation of PKCι/λ, but there is only a fraction of the total cellular PKCι/ζ in the nucleus normally. The antibody used in this experiment recognises both PKCι/λ and PKCζ. Consistent with this, both PKCζ and PKCι have nuclear localisation signals within their zinc finger region (Perander et al., 2001). White and colleagues showed that upon nerve growth factor stimulation, phosphorylation of tyrosine 256 in PKCι occurs and that PKCι accumulates in the nucleus of PC12 cells (White et al., 2002). They suggest that this tyrosine 256 phosphorylation exposes the nuclear localisation signal allowing PKCι entry into the nucleus. Endogenous PKCι/ζ has also been shown to localise to the nucleus in HeLa cells (Sabherwal et al., 2009) and the authors suggest that PKCι/ζ drives cell fate and proliferation in the nucleus of *Xenopus* embryos. Therefore nuclear proteins could be phosphorylation targets of PKCι/ζ.

3.1.4 PKCι and PKCζ Localise to the Centrosomes during Mitosis

It has previously been shown that PKCζ associated with the mitotic spindle in shark rectal gland and Chinese hamster ovary cells (Lehrich and Forrest, 1994). This work used an antibody described previously (Ono et al., 1989), which was raised against the C-terminal region of PKCζ. However, this antibody was made before PKCι was described and may therefore recognise both isoforms. The PKCι isoform is not mentioned.

More recently, Liu and colleagues showed PKCι/ζ staining at the mitotic spindle in HeLa cells and phospho-PKCι/ζ staining at the centrosomes in metaphase, but not anaphase or telophase. They also showed strong staining for both PKCι/ζ and phospho-PKCι/ζ at the midbody in telophase (Liu et al., 2006). In their paper the antibody used for PKCι/ζ is the same as the one used in this work for total atypical PKCι/ζ and recognises both forms of atypical PKC, so the staining seen is for both isoforms. The phospho-PKCζ antibody is different to the one used in this work, but recognises both isoforms of atypical phospho-PKCι/ζ.

PKCι/ζ is found at the centrosomes, colocalising with γ-tubulin in dorsal root ganglion neurones and granule neurones from mice (Mori et al., 2009; Solecki et al.,

2004). Active phospho-PKCι/ζ was also found at the centrosomes in the dorsal root ganglion neurones, but was not tested for in the granule neurones.

Page Baluch and colleagues show PKCζ staining at the meiotic spindle in fertilised mouse eggs is meiosis II (Baluch and Capco, 2008; Page Baluch et al., 2004). The antibody used is the total atypical PKC antibody, which binds both PKCι and PKCζ, therefore one or both of them are found at the meiotic spindle. In mouse meiosis I, phosphorylated PKCζ is found at the centrosomes (Na and Zernicka-Goetz, 2006). The antibody they used is no longer available, so whether it recognises iota and zeta is unknown. This suggests that PKCι/ζ may have a role in meiosis and mitosis and that centrosomal proteins can be considered PKCι candidate phosphorylation targets.

3.2 Aims

The current published PKCι and PKCζ localisation data is widely detailed when it comes to tight junctions, but little has been published about the nuclear and centrosomal localisation of the two isoforms. There has been no data published indicating PKCι/ζ at the centrosomes of MDCK cells, our model system. The aim of this chapter is to describe the localisation of total PKCι/ζ, PKCι, PKCζ as well as the active phospho-PKCι/ζ within MDCK cells during all stages of the cell cycle. MDCK cells are being used as they are a well established polarised cell line that are relatively simple to image.

3.3 Results

To document the cellular localisation of PKCι/ζ, antibodies for active phospho-PKCι/ζ, total PKCι/ζ and PKCι and PKCζ were purchased from commercial sources and the specificity of the PKCι and PKCζ antibodies was tested using overexpressed PKCι or PKCζ protein by our collaborators (Cancer Research Technologies). The antibodies only detected either PKCι or PKCζ and did not cross-react.

3.3.1 PKCι and PKCζ Localise to the Tight Junctions in MDCK Cells

The total PKCι/ζ and phospho-PKCι/ζ data in figure 3.1a and b confirm the published data (see section 3.1.2) that total and phospho-PKCι/ζ localises to the tight junctions in MDCK cells. The results in figure 3.1 c and d, clearly show that the PKCι/ζ antibodies bind the atypical or ι and ζ isoforms directly and that they also localise to the

tight junctions. This confirms that both proteins localise to the tight junctions in MDCK cells.

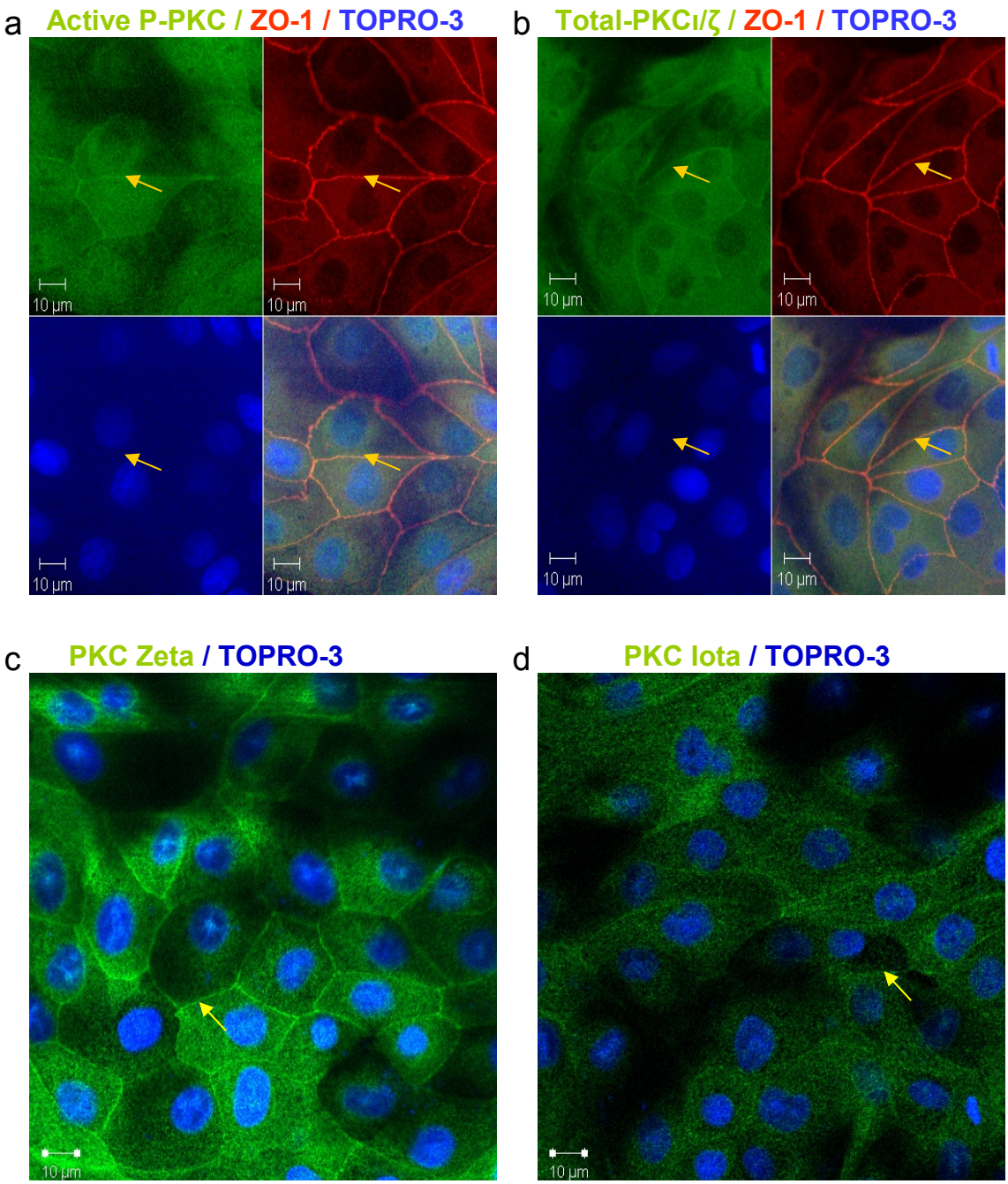

Figure 3.1 PKCι and PKCζ Localise to Tight Junctions in MDCK Cells

Confluent MDCK cells were PFA fixed, stained with PKCι/ζ (green) and ZO-1 (red) antibodies and imaged using confocal microscopy. The nucleus was stained with TOPRO-3 (blue). Arrows indicate tight junctions.

(**a**) Active phospho-PKCι/ζ colocalises with the tight junction marker ZO-1, (**b**) Total PKCι/ζ colocalises with the tight junction marker ZO-1, (**c**) PKCζ localises at the same position as the phospho-PKCι/ζ and total PKCι/ζ antibodies, (**d**) PKCι localises at the same position as the phospho-PKCι/ζ and total PKCι/ζ antibodies.

3.3.2 Nuclear Localisation of PKCι and PKCζ in MDCK Cells

Previous research has indicated that PKCι/ζ localises to the nucleus (see section 3.1.3), but none of these studies have been undertaken in MDCK cells. To establish if MDCK cells had nuclear PKCι or PKCζ, the MDCK cells were stained for each of the PKCι/ζ antibodies and γ-tubulin. No clear nuclear localisation could be seen with any of the PKCι/ζ antibodies (figure 3.2). There was also possible nuclear exclusion seen with the total PKCι/ζ and phospho-PKCι/ζ, but this was not clearly seen with the PKCι and PKCζ antibodies.

3.3.3 PKCι and PKCζ Localisation Alters Dramatically during the Cell Cycle

PKCι/ζ has previously been shown to be on the mitotic apparatus in a few different cell types (see section 3.1.4). However, it has not been shown for MDCK cells so it was decided to stain MDCK cells during different stages of the cell cycle to clarify where, PKCι, PKCζ and active phospho-PKCι/ζ localise. A schematic diagram of the cell cycle is pictured in figure 3.2 to provide a visual representation of the cell cycle.

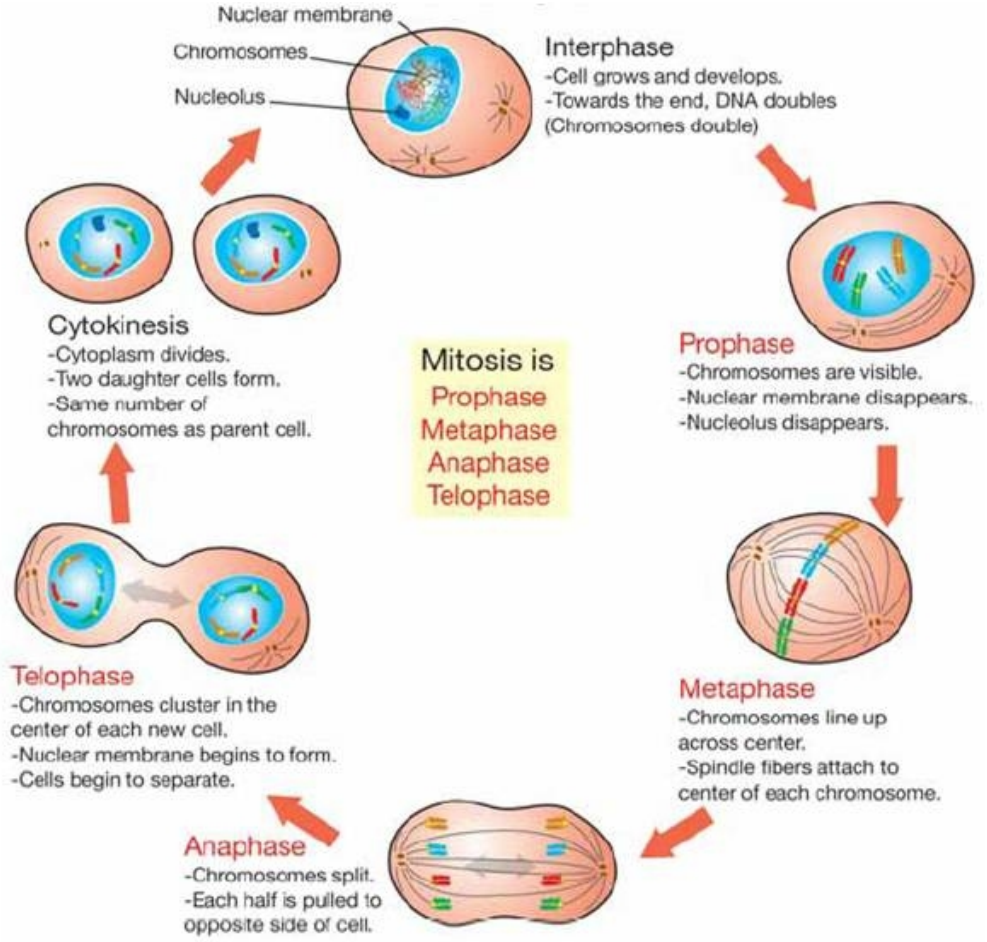

Figure 3.2 The Cell Cycle
A schematic diagram of the cell cycle obtained from 'Cell Biology' www2.mbusd.org/staff/pware/cells on 16/01/11

In the following images (figures 3.3-3.7) the PKCι/ζ antibodies stain the tight junctions as in figure 3.1, but in many cases the tight junctions cannot be seen as the focal plane is at the level of the centrosomes not the tight junctions.

During interphase and prophase all the PKCι/ζ antibodies are localised throughout the cell including cytoplasm and were enriched at the tight junctions (figure 3.3 yellow arrows indicate interphase centrosomes and white arrows indicate prophase centrosomes. Data not shown for tight junctions).

At metaphase the localisation of PKCι and PKCζ changes dramatically (figure 3.4); active phospho-PKCι/ζ staining is stronger and can be seen on the centrosomes from prometaphase onwards (figure 3.4a). The total PKCι/ζ at metaphase has staining on the spindle microtubules and a small amount of staining on the centrosomes (figure 3.4b), however the total cell staining is not as bright as the phospho-PKCι/ζ. The PKCζ staining does not locate directly to the centrosomes (figure 3.4c); however the antibody does stain

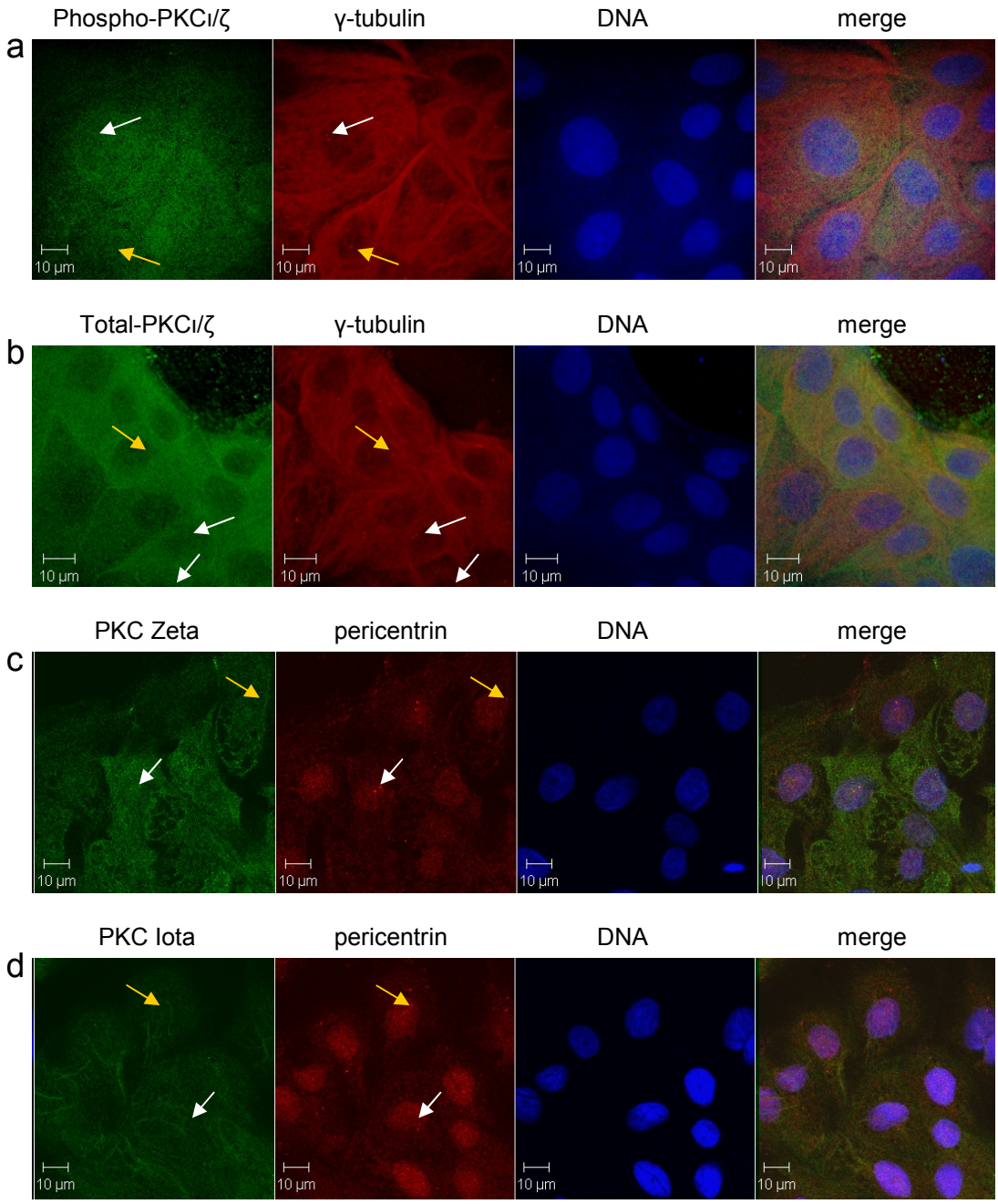

Figure 3.3 PKCι/ζ Localisation during Interphase and Prophase

MDCK cells stained with PKCι/ζ antibodies (green), and γ-tubulin (phospho-PKCι/ζ and total PKCι/ζ) or pericentrin (PKCι and PKCζ) to show the centrosomes (red). The nucleus was stained with TOPRO-3 (blue). Cells were visualised using confocal microscopy. Yellow arrows indicate interphase centrosomes and white arrows indicate prophase centrosomes.

At interphase and prophase there is no nuclear enrichment of PKCι or PKCζ. There may be some nuclear exclusion of total PKCι/ζ.

(**a**) Active phospho-PKCι/ζ, (**b**) Total PKCι/ζ, (**c**) PKCζ, (**d**) PKCι

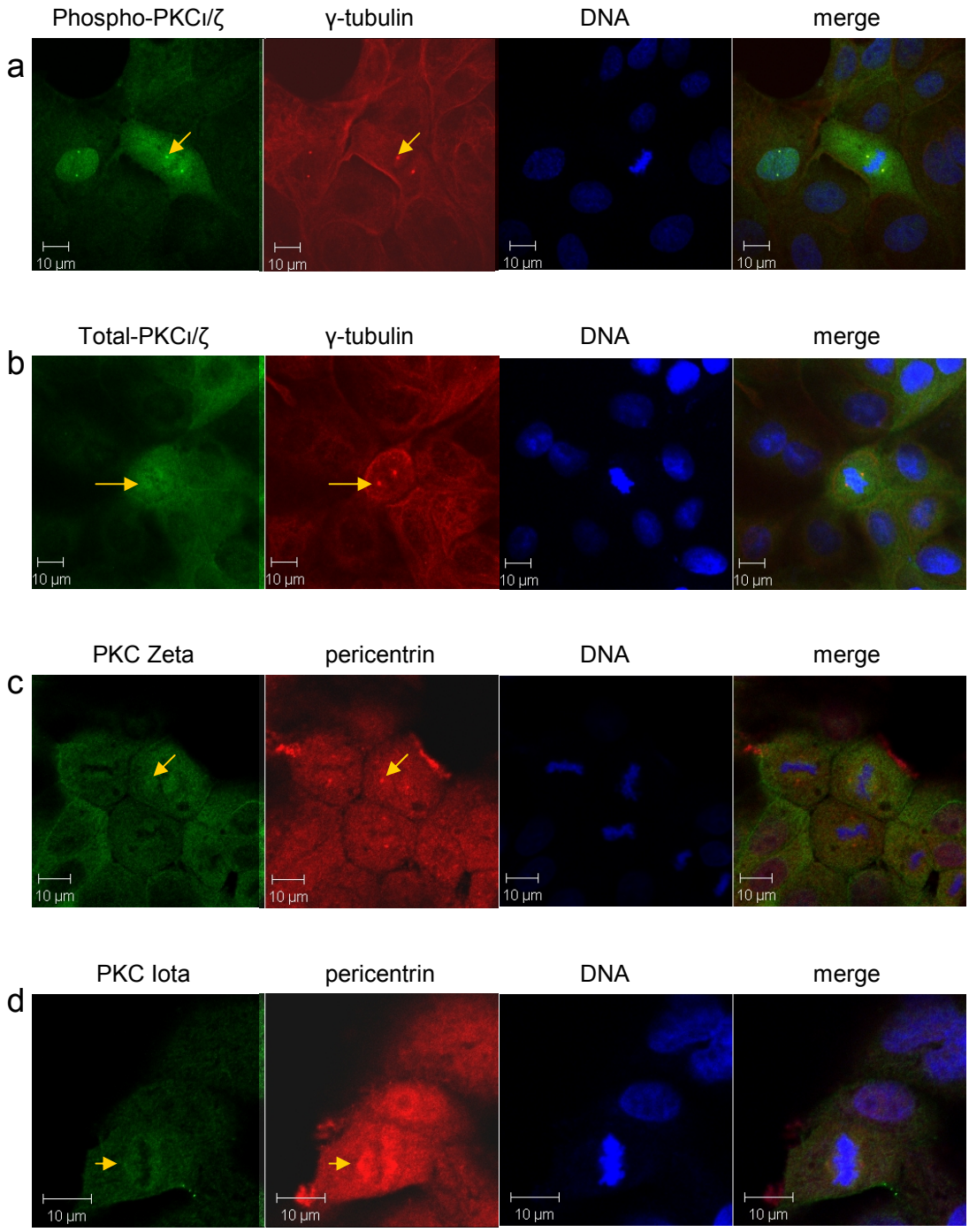

Figure 3.4 PKCι/ζ Localisation during Metaphase

MDCK cells stained with PKCι/ζ antibodies (green), and γ-tubulin (phospho-PKCι/ζ and total PKCι/ζ) or pericentrin (PKCι and PKCζ) to show the centrosomes (red). The nucleus was stained with TOPRO-3 (blue). Cells were visualised using confocal microscopy. (**a**) Phospho-PKCι/ζ staining is bright with a concentration on the centrosomes and spindle microtubules, (**b**) Total PKCι/ζ staining is found on the spindle microtubules, (**c**) PKCζ staining is found on the spindle microtubules, (**d**) PKCι staining is found on the centrosome and mitotic spindle.

the spindle microtubules. There is PKCι staining at the centrosomes indicating that PKCι locates to the centrosomes and combined with the phospho-PKCι/ζ staining, is phosphorylated there (figure 3.4d). All the antibodies stain the mitotic spindle. Therefore, PKCι and PKCζ are found on the spindle microtubules and active phosphorylated PKCι on the centrosomes.

During anaphase, the active phospho-PKCι/ζ can still clearly be seen at the centrosomes and is now on the midbody microtubules (figure 3.5a). The total PKCι/ζ antibody stains the midbody microtubules, but little staining is seen on the centrosomes (figure 3.5b). The PKCζ antibody shows strong midbody microtubule staining (figure 3.5c). The PKCι staining becomes much weaker, in comparison to the metaphase staining, although it is still brighter than the staining in the cells surrounding it which are not dividing, however there is not clear spindle or centrosomal staining (figure 3.5d).

During telophase, active phospho-PKCι/ζ retains its binding to the midbody microtubules and the centrosomes (figure 3.6a). The total PKCι/ζ antibody shows midbody microtubule staining (figure 3.5b). The PKCζ antibodies also show midbody microtubule staining (figure 3.6c). The PKCι staining returns to basal levels during telophase with no staining on the mitotic apparatus (figure 3.6d). So PKCι/ζ is still active at the centrosomes at telophase, however, it is difficult to tell which of the two isoforms it is due to neither of the antibodies showing clear centrosomal staining.

To summarise, active phosphorylated PKCι/ζ is found at the centrosomes and spindle/midbody microtubules throughout metaphase, anaphase and telophase. From the metaphase staining it appears to be PKCι on the centrosomes, however, no staining for PKCι can be found on the centrosomes later on in mitosis. PKCζ locates to the spindle microtubules during metaphase and on the midbody microtubules later on in mitosis and could be phosphorylated at the centrosome. Therefore PKCι and PKCζ may both have a role in regulating mitosis and could have centrosomal phosphorylation targets.

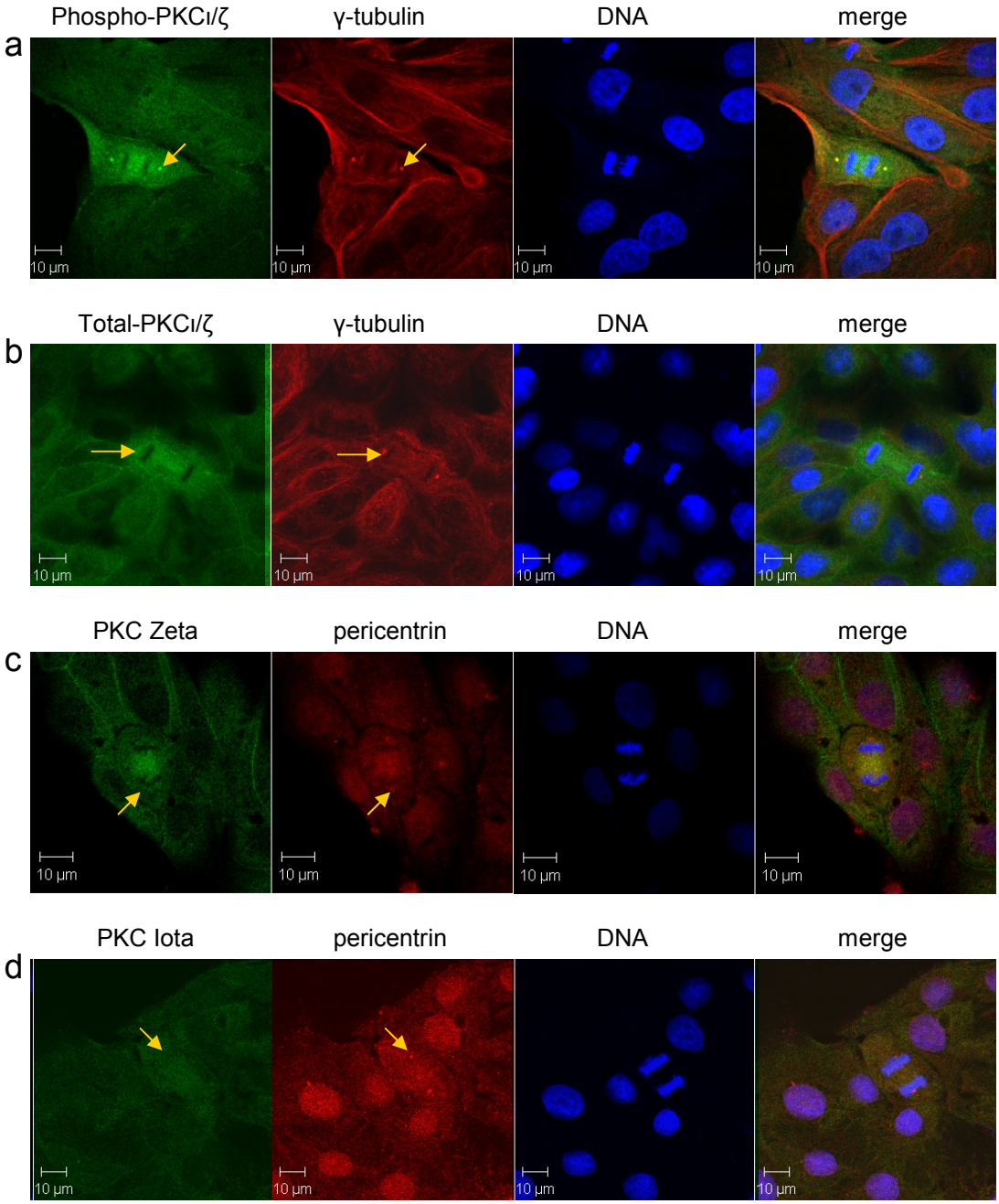

Figure 3.5 PKCι/ζ Localisation during Anaphase

MDCK cells stained with PKCι/ζ antibodies (green), and γ-tubulin (phospho-PKCι/ζ and total PKCι/ζ) or pericentrin (PKCι and PKCζ) to show the centrosomes (red). The nucleus was stained with TOPRO-3 (blue). Cells were visualised using confocal microscopy. (**a**) Phospho-PKCι/ζ staining is bright with a concentration on the centrosomes, spindle and midbody microtubules, (**b**) Total PKCι/ζ staining is found on the spindle and midbody microtubules, (**c**) PKCζ staining is found on the spindle and midbody microtubules, (**d**) PKCι staining is much weaker and stains no particular part of the mitotic apparatus, but is brighter in the cell in anaphase than the cells surrounding it.

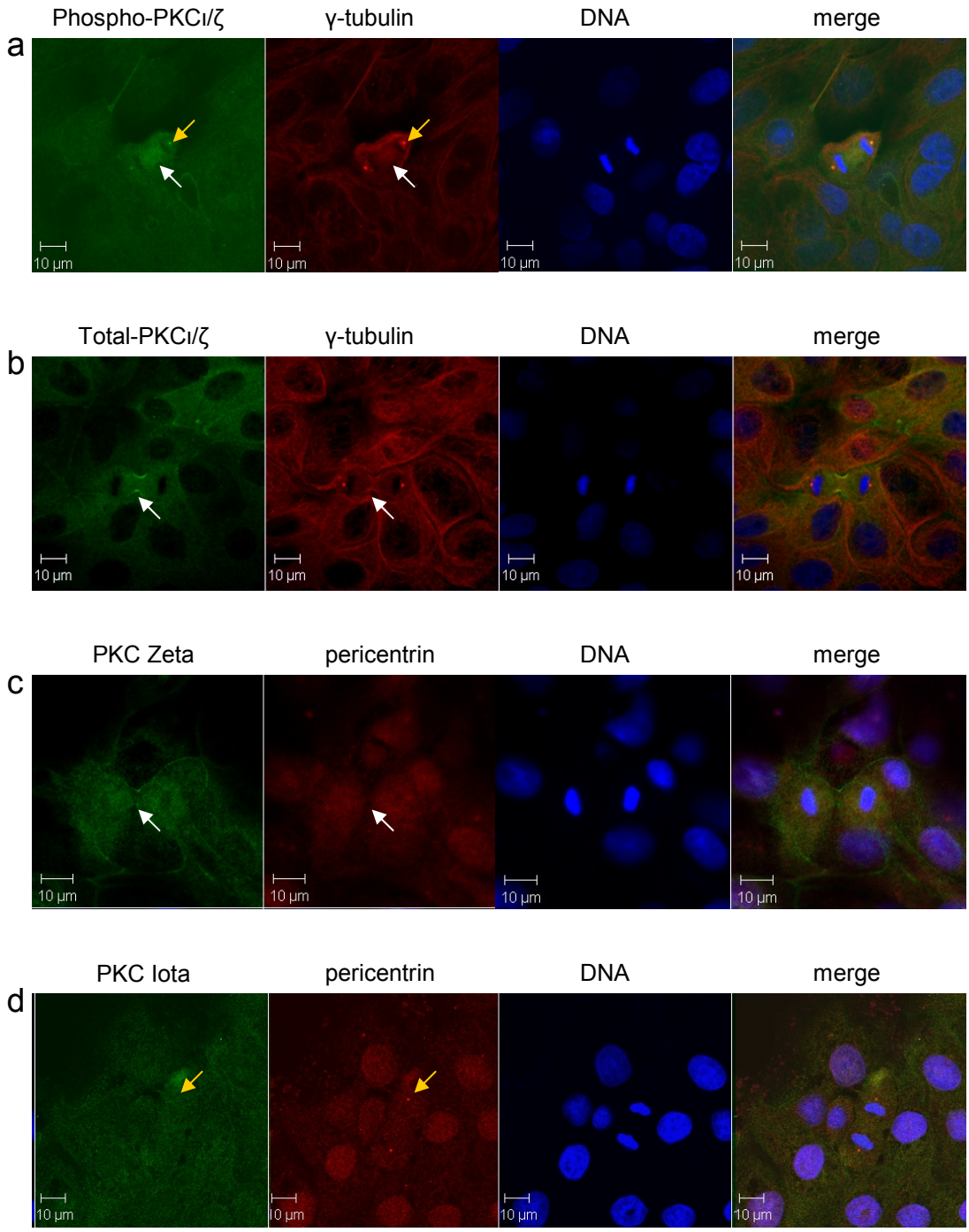

Figure 3.6 PKCι/ζ Localisation during Telophase

MDCK cells stained with PKCι/ζ antibodies (green), and γ-tubulin (phospho-PKCι/ζ and total PKCι/ζ) or pericentrin (PKCι and PKCζ) to show the centrosomes (red). The nucleus was stained with TOPRO-3 (blue). Cells were visualised using confocal microscopy. (**a**) Phospho-PKCι/ζ staining is bright with a concentration on the centrosomes, spindle and midbody microtubules, (**b**) Total PKCι/ζ staining is found on the midbody microtubules, (**c**) PKCζ staining is found on the midbody microtubules, (**d**) PKCι staining is back to basal levels with no staining on the mitotic apparatus.

3.3.4 PKCι and PKCζ Localisation during Metaphase in Caco2 Cells

To ensure that the mitotic staining that had been seen was not an artefact of MDCK cells, the human colorectal adenocarcinoma epithelial cell line, Caco2 was stained in the same way as the MDCK cells (figure 3.7). The staining at metaphase was almost identical to the MDCK staining in figure 3.5, however, The PKCι and PKCζ staining was a lot stronger at the centrosomes of Caco2 cells than on the centrosomes of MDCK cells. The active phospho-PKCι/ζ antibody strongly stained the centrosomes and spindle microtubules (figure 3.7a). The total PKCι/ζ antibody stains the spindle microtubules, but there is no clear centrosomal staining (figure 3.7b). The PKCζ antibody localises to the centrosomes and the spindle microtubules (figure 3.7c). The PKCι antibody stains the centrosomes very strongly with weaker staining on the spindle microtubules (figure 3.7c).

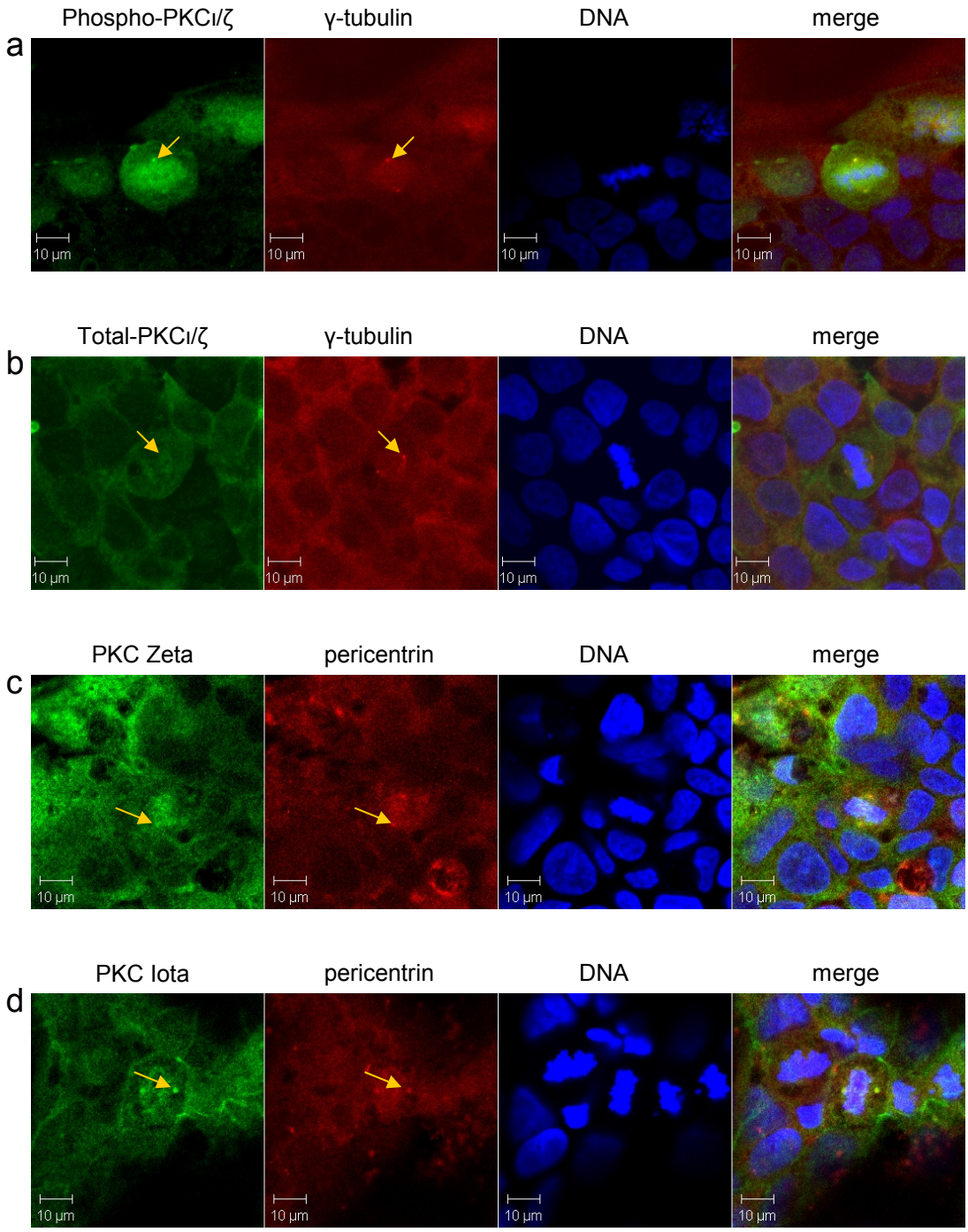

Figure 3.7 PKC Localisation during Metaphase in Caco2 Cells

Caco2 cells stained with PKCι/ζ antibodies (green) and γ-tubulin (phospho-PKCι/ζ and total PKCι/ζ) or pericentrin (PKCι and PKCζ) to show the centrosomes (red). Nucleus stained with TOPRO-3 (blue). Cells were visualised using confocal microscopy. (**a**) Active phospho-PKCι/ζ staining can be seen on the spindle microtubules and the centrosomes, (**b**) Total atypical PKCι/ζ staining can be seen on the spindle microtubules, (**c**) PKCζ staining can be seen on the spindle microtubules and the centrosomes, (**d**) PKCι staining can be seen on the spindle microtubules and the centrosomes.

3.3.5 Active Phosphorylated PKCι/ζ is found at the Centrosomes in Metaphase in other Human Cell Lines

The mitotic data from MDCK and Caco2 cells suggests that the localisation of PKCι/ζ to the mitotic apparatus may be found in many different types of epithelial cells. To confirm the hypothesis the active phosphorylated PKCι/ζ antibody was used. Ovcar-3, the human ovarian carcinoma cell line, HeLa, the human epithelial cervical cancer cell line and the A549 adenocarcinomic human alveolar basal epithelial cell line were stained for active phospho-PKCι/ζ (figure 3.8). The cell lines all showed strong centrosomal staining with the A549 cells having particularly clear centrosomal staining. The Ovcar-3 and HeLa cells also had spindle microtubule staining, but the A549 cells did not. This confirms that phosphorylated PKCι/ζ is found on the spindle and centrosome in a wide range of epithelial cells.

3.3.6 Phosphorylation of PKCι and PKCζ is Increased during Mitosis

The immunofluorescence data in figures 3.4 to 3.7 predicts that phospho-PKCι/ζ and perhaps the individual PKCι and PKCζ proteins are upregulated during mitosis. To confirm if the PKCι and/or PKCζ proteins or the phosphorylation was being up-regulated during mitosis, cells were treated with Nocodazole to produce large numbers of mitotic cells (Zieve et al., 1980) by depolymerising microtubules and causing the cells to arrest in mitosis. DMSO was used as a control because Nocodazole is dissolved in DMSO. The Nocodazole and DMSO treated cells were stained for active phospho-PKCι/ζ and γ-tubulin to act as a positive control and confirm the increase in mitotic cells (figure 3.9 a and b).

The Nocodazole and DMSO treated cells were lysed and subjected to Western blotting with each PKCι/ζ antibody type and α-tubulin as a loading control (figure 3.9 c). The antibodies for total PKCι/ζ, PKCι and PKCζ show similar amounts of protein whether treated with Nocodazole or DMSO, so during mitosis the total amount of each atypical PKC isoform is kept constant. However, the active phospho-PKCι/ζ antibody showed up-regulation when treated with Nocodazole in comparison to DMSO. Therefore, the phosphorylation of either or both atypical PKC isoforms increases during mitosis, but the actual amount of protein is kept at similar levels. This suggests that the activity of PKCι/ζ is increased during mitosis.

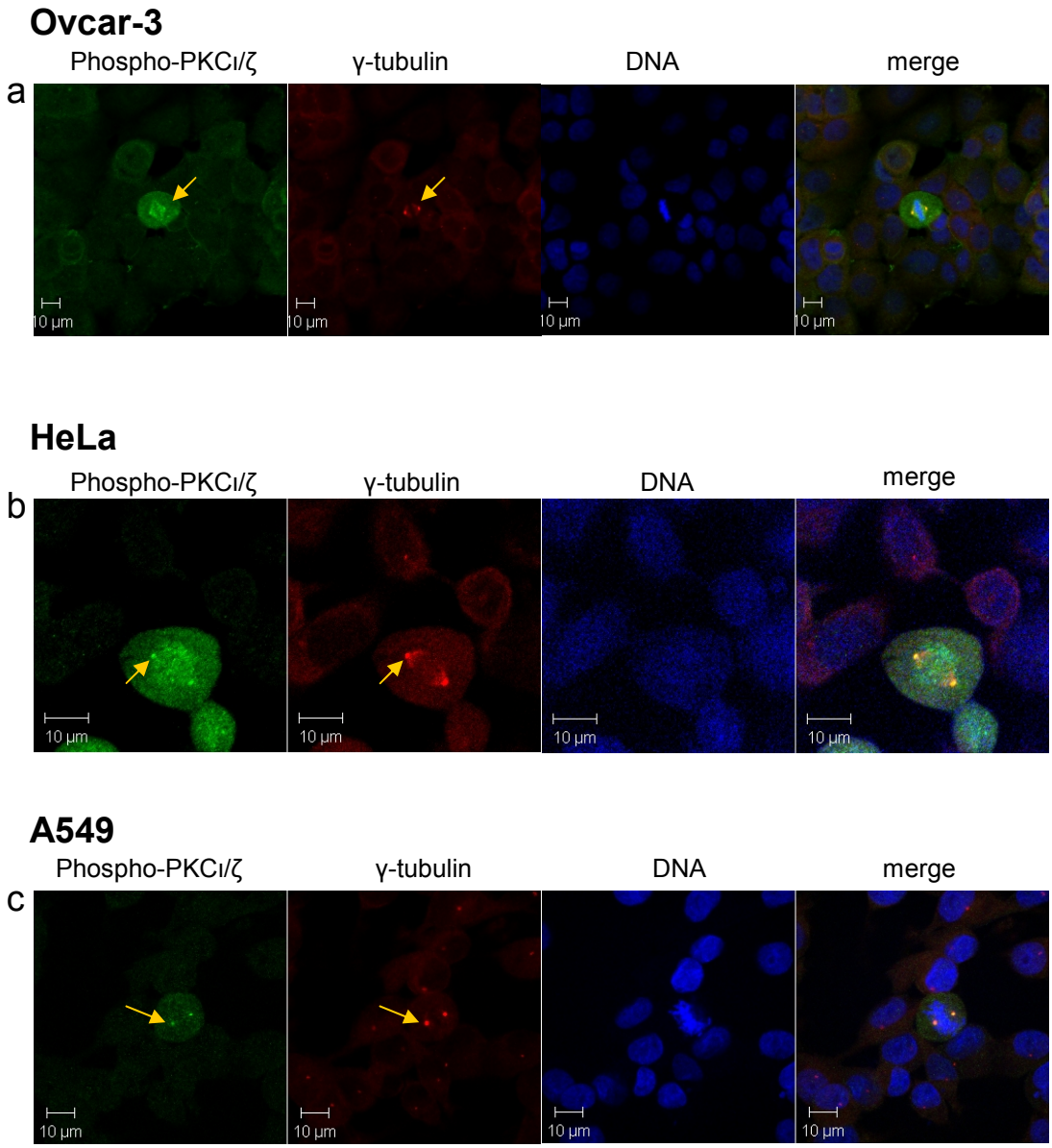

Figure 3.8 Active Phosphorylated PKCι/ζ is found at the Centrosomes in Diverse Epithelial Human Cell Lines

Cell lines were stained with active phospho-PKCι/ζ antibody (green) and γ-tubulin to show the centrosomes (red). The nucleus was stained with TOPRO-3 (blue). Cells were imaged using confocal microscopy.

(**a**) Ovcar-3 cells show strong centrosomal and spindle microtubule phospho-PKCι/ζ staining, (**b**) HeLa cells show strong centrosomal and spindle microtubule phospho-PKCι/ζ staining, (**c**) A549 cells show strong centrosomal but little spindle microtubule phospho-PKCι/ζ staining.

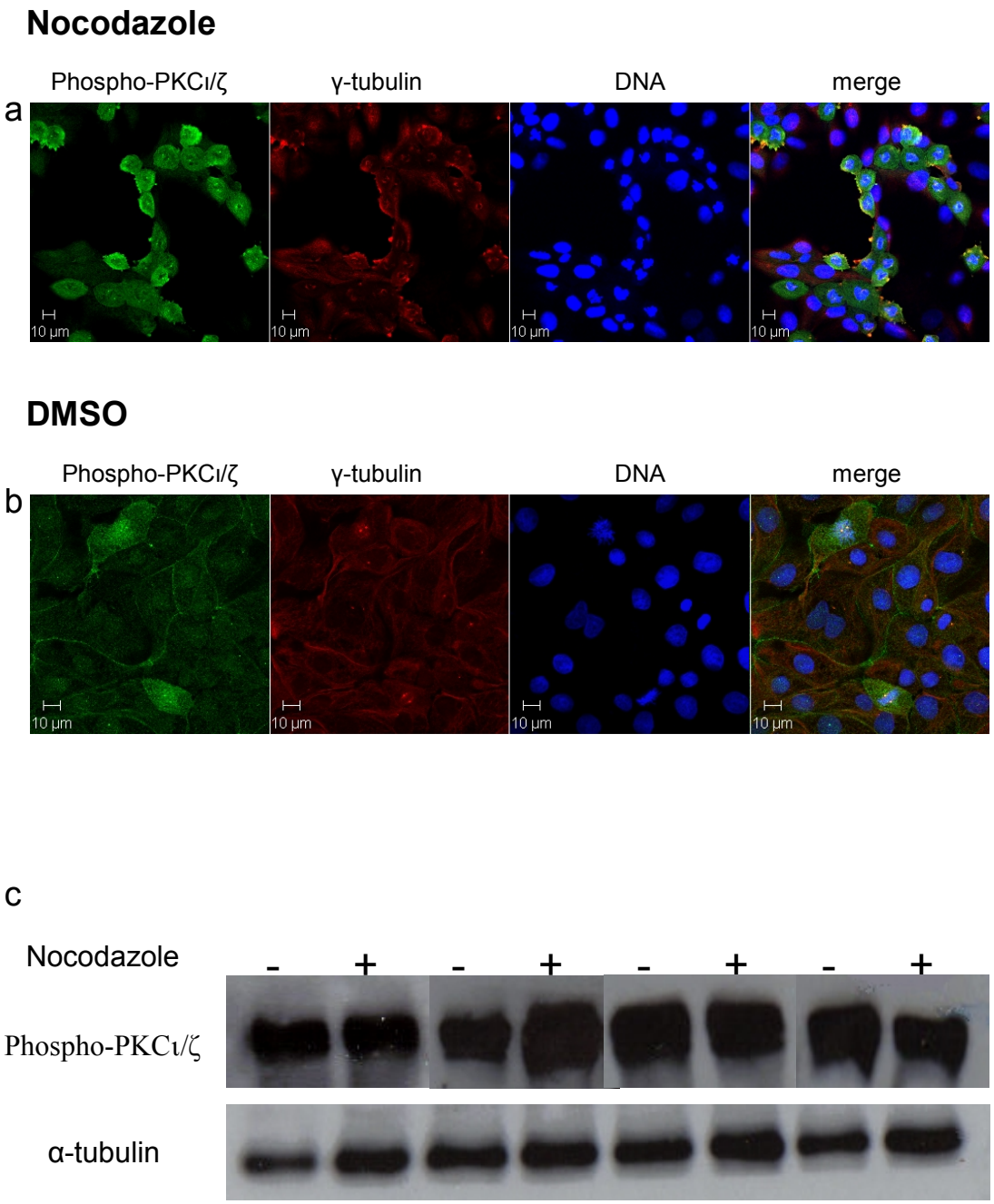

Figure 3.9 Active Phosphorylated PKCι/ζ is Upregulated during Mitosis

MDCK cells were treated with Nocodazole or DMSO and stained with active phospho-PKCι/ζ antibodies (green) and γ-tubulin to show the centrosomes (red). Nucleus stained with TOPRO-3 (blue). Cells were visualised using confocal microscopy. Cell lysates from the Nocodazole and DMSO treated cells were subjected to Western blotting using the PKC antibodies and α-tubulin as a control. This experiment was repeated three times.

(**a**) Cells treated with Nocodazole show high numbers of mitotic cells, (**b**) Cells treated with DMSO show few cells in mitosis, (**c**) The cells were lysed and subjected to Western blotting using the PKC antibodies and α-tubulin loading as a control.

3.4 Discussion

3.4.1 Tight Junction Localisation

In figure 3.1 it has been shown that the atypical PKC antibodies localise to the tight junctions, confirming previous data (Izumi et al., 1998; Nunbhakdi-Craig et al., 2002). The PKCζ antibody (figure 3.1 c) seems to bind the tight junctions more than the PKCι antibody as the PKCι (figure 3.1 d) staining is less pronounced or specific for the tight junctions. This could suggest that there is more PKCζ at the tight junctions or that the PKCζ is a better antibody in MDCK cells than the PKCι antibody. To test this more PKCι and PKCζ specific antibodies could be tested, especially those that have been raised against canine PKCι and PKCζ.

3.4.2 Nuclear Localisation

The nuclear localisation of PKCι/ζ was also investigated (figure 3.3). No clear nuclear staining was visualised, however, this is in resting cells. PKCι/ζ has been reported to shuttle in and out of the nucleus (Perander et al., 2001), so the amount of PKCι or PKCζ in the nucleus at any one time could be quite small and difficult to detect. To determine if either atypical PKC isoform localises to the nucleus, the MDCK cells could be treated with Leptomycin B, which prevents nuclear export. PKCι or PKCζ would then accumulate in the nucleus and would be easily visualised using antibody staining.

3.4.3 Cell Cycle Localisation

There are a number of results that can be inferred from figures 3.3-3.6, firstly, active phospho-PKCι/ζ localises to the centrosomes, spindle and midbody microtubules during metaphase, anaphase and telophase. The total PKCι/ζ localises to the spindle and midbody microtubules during metaphase, anaphase and telophase. PKCζ also localises to the spindle and midbody microtubules during metaphase, anaphase and telophase, but little staining is seen on the centrosomes. PKCι localises to the centrosomes and spindle microtubules during metaphase, however, in anaphase and telophase the staining is reduced. The PKCι staining is in contrast to the Caco2 staining, which shows clear PKCι at the centrosomes (figure 3.7d). The PKCζ staining in the Caco2 cells is also more pronounced at the centrosomes of the Caco2 cells than the MDCK cells (figure 3.7c). This discrepancy could be due to the antibodies not being raised against canine PKCι and

PKCζ. The PKCι and PKCζ antibodies may much more readily bind human PKCι/ζ than canine. To confirm this, a Western blot with the same amount of PKCι/ζ protein, from different species, could be utilised to demonstrate whether there is weaker binding to the canine PKCι/ζ than other species of PKCι/ζ. Future work would also include obtaining an antibody, specific for PKCι that does recognise the canine PKCι and using it to confirm that PKCι does localise to the centrosomes during mitosis. Another possibility is that there is actually more PKCι/ζ at the centrosomes in Caco2 cells as Caco2 cells are a cancer derived cell line and PKCι/ζ is upregulated during cancer. To determine if this is the case, the study could be extended to look in more cell lines derived from both cancer cells and normal cells to determine if there are any differences in the amount of PKCι or PKCζ at the centrosomes.

Liu and colleagues showed PKCι/ζ staining at the mitotic spindle in HeLa cells and phospho-PKCι/ζ staining at the centrosomes in metaphase, but not anaphase or telophase (Liu et al., 2006). The slight differences seen in the staining at the centrosomes in anaphase and telophase may be due to different antibodies being used. In their paper the antibody used for PKCι/ζ is the same as the one used in this work for total PKCι/ζ however, the phospho-PKCι/ζ antibody is different to the one used in this work, but does recognise both isoforms of phospho-PKCι/ζ. The phospho-PKCι/ζ antibody may not bind phospho-PKCι/ζ as well at the one we used. To test this HeLa cells could be stained with the phospho-PKCι/ζ antibody used in this work and the phospho-PKCι/ζ antibody used by Liu and colleagues, through all stages of the cell cycle. If only the phospho-PKCι/ζ antibody used in this work binds the mitotic apparatus throughout cell division, it would confirm that the differences in staining are due to the specificity of the antibodies.

Localisation and Western blotting data suggest that both PKCι and PKCζ are likely to be activated during mitosis. To determine which PKCι/ζ isoform is activated, cells can be arrested in metaphase using Nocodazole and the phospho-PKCι/ζ used to immunoprecipitate the active PKCι/ζ. This could then be subjected to Western blotting with the PKCι and PKCζ antibodies to see which one is more prevalent in mitosis. From the immunofluorescence data, especially the Caco2 images (figure 3.8) it would be expected that both are found at the centrosomes, but PKCι may be more prevalent as it is much brighter in the Caco2 images.

Active phospho-PKCι/ζ is found at the centrosomes in metaphase in a variety of epithelial cells (figure 3.8) which suggests a key role in mitosis; however in this study only epithelial cells have been tested. It will be interesting to test non-epithelial cell lines such a blood cells or fibroblasts to determine whether PKCι/ζ is active at the centrosomes in all cells.

In figure 3.9 it was shown that it is the threonine 410 (T410) activating phosphorylation of the atypical PKCs that is increased in mitosis, not the protein levels. Phosphorylation of PKCι/ζ on T410 is autophosphorylation and indicates that PKCι/ζ is active. PKCι and PKCζ are therefore they are likely to be translocated to the centrosomes and spindle microtubules early on in mitosis and phosphorylated there. T410 phosphorylation indicates active atypical PKC therefore they are active on the centrosomes and the spindle microtubules. Further work is required to elucidate what activates PKCι at the centrosomes and spindle microtubules. Cdc42 activates PKCι/ζ by releasing the inhibitory affect on PKCι/ζ by Par-6 and Cdc42 is found near the centrosomes in MDCK cells (Rodriguez-Fraticelli et al., 2010), so it is likely that PKCι/ζ is being activated by Cdc42 at the centrosomes. To test this Cdc42 can be knocked down and if no PKCι/ζ autophosphorylation at the centrosomes occurs, then Cdc42 is responsible for the PKCι/ζ activation at the centrosomes and spindle microtubules.

PKCι/ζ can cause the phosphorylation of GSK3β on serine 9, inactivating GSK3β (Etienne-Manneville and Hall, 2003a). GSK3β is also found on the centrosomes and spindle microtubules during mitosis (Bobinnec et al., 2006; Wakefield et al., 2003) and is inactive at the centrosomes at this time (Wakefield et al., 2003). It is plausible that PKCι/ζ is responsible for the GSK3β phosphorylation and inactivation at the centrosomes. To test this PKCι/ζ can be knocked down and if no GSK3β phosphorylation occurs then it is very likely that PKCι/ζ is responsible for the phosphorylation.

In summary, there are two sites of PKCι/ζ localisation and activation; the tight junctions and mitotic apparatus and potentially the nucleus. The following chapters will consider potential phosphorylation targets at these sites.

Chapter 4

Establishing a Method to Identify Proteins Phosphorylated by PKCι

4.1 Introduction

The aim of the project is to find novel PKCι phosphorylation targets, so a method was needed to test potential candidates. There are many different ways of finding and verifying kinase targets (Johnson and Hunter, 2005). In this chapter the aim is to establish a method to determine whether a potential candidate is an actual PKCι phosphorylation target.

4.1.1 Phosphorylation Prediction Methods

One way of identifying targets is to use computer based prediction programs. The four main web tools are Scansite (http://scansite.mit.edu/), PhosphoELM (http://phospho.elm.eu.org/), NetPhos (http://www.cbs.dtu.dk/services/NetPhos/) and Human protein Reference Database HPRD (http://www.hprd.org/).

Scansite, PhosphoELM and NetPhos all use algorithms to predict kinase phosphorylation sites. However, publishers retain the copyright information about the algorithms, so exact details are not known, the details known are described below.

Scansite uses an algorithm based on a Position Specific Scoring Matrix (PSSM) (Obenauer et al., 2003). A PSSM compares known phosphorylation sites from experimental data, for one kinase and scores which amino acids are strongly favoured or strongly disliked either side of the phosphorylation site. On the basis of this an algorithm can be written to scan a protein sequence to find predicted phosphorylation sites.

PhosphoELM uses an algorithm based on a manual phospho-protein database, made up of high throughput data sets from the published literature (Diella et al., 2008). From these data sets they have written an algorithm to predict phosphorylation sites in a substrate for a given kinase.

NetPhos uses an artificial neural network method to predict protein phosphorylation (Blom et al., 1999). Like PhosphoELM, the network is based on large data sets from the published literature. Within the network both the protein sequence and the structure are used, when available. The structural data should make the prediction more accurate as the protein folding around a phosphorylation site can be important for recognition by a kinase.

The HPRD is different from the other search method. It does not use an algorithm, instead it reports the presence of kinase motifs found in the literature (Amanchy et al., 2007). The database is manually updated from the literature.

The advantages of using the above online tools are that they are quick and easy to use and a large number of proteins can be rapidly tested. A disadvantage is that they are not completely accurate (see section 4.2).

4.1.2 *In vitro* Methods for Determining PKCι Phosphorylation

An alternative to computer based prediction programs is to carry out *in vitro* kinase assays to test a potential kinase substrate. The main way of showing a protein is phosphorylated *in vitro* is to use the purified substrate mixed with the purified kinase and radio-labelled ATP^{32}. The P^{32} is incorporated into the substrate and can be viewed via autoradiography. Lgl was shown to be phosphorylated by PKCι using an Lgl-GST fusion protein, that had been expressed in bacteria, and commercially available purified PKCι. (Betschinger et al., 2003). Par-1b was shown to be phosphorylated in a slightly different way, the Par-1b was a GST fusion protein, but the PKCι was flag tagged and produced in Hek293 cells (Hurov et al., 2004). Both papers mentioned above went on to show *in vivo* PKCι phosphorylation. The advantage with this method is that it is relatively quick, although slower than the prediction programs. However the disadvantages are that it requires radioactivity and that kinases may be able to phosphorylate a substrate *in vitro*, but the phosphorylation may not occur *in vivo*. This means that a phosphorylation site identified *in vitro* needs to be confirmed *in vivo*.

Another *in vitro* method is KESTREL (kinase substrate tracking and elucidation) (Cohen and Knebel, 2006). Hela cell extracts are depleted of ATP, and a high concentration of kinase plus radio-labelled ATP added. The cell extract is then separated by electrophoresis and phosphorylation viewed using autoradiography. Phosphorylated proteins can then be purified and identified using mass spectrometry. This method was used to demonstrate the phosphorylation of PAPK4/p38δ by eEF2 kinase (Knebel et al., 2001). The advantages of this method are that it tests all the proteins in a cell and is relatively quick to carry out. The disadvantages are that it requires radioactivity and that it may yield proteins that can be phosphorylated by a kinase, but are not normally as they are sequestered in different parts of the cell.

Another *in vitro* phosphorylation method is the screening of expression libraries. A cDNA library can be constructed with each cDNA tagged to GST. The GST-fusion proteins are then expressed in E.coli by bacteria phage and then transferred to a nitrocellulose membrane. The kinase of interest and radiolabelled ATP are added to the membrane and then removed by washing. Phosphorylation can be visualised by autoradiography to see which plaques were phosphorylated by the kinase. The cDNA in the phosphorylated plaque can then be sequenced to find which protein was expressed and phosphorylated by the kinase of interest. This method was used to determine the phosphorylation of MNK1 by ERK MAP kinase (Fukunaga and Hunter, 1997). The advantage of this method is that it is a random unbiased screen; however, the disadvantage with the approach is that you might identify a target in a biological process you are not interested in.

4.1.3 *In vivo* Methods for Determining PKCι Phosphorylation

There are numerous ways of showing that a protein is phosphorylated *in vivo*. A kinase can be inhibited or knocked down using siRNA and a reduction in the amount of phosphorylation of the protein of interest can indicate phosphorylation by that particular kinase. The phosphorylation can be visualised using a phospho specific antibodies, particular for the substrate of interest, on a Western blot. This method was used to show PKCι phosphorylation of GSK3β (Etienne-Manneville and Hall, 2003a) and Lgl (Betschinger et al., 2003). The advantages of this method are that it is *in vivo* and quick to carry out. The disadvantage is that it may not show direct phosphorylation, the kinase may phosphorylate another kinase causing it to phosphorylate the protein of interest. Another disadvantage is that you need phospho-specific antibodies which are expensive and time consuming to make.

A more direct method of showing *in vivo* protein phosphorylation is to overexpress both proteins at the same time in the same cell and then assess for phosphorylation. This method was used to show the phosphorylation of FoxG1 by CKIδ (Regad et al., 2007). *Xenopus* embryos were co-injected with RNA for GFP tagged CKIδ and GFP-FoxG1, the embryos then expressed the proteins and phosphorylation occurred. The GFP-FoxG1 was immunoprecipitated and the phosphorylation visualised by Western blotting using a pan phosphoserine antibody. The advantages of this method are that it is quick to undertake, is *in vivo* and probably direct between the kinase and the substrate due to overexpression.

The disadvantage is that over expressing two proteins may not mimic the true situation and phosphorylation that would not normally occur due to spatial differences of the protein within the cell may occur with this method.

Chen and colleagues showed the phosphorylation of adducin by transfecting cells with wild type (WT) and kinase dead (KD) novel PKC. The authors showed that adducin phosphorylation was increased in the cells transfected with WT but not those transfected with KD novel PKC the phosphorylation was visualised using a phospho-specific antibody (Chen et al., 2007). The advantages of this method are that it is *in vivo* and does not require radioactivity. The disadvantage is that the kinase is overexpressed and may cause the phosphorylation of proteins it would not normally have contact with and that it is may not be direct; the kinase may phosphorylate another kinase causing it to phosphorylate the protein of interest.

A particularly clever *in vivo* phosphorylation assay involves mutation of the ATP binding pocket of the kinase so that it preferentially binds a radio-labelled analogue of ATP that cannot be bound by other kinases. The DNA for the mutated kinase is transfected into cells, expressed and the radiolabelled ATP analogue added. The cell extract is then separated by electrophoresis and visualised using autoradiography and the substrates identified using mass spectrometry. This technique was used to discover phosphorylation of Cofilin and Dok-1 by v-Src (Shah and Shokat, 2002). The advantages of this method are that it is *in vivo* and quick once the kinase mutant has been made. However, the disadvantage can be that it may take a long time to make the kinase mutant. Another disadvantage is that the kinase is over expressed; therefore, it may phosphorylate proteins it wouldn't usually have contact with. As with all the *in vitro* methods, to show that the phosphorylation seen *in vivo* is direct an *in vitro* kinase assay needs to be carried out.

A candidate approach was chosen to enable the project to focus on proteins of interest rather than the many proteins that can be found using a screening program such as KESTREL. The project was started by testing phospho-prediction programs.

4.2 Results

4.2.1 Testing Phosphorylation Prediction Methods

The aim of the project was to test a large number of candidates that could be phosphorylated by PKCι, the available phosphorylation prediction tools on the web were tested first.

To test the reliability of these prediction methods four known PKCι targets were chosen and assessed using the online tools. The four substrates chosen were Lgl, Par-1b, GSK3β and Numb. Mouse Lgl is phosphorylated by PKCι on five serines, S654, 658, 662, 669 and 672 (Plant et al., 2003). Human Par-1b is phosphorylated by PKCι on one threonine, T595 (Hurov et al., 2004). Rat GSK3β is phosphorylated by PKCι on one serine, S9 (Etienne-Manneville and Hall, 2003a). Human Numb is phosphorylated by PKCι on two serines, S7 and 295 (Smith et al., 2007). The results of these proteins when inputted into the prediction tools are shown in table 3.1

WEB BASED TOOLS				
Known Target	Scansite ZETA	Phospho ELM	NetPhos	HPRD
Lgl	✓A	✗	✗	✗
Par-1b	✗	✗	✗	✗
GSK3β	✗	✗	✗	✗
Numb	✓B	✗	✓	✓

Table 4.1 Results from the Four Phosphorylation Prediction Tools on Four Known PKCι Substrates

(A) denotes only four of the five known sites predicted. The accession numbers for the proteins are in the methods. (B) denotes only one of the two known sites predicted.

When comparing the web based tools with known results Scansite correctly predicted some of the residues found in Lgl and Numb, but not all of them. It did not predict the correct sites for Par-1b or GSK3β. PhosphoELM was unable to predict any of the known PKCι phosphorylation sites even though they state that they use published data.

It is likely that they have used only limited data and not the data from the known targets we are using. NetPhos shows total PKC phosphorylation not the individual PKC family members, so the results are limited. Netphos correctly predicted all the known residues phosphorylated by PKC on Numb, but failed to predict any of the other residues in the other three known PKCι targets; Lgl, Par-1b and GSK3β. The PhosphoELM was unable to predict the phosphorylation of Lgl, Par1b or GSK3β, but it did correctly predict the phosphorylation of Numb. However, all of the tools incorrectly predicted other sites, apart from HPRD which only lists substrates known for the particular kinase. For Lgl and Par-1b the published data proves that the sites predicted are false positives. Plant and colleagues created recombinant fusion proteins that spanned the length of Lgl (Plant et al., 2003). Only two of these fusion proteins, corresponding to amino acids 418-1034 were phosphorylated by PKCζ, however, scansite predicts two sites which are not in this region and therefore not phosphorylated by PKCζ and are false positives. Netphos predicts thirty-five other PKC sites that are false positives for PKCι/ζ but may be positives for the other PKC subtypes. Similarly, Hurov and colleagues mutated the threonine 595 to alanine in Par-1b and abolished PKCζ phosphorylation (Hurov et al., 2004), however Scansite predicts three other Par-1b sites which are not phosphorylated by PKCζ and are therefore false positives. NetPhos predicts thirty-four other Par-1b PKC sites which are false positives for PKCι/ζ but may be positive for other PKC subtypes. The HPRD only describes PKC phosphorylation sites; it does not specify which PKC. For each of the proteins many sites were predicted, indicating many false positives. This indicates that the parameters used by the algorithms are not specific and many false positives can be given and so the prediction tools alone are not sufficient to determine if PKCι phosphorylates a protein. Scansite, as it predicts PKCζ substrates, might be a useful tool once phosphorylation has been established to help find the exact site phosphorylated by PKCι.

4.2.2 *In vivo Xenopus* Method

The prediction programs were not suitable so another approach had to be found. The *Xenopus* method was tested because it is a relatively quick *in vivo* candidate approach. Two well established PKCι targets are Lgl and Par-1b (Betschinger et al., 2003; Hurov et al., 2004; Plant et al., 2003), were chosen to test the *in vivo Xenopus* method. Lgl is phosphorylated on serines (Plant et al., 2003) and Par-1b is phosphorylated on a threonine (Hurov et al., 2004).

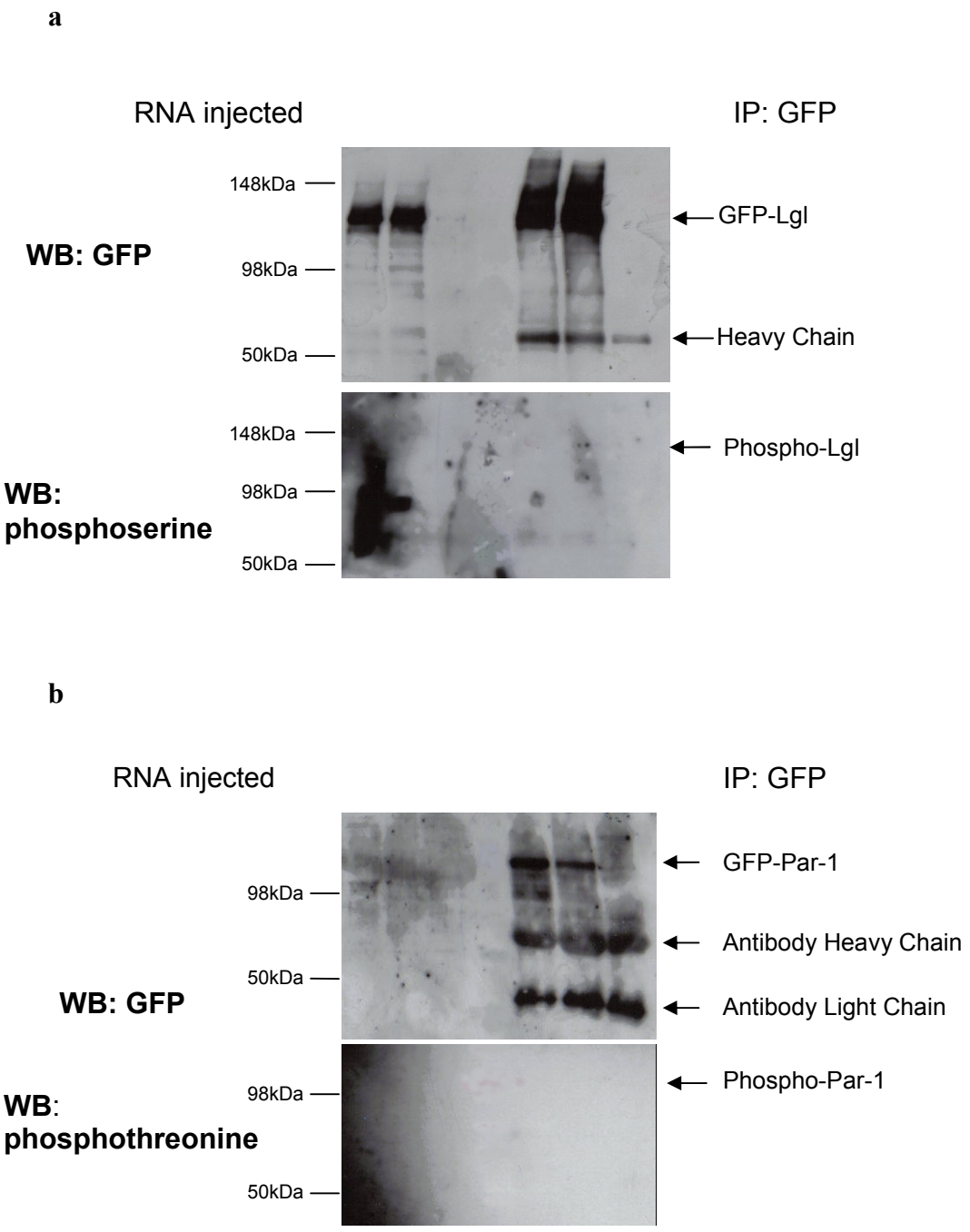

Figure 4.1 The *in vivo Xenopus* Method did Not Detect Phosphorylated Lgl or Par-1b. Proteins were expressed in *Xenopus* embryos and then IP using a GFP antibody and probed with pan phosphoserine and phosphothreonine antibodies.

(a) Lgl is clearly expressed by the *Xenopus* embryos (top panel) however the phosphoserine antibody was unable to detect Lgl phosphorylation (lower panel),

(b) Par-1b is clearly expressed by the *Xenopus* embryos (top panel) however the phosphothreonine antibody was unable to detect Par1b phosphorylation (lower panel).

Using these two proteins gives the opportunity to test the detection of both types of PKCι phosphorylation.

mRNA of each GFP fusion proteins were injected into 2 cell stage *Xenopus* embryos with and without a PKCι construct. At approximately stage 9 the embryos were lysed and the GFP fusion proteins were immunoprecipitated using a GFP antibody. The presence of the fusion protein was determined by a Western blot using a GFP antibody and the presence of phosphorylation assessed using a phosphoserine antibody for Lgl and a phosphothreonine antibody for Par-1b. Both of the GFP fusion proteins were expressed highly even in the presence of PKCι (figure 4.1 a top panel and b top panel). However, the phosphoserine and phosphothreonine antibodies could not detect any phosphorylation (figure 4.1 a and b, bottom panel). This is probably due to the phospho antibodies not being able to recognise all phosphorylated serines or threonines. As the antibodies do not recognise known PKCι phosphorylation sites it is unlikely they will recognise any PKCι phosphorylation sites, as the consensus sequence around the phosphorylation site is likely to be similar to that around the phosphorylation sites in Lgl and Par-1b. PKCι was not blotted for, so it cannot be proven that it was present, but the embryos had cell apicalisation, so it is likely that it was present.

4.2.3 Setting up an *in vitro* Kinase Assay

Due to the *in vivo Xenopus* method not being suitable for established PKCι targets and therefore not suitable for finding novel PKCι phosphorylation targets an alternative method to measure phosphorylation was tested. The *in vitro* kinase assays were chosen as it is quick and shows direct phosphorylation. MBP is a known PKC substrate (Kishimoto et al., 1985) that can be purchased from Sigma. PKCι can also be purchased from Calbiochem. Therefore, MBP was used to test the kinase assay conditions set out by Calbiochem and also act as a positive control.

MBP was added to PKCι and radiolabelled ATP, then incubated, the reaction was stopped using sample buffer and the mixture run on an SDS-Page gel and visualised using autoradiography. PKCι can phosphorylate MBP (figure 4.2), showing that the kinase assay conditions are suitable for PKCι substrate phosphorylation and MBP can be used as a positive control in future kinase assays.

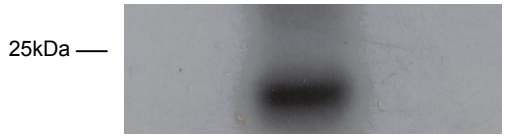

Figure 4.2 MBP is Phosphorylated by PKCι

An *in vitro* kinase assay was performed with MBP as the substrate and commercial PKCι as the kinase, the kinase assay mixture was separated by electrophoresis and visualised using autoradiography.

4.2.4 Testing an *in vitro* Kinase Assay Method which used GFP tagged Lgl and Par-1b Expressed in *Xenopus* Embryos.

Xenopus embryos were used to make the proteins as that has already been successfully completed (figure 4.1) Par-1b and Lgl, known PKCι phosphorylation targets were chosen as substrates to test the *in vitro* kinase assay using proteins expressed in *Xenopus* embryos. GFP tagged Lgl and Par-1b were expressed in *Xenopus* embryos and purified by immunoprecipitation using a GFP antibody (figure 4.3 a). The purified fusion proteins were then added to PKCι and ATP^{32}, and the kinase assay carried out. Par-1b phosphorylation was not detected in this assay (figure 4.3 b). This may be due to not making enough Par-1b protein and a disadvantage with this approach is that it is not possible to quantitate the amount of protein because of the IgG protein from the IP. In contrast, Lgl was clearly phosphorylated (figure 4.3 b), however, this phosphorylation occurs with and without PKCι. It was hypothesised that Lgl was being phosphorylated without PKCι being added because PKCι may have co-immunoprecipitated with the Lgl from the *Xenopus* extracts. To test this a Western blot for PKCι was carried out. The results shown in figure 4.3 c show a strong band of PKCι in the whole embryo extracts and a lighter band in the GFP IP for Lgl. This indicates that the phosphorylation seen in the kinase assay was due to the PKCι co-immunoprecipitating with the Lgl. Due to this possibly happening with other candidate proteins and Par-1b phosphorylation not being detected it was decided to use an alternative method to express the proteins.

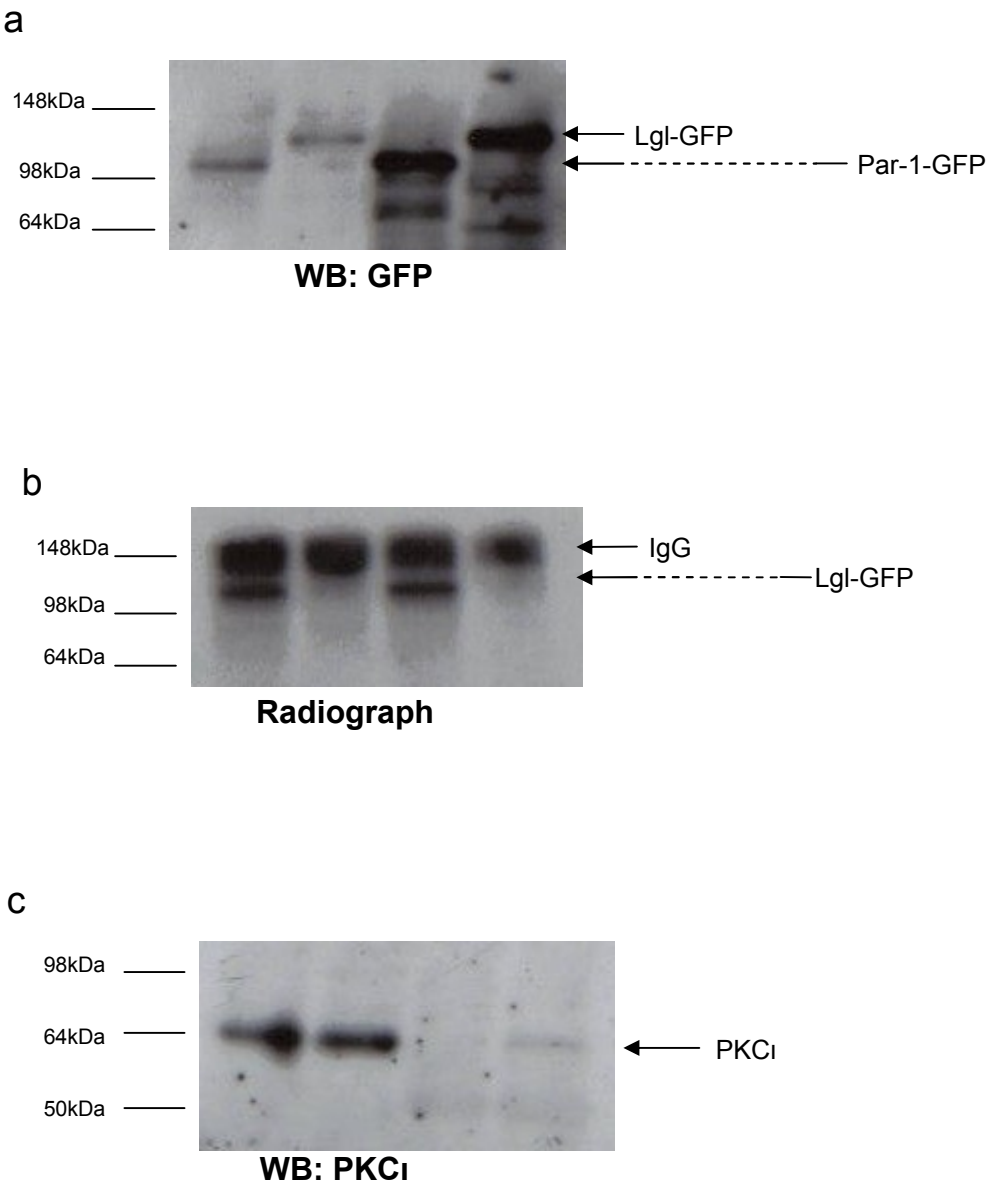

Figure 4.3 Testing the *in vitro* Kinase Assay using GFP tagged Lgl and Par-1b Expressed in Xenopus Embryos.

GFP tagged Lgl and Par-1b were expressed in *Xenopus* embryos, purified by IP and either used for a Western blot or a kinase assay with commercial PKCι.

(a) A Western blot for GFP showing GFP tagged Lgl and Par-1b are expressed by the Xenopus embryos and are efficiently immunoprecipitated, **(b)** In the kinase assay Lgl is clearly phosphorylated; however, this occurs with and without the presence of PKCι. Par-

1b phosphorylation is not detected, **(c)** A Western blot for PKCι shows that PKCι co-immunoprecipitates with Lgl from the *Xenopus* extracts.

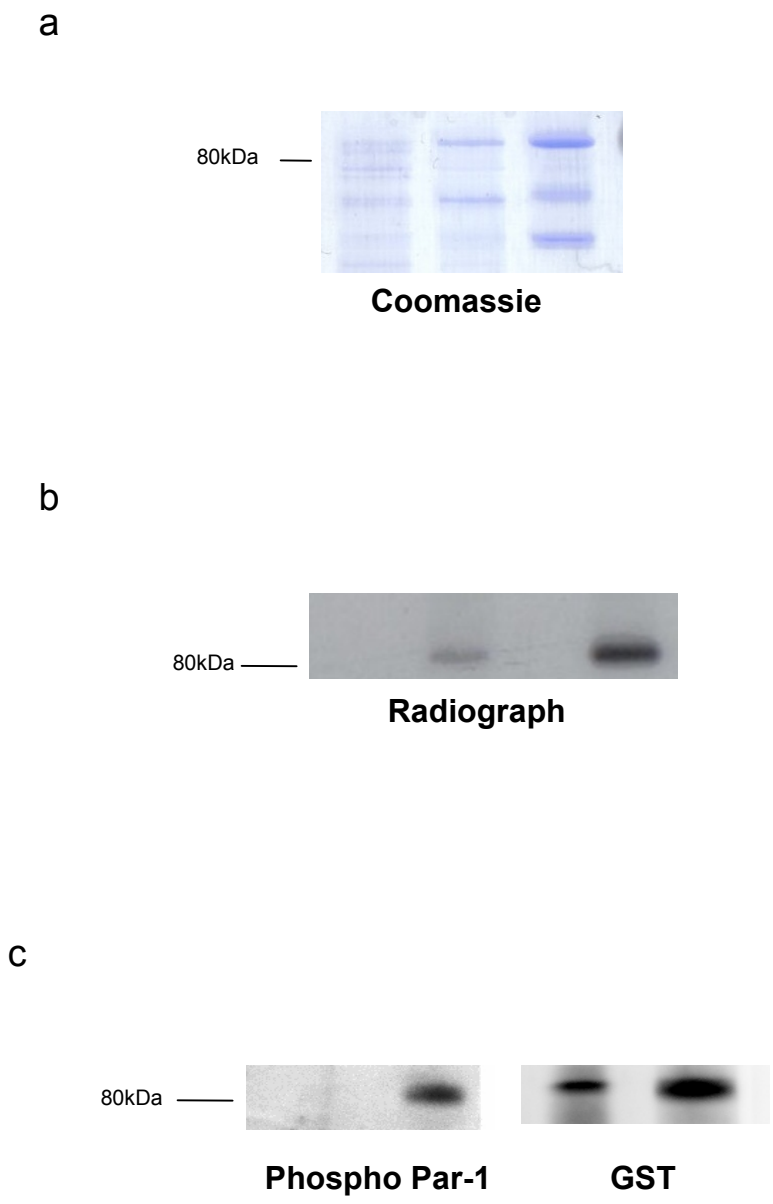

Figure 4.4 Bacterially Produced Par-1b is Phosphorylated in an *in vitro* Kinase Assay
GST-Par-1b was expressed in and purified from E.*coli* and subjected to a kinase assay and a Western blot.
(**a**) GST-Par-1b is expressed after induction and purified successfully, (**b**) Par-1b is phosphorylated when mixed with PKCι, however there is a small band of the same size present when PKCι is mixed with ATP^{32} alone which is probably PKCι autophosphorylation, (**c**) A Western blot for phospho-Par-1 clearly shows Par-1b is

phosphorylated by PKCι. A western blot for GST shows PKCι and Par-1b are the same size.

4.2.5 Bacterially Produced GST-fusion Proteins are Phosphorylated in an *in vitro* Kinase Assay

Due to PKCι co-immunoprecipitating with fusion proteins produced in *Xenopus* it was decided that bacterially expressed GST fusion proteins would be used instead as these should not contain PKCι when purified. This would prevent any PKCι co-immunoprecipitation and hopefully allow for a cleaner kinase assay. The GST fusion proteins would be purified using glutathione beads. Par-1b was chosen as a known PKCι phosphorylation target to test the kinase assay and Par-1b tagged to GST was kindly donated by H.Piwnica-Worms (Hurov et al., 2004). There is clear induction of bacterial expression of GST-Par-1b and purification using glutathione coated sepharose beads (Figure 4.4 a). The purified fusion protein was added to PKCι and ATP^{32} and the kinase assay carried out. The autoradiograph in figure 4.4 (b) shows Par-1b phosphorylation when PKCι is added to the kinase assay. However, there is also a weaker band in the PKCι and ATP^{32} lane. The commercial PKCι is GST tagged and is the same size as Par-1b-GST. It is likely that the small band seen in the PKCι and ATP^{32} lane is PKCι autophosphorylation. To prove that Par-1b is being phosphorylated a Western blot for phospho-Par-1b on T595 was carried out (figure 4.4 c left hand panel). The antibody recognises phosphorylation on threonine 595, the site phosphorylated by PKCι (Hurov et al., 2004). Par-1b is phosphorylated by PKCι. The right hand panel in figure 4.4 (c) shows a Western blot for GST. Par-1b-GST and PKCι-GST are both present and are the same size. It can be concluded that a working method for testing whether a protein is phosphorylated by PKCι has been established.

4.3 Discussion

The web based phosphorylation prediction methods were found to be unsuitable for predicting phosphorylation of suspected PKCι substrates as many false positives were predicted. With NetPhos and HPRD, only predicted sites for all the PKC subtypes are shown. This limits the usefulness of these sites as the predicted phosphorylation could be due to any of the PKC subtypes, not just PKCι. PhosphoELM lists predicted PKCι substrates, however, if the substrate of interest is not in this list it is of little use. Scansite appears to be the best tool to because it predicts PKCζ phosphorylation sites specifically.

However, the results can only be used as a guide as Scansite, like the other programs, does predict false positives. In future the programs may be improved and therefore it will be worth keeping up to date with developments in this area.

The *in vivo Xenopus* assay to determine PKCι phosphorylation did not detect PKCι phosphorylation of Lgl or Par-1b (Figure 4.1). This is probably due to the phospho antibodies not being able to recognise all phosphorylated serines or threonines. The antibodies are designed to recognise phosphorylated serines and threonines, but if the PKCι consensus sequence for phosphorylation was not used when designing the antibodies they will not recognise substrates phosphorylated by PKCι. Pan phosphoserine and phosphothreonine antibodies also tend to have a low affinity for their target, so may not bind with a high enough level to be detected (Johnson and Hunter, 2005).

The *in vitro* kinase assay using GFP-tagged Lgl and Par-1b also failed to detect Par-1b phosphorylation, but did detect Lgl phosphorylation (figure 4.3). The lack of Par-1b phosphorylation may be due to it already being phosphorylated in the *Xenopus* embryo or that the band is too faint to be seen. Lgl is phosphorylated at least five times, and Par-1b only once, it may be that the Par-1b phosphorylation band is too faint in comparison to the Lgl phosphorylation band. Further exposure of the kinase assay resulted in over exposed film (data not shown). More Par-1b protein was needed than the amount that could be gained from the *Xenopus* embryos, hence using bacteria to produce the protein. Lgl was phosphorylated with and without PKCι being added to the kinase assay. This has been shown before, Plant and colleagues showed that Lgl could be phosphorylated by PKCι that associated with it before the 293T cells were lysed (Plant et al., 2003). This was an unexpected problem of making protein in embryos. It may also occur with candidate proteins and may not be PKCι that is immunoprecipitated, leading to false positives. This would not occur if the protein were made in bacteria.

The *in vitro* kinase assay using GST-fusion proteins was shown to be effective in showing Par-1b phosphorylation (figure 4.4). However, the disadvantage of using this method is that the proteins are made in bacteria and are not subjected to post-translational modifications that may occur when the proteins are expressed in mammalian cells. This problem will have to be considered when novel PKCι phosphorylation targets are elucidated using this method. Once novel *in vitro* phosphorylation has been established it will have to be shown *in vivo*, but this *in vitro* kinase assay approach is a useful method as

the main aim of this thesis is to test candidate genes to see if they are phosphorylated by PKCι.

Chapter 5

Investigating Novel PKCι Phosphorylation Targets

5.1 Introduction

Cell polarity is the asymmetric distribution of constituents within a single cell that produces the asymmetry of cellular functions (Suzuki and Ohno, 2006). Epithelial cells are polarised along their apico-basal axis, the apical side of the cells is separated from the basal by tight junctions. The tight junctions have two functions; they provide a barrier between cells and they prevent the mixing of the transmembrane proteins between the apical and basal domains (Balda and Matter, 1998).

There are four main polarity complexes that are required to maintain polarity: the apical PKCι/ζ/Par-3/Par-6 complex, the apical Crumbs/Pals-1/Patj complex, the basolateral Lgl/Dlg/Scribbles group and the Yurt, Coracle, Neurexin IV and Na^+, K^+-ATPase group, as well as the basolateral protein Par-1. These complexes are evolutionarily conserved (Hurd et al., 2003; Izumi et al., 1998; Joberty et al., 2000; Laprise et al., 2009; Lin et al., 2000; Plant et al., 2003; Yamanaka et al., 2003) and are required to establish and maintain epithelial polarity.

Par-3 is known to be phosphorylated by PKCι/ζ (Nagai-Tamai et al., 2002) and Par-6 has been reported as not being phosphorylated by PKCι/ζ. Lgl is also known to be phosphorylated by PKCι/ζ (Yamanaka et al., 2003). *Drosophila* Crumbs has also been shown to be a human PKCι phosphorylation target in an *in vitro* kinase assay (Sotillos et al., 2004). Consequently these four proteins were not chosen as potential PKCι phosphorylation targets to be tested in this project. The Yurt, Coracle, Neurexin IV and Na^+, K^+-ATPase group was not described as a polarity complex until later in this work, so unfortunately none of them were included. The proteins chosen for testing in an *in vitro* kinase assay were, Patj, Scribble, Pals-1 and Dlg.

In addition to its role at tight junctions, PKCι/ζ is active at the centrosomes (chapter 3), which are cellular organelles that are composed of two centrioles surrounded by pericentriolar material (Alieva and Uzbekov, 2008; Schatten, 2008). This structure is a microtubule organising centre that plays a role in a wide variety of cellular functions

including, cell division, vesicle transport, cell motility and cell shape maintenance (Schatten, 2008). Defective centrosome function has also been linked to tumour progression (Nigg, 2002). Proteins associated with the centrosome can be split into three groups; the centriolar matrix, the pericentriolar matrix and centrosome associated proteins (Alieva and Uzbekov, 2008). Over 500 centrosomal proteins have been identified in a mass spectroscopy study (Andersen et al., 2003), however, these may not be present at all stages of the cell cycle and the role of many of these proteins is not understood. It would not be possible to test such a large number of proteins and it was decided to test two proteins which appeared to be particularly good candidates. Two proteins described below localise to the centrosome and are candidate PKCι phosphorylation targets that will be tested in this project.

5.1.1 LGN

LGN was first cloned in 1996; it is a 76kDa protein with Leu-Gly-Asn repeats, and so was called LGN. The mRNA for LGN is expressed in a wide variety of tissues including kidney, lung and skeletal muscle (Mochizuki et al., 1996). LGN is the mammalian homologue of *Drosophila* Partner of Inscuteable (Pins) and they share a 63% similarity (Yu et al., 2000). In *Drosophila* neuroblasts Pins localises to a crescent in the apical cortex. It binds Inscuteable (Insc) and is required for the maintenance of Insc at the apical cortex. Insc links Baz and the Par-aPKC complex to Pins (Yu et al., 2000). Pins can localise asymmetrically in neuroblasts and lead to asymmetric spindle orientation by associating with microtubules and working in conjunction with DaPKC this leads to asymmetric neuroblast divisions (Bowman et al., 2006; Cai et al., 2003).

In mammalian cells, the localisation of LGN seems to depend on the cell type. In MDCK cells, endogenous LGN is found throughout the cytoplasm in interphase, but during mitosis, LGN relocates to a crescent at each spindle pole and the mitotic apparatus (Du et al., 2001). In MDCK cells stably expressing YFP-LGN there is clear staining of the spindle poles during metaphase (Du and Macara, 2004). Overexpressed LGN localises to the cell cortex in mitotic: WISH, PC12 and NRK cells but not in Cos7 cells (Kaushik et al., 2003). In HeLa cells, LGN protein levels increase during mitosis as shown by Western blotting (Du and Macara, 2004). In PC12 cells, loss of or overexpression of LGN causes cell cycle progression defects; the cells arrest at the G1/S phase checkpoint (Kaushik et al., 2003). In MDCK cells, overexpression of LGN causes misorientated spindles during

metaphase and mis-segregation of chromosomes during anaphase. The same effect is observed in HeLa cells when LGN is knocked out using siRNA (Du et al., 2001), showing that LGN has a key role in mitosis.

LGN has also been shown to bind PKCι/ζ, Par-6 and Lgl during mitosis in HEK293 cells (Yasumi et al., 2005). The Hek293 cells were synchronised using thymidine and Nocodazole, lysed and then subjected to an immunoprecipitation using an anti-LGN antibody and subsequent Western blotting using anti-PKCι/ζ, Par-6 and Lgl antibodies. This revealed that LGN formed a complex with PKCι/ζ, Par-6 and Lgl and when compared to the non-synchromised cells, the formation of this complex increased during mitosis. PKCι/ζ, Lgl and LGN also colocalise at the cell periphery during metaphase in HEK293 cells.

LGN also binds NuMa and they colocalise at the centrosomes during mitosis in MDCK cells and the overexpression of LGN disrupts the localisation of NuMa at the centrosomes (Du et al., 2001). LGN and NuMa function together to regulate spindle formation and spindle pole organisation during mitosis. NuMa is required for the stability of microtubules; it prevents them from dissociating into tubulin subunits. LGN prevents NuMa from binding microtubules by binding the region of NuMa that binds microtubules. Therefore, LGN regulates the binding of NuMa to the microtubules at the spindle poles (Du et al., 2002). However, how LGN is regulated is unknown, although interestingly it does contain potential PKC phosphorylation sites according to Prosite (Mochizuki et al., 1996) and may be regulated by PKC phosphorylation at the centrosomes. Therefore, it was decided to test if PKCι could phosphorylate LGN.

5.1.2 Glycogen Synthase Kinase 3β

GSK3β was first described in 1992 as a component of a metabolic pathway (Plyte et al., 1992) but is now linked to many cellular processes, including, Wnt, NFκB and hedgehog signalling, cell fate and cell polarity (Kim and Kimmel, 2006). GSK3β localises to the centrosome and spindle microtubules during mitosis in mammalian HeLa cells (Fumoto et al., 2006; Izumi et al., 2008; Wakefield et al., 2003). GSK3β phosphorylates microtubule associated proteins, such as Tau, decreasing their ability to stabilise microtubules (Lovestone et al., 1996). During mitosis microtubule dynamics increase and microtubule nucleation at the centrosome occurs (Compton, 2000). GSK3β is phosphorylated on S9 during mitosis at the centrosome (Wakefield et al., 2003) and

inactivated (Harwood, 2001). GSK3β may also play a role in centrosomal protein transport, such as ninein, by interaction with Bicaudal-D. This requires GSK3β activity, again indicating that GSK3β is active on the spindle microtubules (Fumoto et al., 2006). GSK3β has also been shown to regulate microtubule dynamics through GCP5 (γ-tubulin complex protein-5) which is part of the centrosome. The inhibition of GSKβ at the centrosomes increases the recruitment of GCP5 and γ-tubulin to the centrosome leading to more microtubules at the centrosome (Izumi et al., 2008). If GSK3β is totally inhibited in synchronised HeLa cells during mitosis, there are defects in microtubule and chromosome alignment, therefore active GSK3β is needed for chromosome alignment. The GSK3β at the centrosomes is already phosphorylated and inactivated at the centrosomes, so it must be GSK3β on the spindle microtubules and elsewhere in the cytosol that is responsible for chromosome and microtubule alignment (Wakefield et al., 2003). There is temporal and spatial phosphorylation and therefore inhibition of GSK3β.

Wakefield and colleagues suggest that it is PKB that is phosphorylating GSK3β, as PKB is active at the centrosomes. However, the staining is similar to the staining for phospho-PKCι/ζ shown in chapter 3 of this work, so it is possible that is it PKCι phosphorylating GSK3β. In support of this hypothesis, GSK3β has also been shown to be a phosphorylation target of PKCζ, however, not directly (Etienne-Manneville and Hall, 2003a). GSK3β is phosphorylated at S9 at the leading edge of migrating astrocytes. The authors showed that GSK3β and PKCζ form a complex by IP and Western blotting. Phospho-GSK3β was not detected in the Western blot indicating that PKCζ cannot bind phospho-GSK3β. Inhibition of PKCζ prevented GSK3β phosphorylation and transfection of wild-type but not kinase dead PKCζ causes GSK3β phosphorylation. This suggests that GSK3β is a phosphorylation target of PKCι, but it has not been shown to be direct. It was within this paper that the role of GSK3β in cell polarity was elucidated. GSK3β phosphorylation on serine 9 occurs at the leading edge of migrating astrocytes. A S9A mutant of GSK3β injected into the leading edge prevents centrosome reorientation and polarity establishment. GSK3β phosphorylation is needed to inactivate GSK3β allowing that accumulation of β-catenin at the leading edge and the association of adenomatous polyposis coli (APC) with the plus ends of microtubules. β-catenin is not necessary for cell polarisation, but APC is. However, how APC is involved in polarity remains unclear (Etienne-Manneville and Hall, 2003a).

5.2 Aims

Due to the large number of polarity proteins that are involved in similar processes to the Par-PKCι/ζ complex, but which have not been reported as positive PKCι phosphorylation targets, the aim was to test some of these polarity proteins using the GST-fusion protein kinase assay method developed in chapter four. The polarity proteins chosen were; Patj, Pals-1, Scribble and Dlg. To begin to understand the role of PKCι at the centrosome, another aim was to test two known centrosomal proteins, LGN and GSK3β, to see if they are directly phosphorylated by PKCι.

5.3 Results

Plasmids for each of the suspected polarity phosphorylation candidates were requested from other researchers. Patj was kindly provided by A Le Bivic (Lemmers et al., 2002), Scribbles was kindly provided by I Macara (Qin et al., 2005), Dlg was kindly provided by L Banks (Massimi et al., 2006) and Pals-1 was kindly provided by B. Margolis (Kamberov et al., 2000). All the genes had different tags on them so had to be cloned into a GST vector using the Gateway® Cloning kit (stratagene), to allow expression in bacteria and purification. LGN-GST was kindly provided by V. Slepak (Nair et al., 2005) and GSK3β-GST was kindly provided by H. Paudel (Sun et al., 2002) and as they were already in GST expression vectors they could be used immediately.

5.3.1 Patj and Scribble

Patj contains one L27 domain and ten PDZ domains. The L27 is a protein-protein binding domain that binds to the L27 domain of Pals-1 (Li et al., 2004). PDZ domains are also protein-protein interaction domains (Ponting et al., 1997). No PKCι/ζ phosphorylation sites were predicted by Scansite. Primers were designed for Patj as per manufacturers' instructions. The Patj PCR was successful and a clear band at 4.7kb could be seen (figure 5.1b). The TOPO® reaction was then carried out using the PCR product, amplified by E.coli, mini-prepped, and the products cut with the restriction enzyme BSRG1. The TOPO® vector has BSRG1 sites at the recombination sites, so using BSRG1 should excise the PCR product. This did not occur for Patj. The only band seen on cutting the plasmid was that of the self-ligated TOPO® vector (fig 5.1c). The TOPO® reaction was repeated six times altering the length of the TOPO® reaction and the temperature, but to no avail.

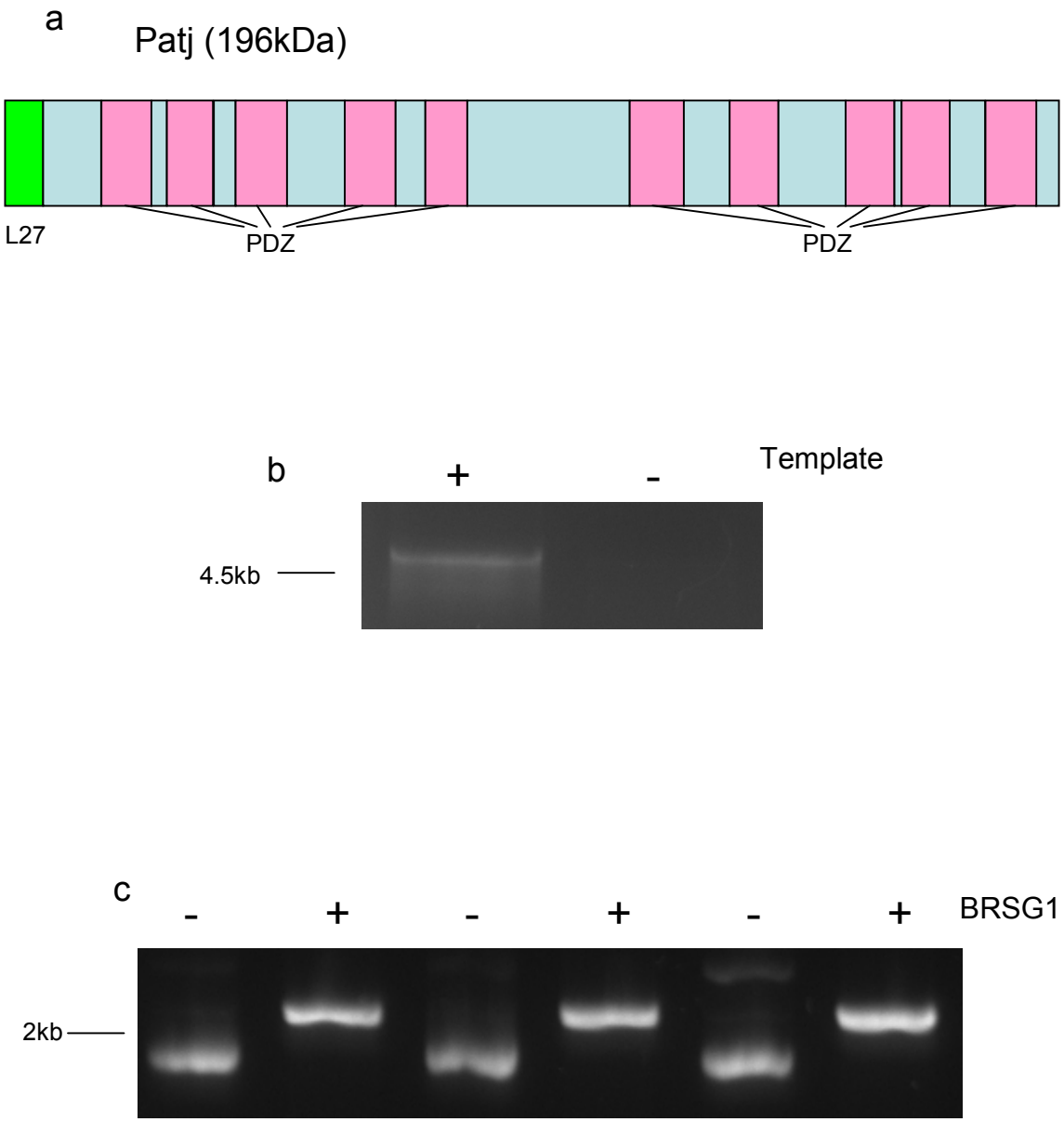

Figure 5.1 Unsuccessful Attempt to make a GST-fusion Protein of Patj

(a) A schematic diagram of the domains in Patj. Scansite did not predict any PKCζ phosphorylation sites, **(b)** Patj PCR was successful. The Patj PCR product should be 4.7kb, **(c)** Patj TOPO™ reaction product, cut with the restriction enzyme BSRG1, should have produced a 4.7kb and a 2.5kb product, only the 2.5kb vector was present. This shows that there is no insert present. A few clones were also sequenced which contained no insert.

A few Patj TOPO® constructs were sent for sequencing and some returned showing the TOPO® linker sequence and around 100bp of the Patj gene indicating that a truncated piece of the Patj was being incorporated into the TOPO® vector and some contained no Patj at all.

Scribble contains four PDZ domains, that are protein-protein interaction domains (Ponting et al., 1997). No PKCι/ζ phosphorylation sites were predicted by Scansite. Primers were designed for Scribble as per manufacturers' instructions. The Scribble PCR was not successful initially, only smears could be seen on the gel (figure 5.2b). DMSO can help break secondary structures in GC rich DNA allowing the polymerase easier access to the template DNA. On this basis 0%, 5% and 10% DMSO was added to each reaction and 4.8kb PCR product of Scribble was achieved with 10% DMSO (figure 5.2c). The Scribble PCR product was then added to the TOPO® reaction, the reaction performed, the reaction product amplified by E.coli, mini-prepped, and the products cut with the restriction enzyme BSRG1. The TOPO® vector has BSRG1 sites at the recombination sites, so using BSRG1 should excise the whole 4.8kb PCR product. This did not occur for Scribble. The only band seen on cutting the plasmid was that of the self-ligated TOPO® vector (fig 5.2d). The TOPO® reaction was repeated twice, altering the length of time the reaction took place for, but to no avail. No TOPO® reaction products were sent for sequencing as none of them contained any inserts.

Due to the difficulties in cloning Patj and Scribble, it was decided to focus on other candidates.

5.3.2 Pals-1 is not Phosphorylated by PKCι *in vitro.*

Pals-1 contains two L27 domains, one PDZ, one SH3 and one guanylate kinase-like domain. The L27 domain is a protein-protein binding domain that binds to the L27 domain of Patj (Li et al., 2004). The PDZ domain is also a protein-protein interaction domain (Ponting et al., 1997). The SH3 domain is also a protein-protein interaction domain (Pawson and Schlessingert, 1993). Primers were designed for Pals1 as per manufacturers' instructions. The PCR was successful and the product the correct size. The product was ligated into the TOPO® vector and finally the GST vector via the Gateway® Cloning kit (Invitrogen) (data not shown). The schematic in figure 5.3a shows the domains of Pals-1 fused to the GST tag.

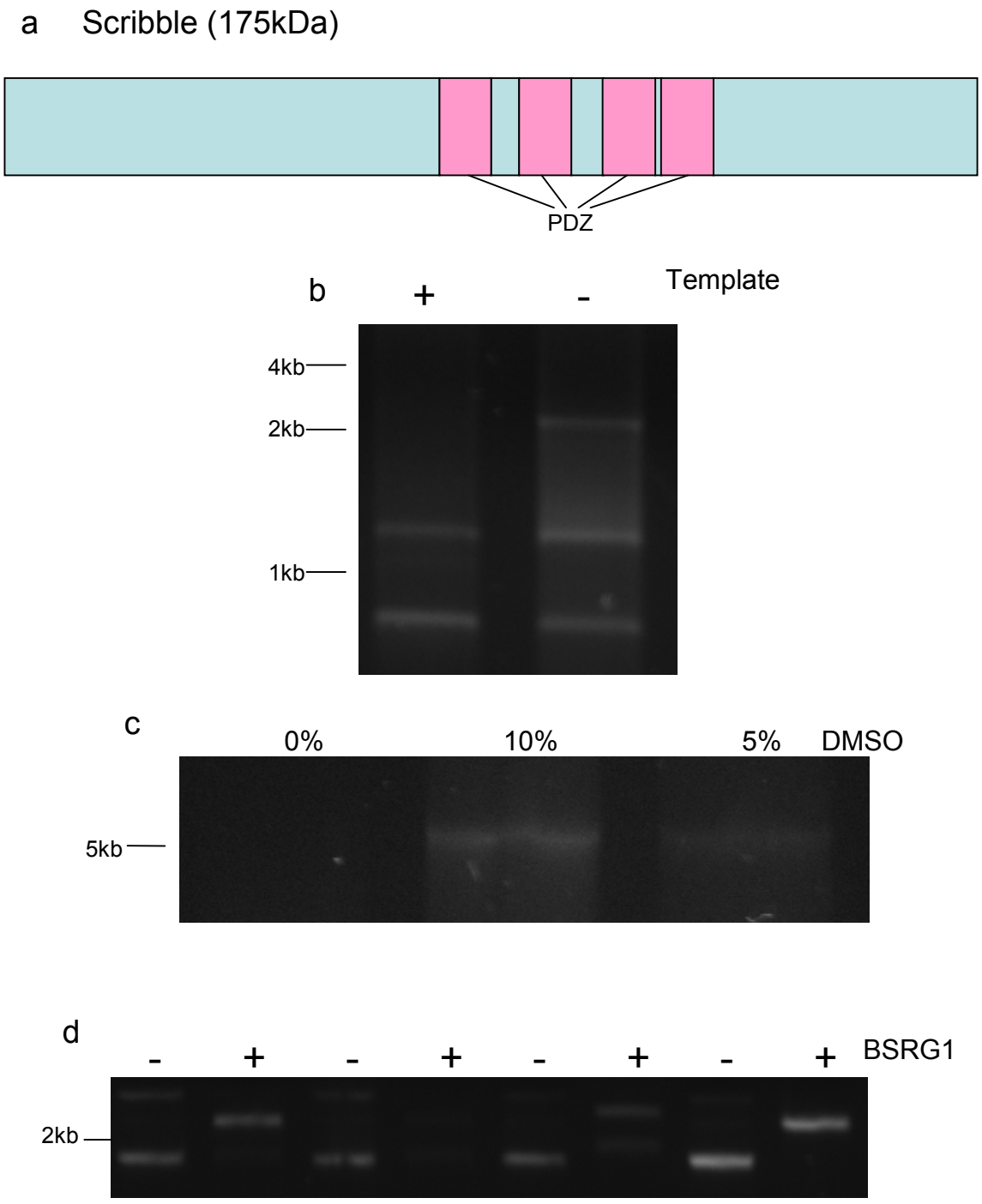

Figure 5.2 Unsuccessful Attempt to Make a GST-fusion Protein of Scribble

(a) A schematic diagram of the domains in Scribble. Scansite did not predict any PKCζ phosphorylation sites, **(b)** The initial Scribble PCR did not work, **(c)** Addition of DMSO to the PCR reaction mixture enabled Scribble PCR to work and a band of 4.8kb, the size of scribble was present, **(d)** Scribble TOPO™ reaction product, cut with the restriction enzyme BSRG1, should have produced a 4.8kb and a 2.5kb product, only the 2.5kb vector was present. This shows that there is no insert present.

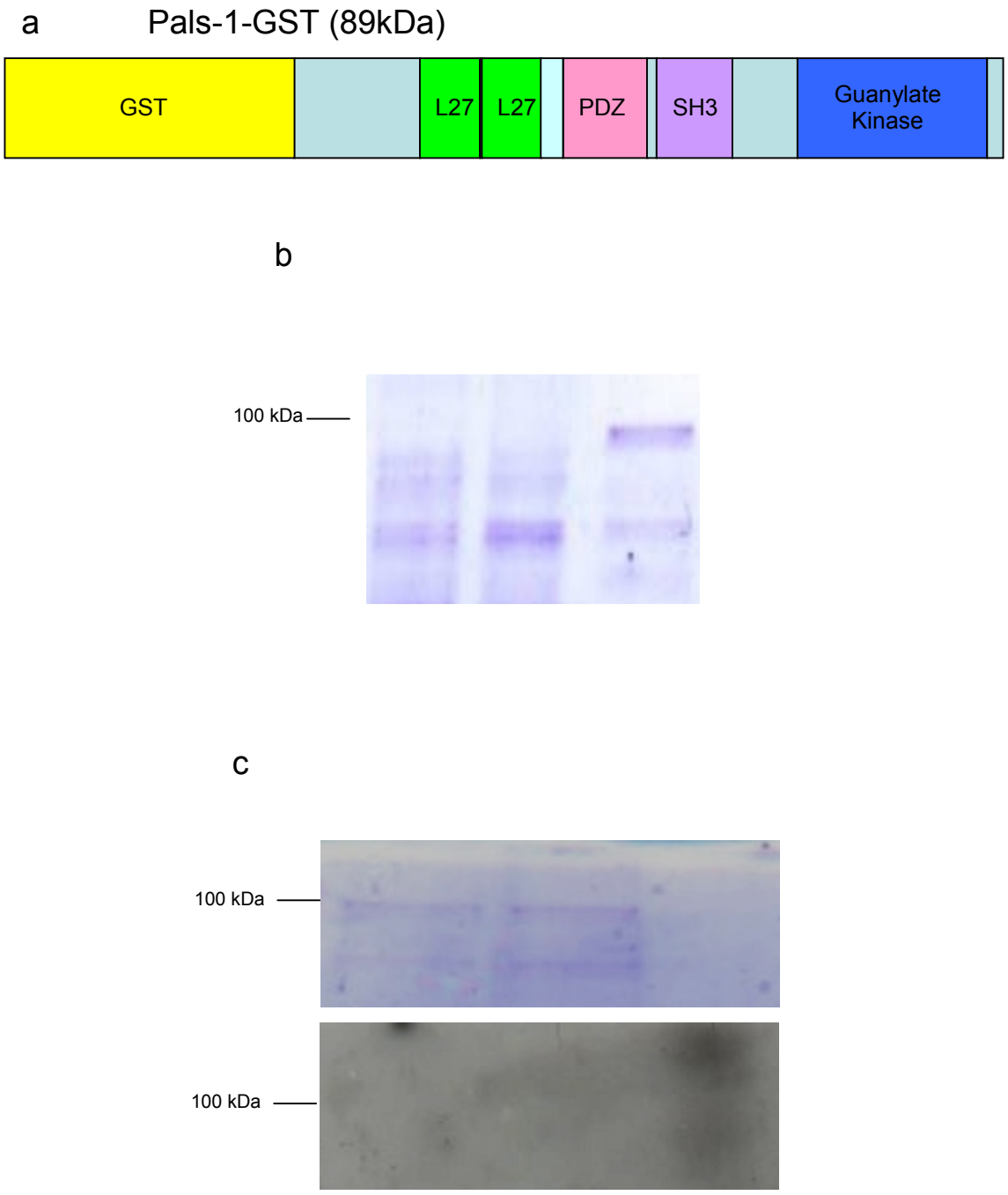

Figure 5.3 Pals-1 is not Phosphorylated by PKCι in an *in vitro* Kinase Assay

(a) A schematic diagram of the domains in Pals-1 tagged to GST. Scansite did not predict any PKCζ phosphorylation sites, **(b)** Pals-1 is expressed in E.coli following the addition of L-arabinose and successfully purified using glutathione sepharose beads, **(c)** The Pals-1-GST fusion protein was used in a kinase assay with PKCι, but no phosphorylation was detected by autoradiography (bottom panel). The purified Pals1 protein could be seen on the Coomassie stained kinase assay SDS-PAGE gel (top panel).

The finished GST-tagged Pals-1 plasmid was transformed into BL21-A1 E.coli, the bacteria grown to the log phase and then L-arabinose added to induce expression of the protein. Upon L-arabinose addition the protein was expressed and purified using glutathione sepharose beads (figure 5.3b) in the centre lane in figure 5.3b the induction of Pals-1 cannot be seen clearly; however, the purified protein is much clearer in the right hand lane.

The purified GST-Pals-1 fusion protein was added to a kinase assay containing PKCι and the reaction carried out. The reaction was quenched using sample buffer and the mixture separated by an SDS-PAGE gel and visualised using autoradiography. The top panel in figure 5.3c shows the Coomassie stained gel that contains the kinase assay mixture and the Pals-1 protein can clearly be seen. The bottom panel in figure 5.3c shows the autoradiograph, no phosphorylation band can be seen at the size of Pals-1. The autoradiograph was further exposed and no phosphorylation bands were seen (data not shown), so no phosphorylation of Pals-1 by PKCι could be detected (figure 5.3c). MBP was used as a positive control and was phosphorylated (data not shown).

5.3.3 Dlg is not Phosphorylated by PKCι *in vitro,* but Increases PKCι Autophosphorylation

Dlg contains one L27 domain, three PDZ domains, one SH3 domain and a guanylate kinase domain that is inactive (Kistner et al., 1995). Primers were designed for Dlg as per manufacturers' instructions. The PCR was successful and the product the correct size. The Dlg PCR product was ligated into the TOPO® vector and finally the GST vector via the Gateway® Cloning kit (Stratagene) (data not shown). The schematic in figure 5.4a shows the domains of Dlg fused to the GST tag. The finished GST-tagged Dlg plasmid was transformed into BL21-A1 E.coli, the bacteria grown to the log phase and then L-arabinose added to induce expression of the protein. Upon L-arabinose addition the protein was expressed and purified using glutathione sepharose beads (figure 5.4b). The purified GST-Dlg fusion protein was added to a kinase assay containing PKCι and the reaction carried out. The reaction was quenched using sample buffer and the mixture separated by an SDS-PAGE gel and visualised using autoradiography. A band was seen by autoradiography, but Dlg phosphorylation by PKCι was not detected (figure 5.4c), when the top and lower panels are overlaid the phosphorylation band is much lower than the Dlg protein band on the Coomassie stained gel.

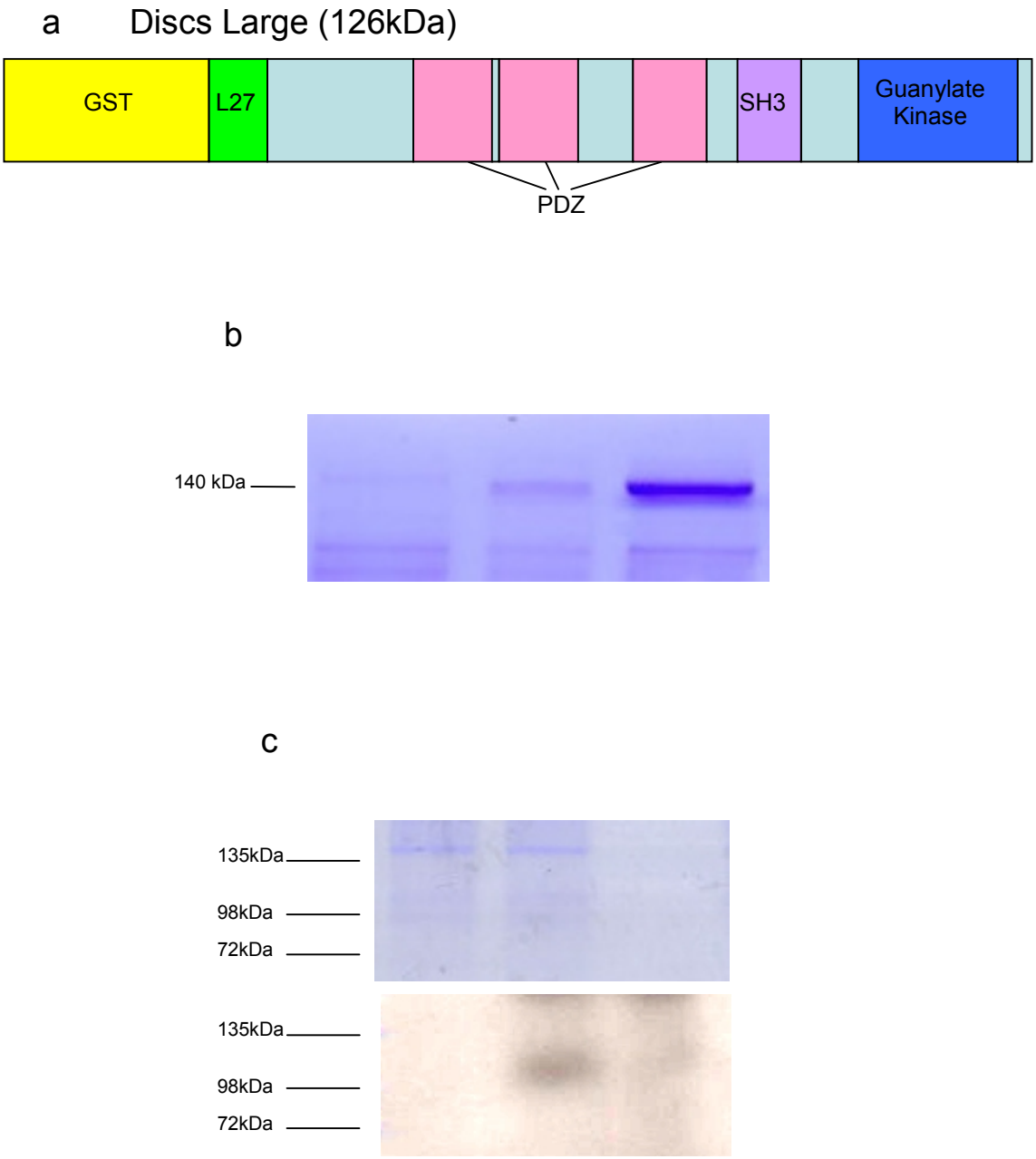

Figure 5.4 Dlg is not Phosphorylated by PKCι but Increases PKCι Autophosphorylation

(a) A schematic diagram of the domains in Dlg tagged to GST. Scansite did not predict any PKCζ phosphorylation sites, **(b)** Dlg was expressed in E.coli following the addition of L-arabinose and successfully purified using glutathione sepharose beads, **(c)** The Dlg-GST fusion protein was used in a kinase assay with PKCι, but no Dlg phosphorylation was visualised at the correct size (bottom panel). However there is a clear phosphorylation band at the same size as PKCι. The purified Dlg protein can be seen on the Coomassie stained kinase assay SDS-PAGE gel (top panel) and is larger than the band seen by autoradiography.

This proves that it is not Dlg phosphorylation on the autoradiograph. The only other component within the mixture is PKCι and the phosphorylation band on the autoradiograph is the same size as PKCι (98 kDa), so it is highly likely that the band is PKCι autophosphorylation. However lane 3 contains the same amount of PKCι as lane 2 and at this exposure time no autophosphorylation band is seen on the autoradiograph in this lane. This indicates that more PKCι autophosphorylation is taking place when Dlg is added to the kinase assay mixture. However, Dlg does not contain an active kinase domain, so appears to be increasing the autophosphorylation of PKCι. This experiment was repeated four times.

5.3.4 LGN is not Phosphorylated by PKCι *in vitro*

LGN contains six tetratricopeptide repeat (TPR) domains and four Go-Loco motifs. The TPR motifs mediate the interaction of LGN with NUMA (Du et al., 2001), Lgl also binds the N-terminal region of LGN, but it is unclear if this is via the TPR motifs (Yasumi et al., 2005). Go-Loco motifs associate with the Gα subunits of heterotrimeric G-proteins and are responsible for the localisation of LGN (Kaushik et al., 2003). The schematic diagram in figure 6.1a shows the domains of LGN fused to the GST tag, including the potential PKCζ phosphorylation sites predicted by Scansite. The GST-tagged LGN plasmid was transformed into BL21-A1 E.coli, the bacteria grown to the log phase, and then L-arabinose added to induce expression of the protein. Upon L-arabinose addition, the protein was expressed and then purified using glutathione sepharose beads (figure 6.1b). The purified protein is clear in the right hand lane of the Coomassie stained gel. The purified GST-LGN fusion protein was added to a kinase assay containing PKCι and the reaction carried out. The reaction was quenched using sample buffer and the mixture separated by an SDS-PAGE gel and visualised using autoradiography. Phosphorylation of LGN could not be detected (figure 6.1c). The top panel in figure 6.1c shows the Coomassie stained gel that contains the kinase assay mixture, LGN-GST can clearly be seen. The bottom panel in figure 6.1c shows the autoradiograph, no phosphorylation band can be seen at the size of LGN-GST. The autoradiograph was further exposed and no phosphorylation bands were seen (data not shown). MBP was used as a positive control and was phosphorylated (data not shown).

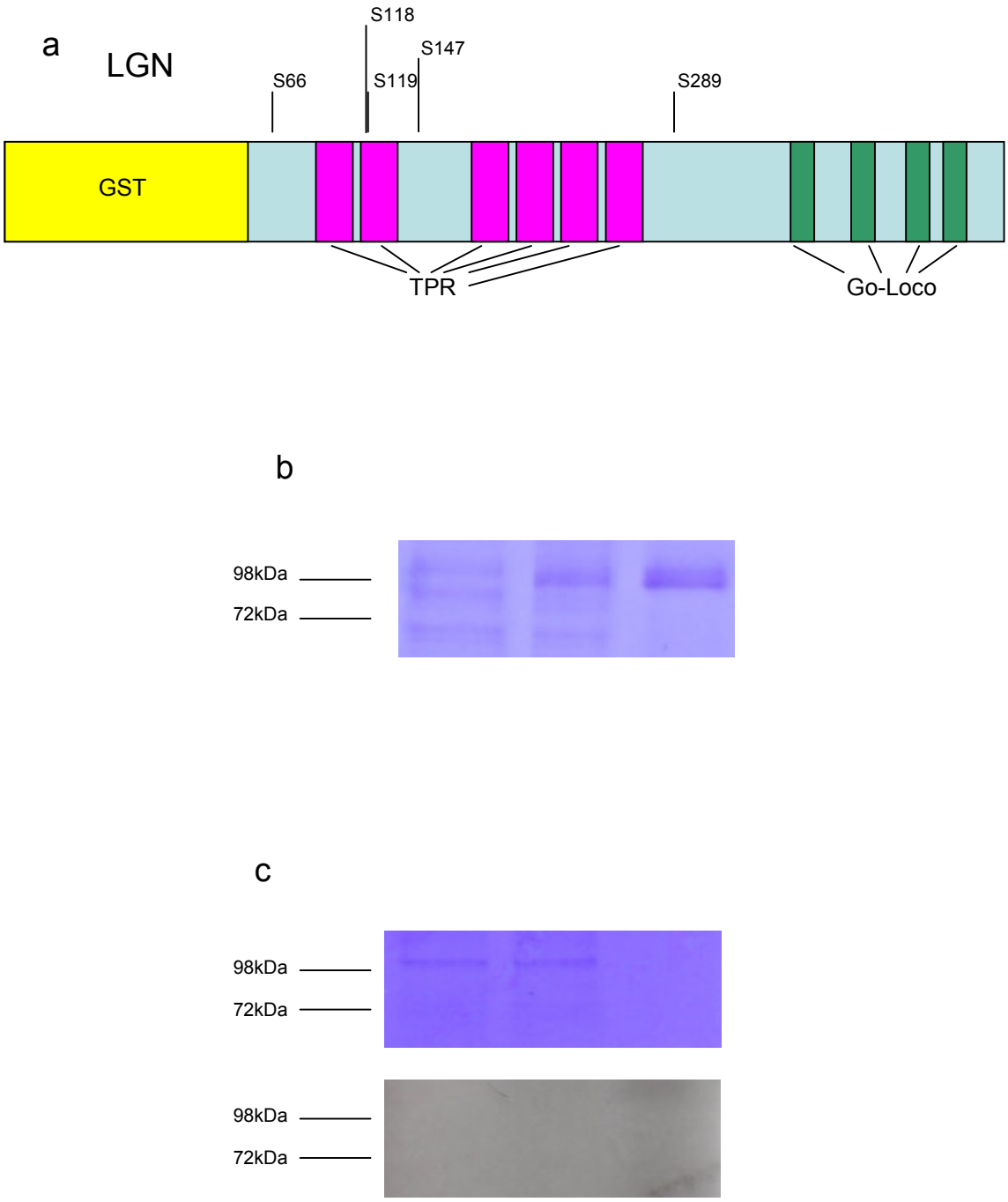

Figure 5.5 LGN is not Phosphorylated by PKCι in an *in vitro* Kinase Assay.
(a) A schematic diagram of the domains in LGN tagged to GST including the potential phosphorylation sites predicted by Scansite, **(b)** LGN-GST is expressed in E.coli following the addition of L-arabinose and successfully purified using glutathione sepharose beads, **(c)** The LGN-GST fusion protein was used in a kinase assay with PKCι, but no phosphorylation was detected by autoradiography (bottom panel). The purified LGN-GST protein can be seen on the Coomassie stained kinase assay SDS-PAGE gel (top panel).

5.3.5 GSK3β is not Phosphorylated by PKCι *in vitro*

The schematic diagram in figure 5.6a shows the domains of GSK3β fused to the GST tag, including the potential PKCζ phosphorylation sites predicted by Scansite. The GST-tagged GSK3β plasmid was transformed into BL21-A1 E.coli, the bacteria grown to the log phase and then L-arabinose added to induce expression of the protein. Upon L-arabinose addition the protein was expressed and then purified using glutathione sepharose beads (figure 5.6b). The purified protein is clear in the right hand lane of the Coomassie stained gel.

The purified GST- GSK3β fusion protein was added to a kinase assay containing PKCι and the reaction carried out. The reaction was quenched using sample buffer and the mixture separated by an SDS-PAGE gel and visualised using autoradiography. Phosphorylation of GSK3β could not be detected (figure 5.6c). The top panel in figure 5.6c shows the Coomassie stained gel that contains the kinase assay mixture, GSK3β -GST can clearly be seen. The bottom panel in figure 5.6c shows the autoradiograph, no phosphorylation band can be seen at the size of GSK3β-GST. The autoradiograph was further exposed and no phosphorylation bands were seen (data not shown). MBP was used as a positive control and was phosphorylated by PKCι (data not shown).

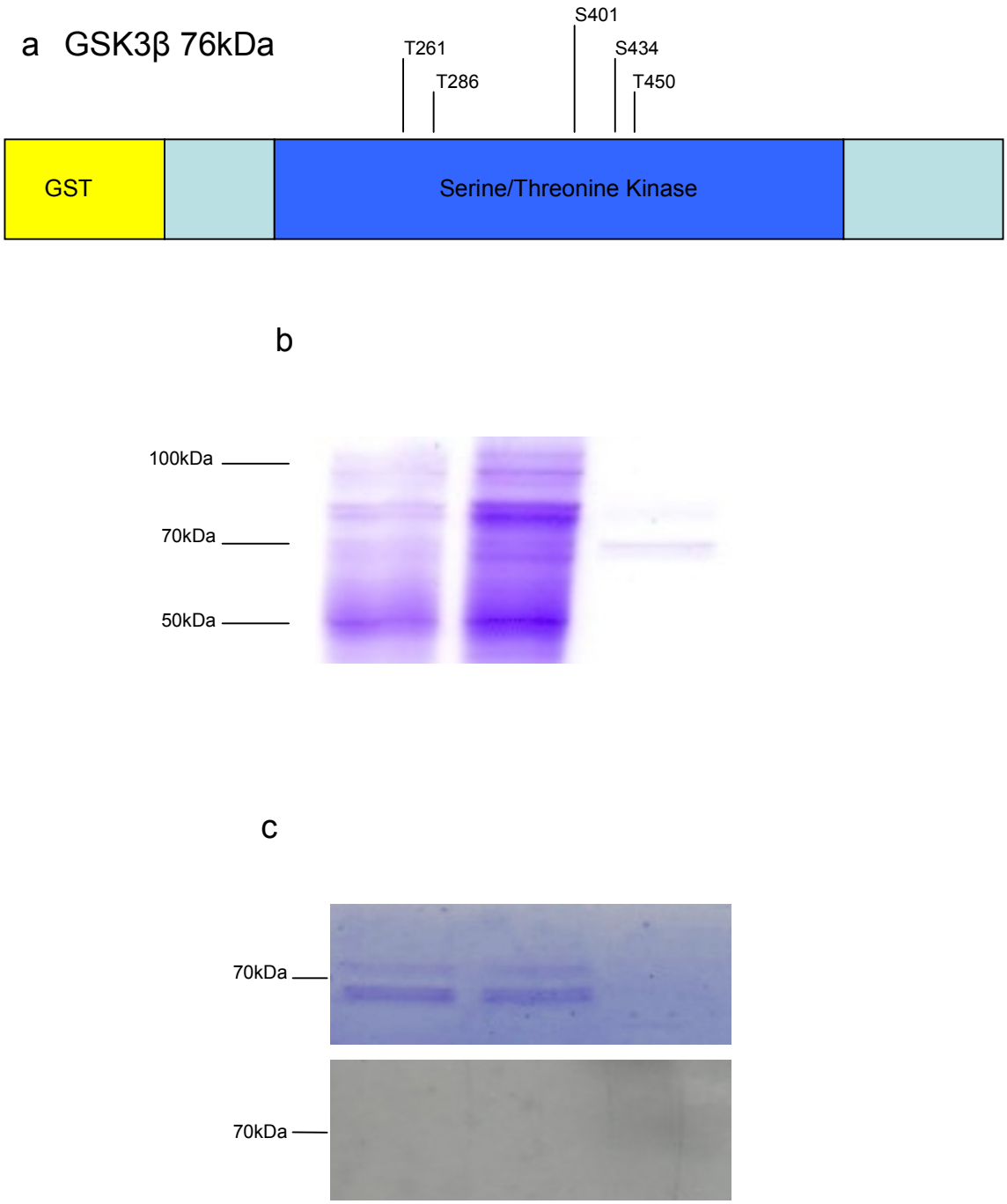

Figure 5.6 GSK3β is not Phosphorylated by PKCι in an *in vitro* Kinase Assay

(a) A schematic diagram of the domains in GSK3β tagged to GST including the potential phosphorylation sites predicted by Scansite, **(b)** GSK3β-GST is expressed in E.coli following the addition of L-arabinose and successfully purified using glutathione sepharose beads, **(c)** The GSK3β-GST fusion protein was used in a kinase assay with PKCι, but no phosphorylation was detected by autoradiography (bottom panel). The purified GSK3β - GST protein can be seen on the Coomassie stained kinase assay SDS-PAGE gel (top panel).

5.4 Discussion

In this chapter the unsuccessful cloning of Scribble and Patj, into GST vectors has been described as well as the successful cloning of Pals-1 and Dlg. Pals-1, LGN and GSK3β kinase assays with PKCι that could not detect phosphorylation have also been described. The results of these experiments are summarised in table 5.1. Also in this chapter it has been shown that Dlg unexpectedly increases the phosphorylation of PKCι.

DNA	PCR	TOPO®	KA
Patj	✓	✗	N/A
Scribble	✓	✗	N/A
Pals-1	✓	✓	✓
Dlg	✓	✓	✓
LGN	N/A	N/A	✓
GSK3β	N/A	N/A	✓

Table 5.1 A Summary of the Progress made with Cloning of the Genes into GST Vectors and the Following Kinase Assays.

The unsuccessful attempts to make Patj and Scribble GST fusion proteins may have been due to the large size of the transcripts. Patj is 4.7 kb and Scribble is 4.8kb. Dlg and Pals-1 which were successful are 2.7kb and 2kb respectively. The TOPO® manufacturers indicate that the TOPO® vector will take sequences up to 10kb, however, they do say that longer ligation times may be required for larger plasmids. If more time was available, the Patj and Scribble could have been cut into two parts and put into the TOPO® vector separately. This would hopefully allow the incorporation of the smaller piece of DNA into the TOPO® vector. However, when the protein is expressed, only half of it would be there at any one time and this may affect the folding of the protein and possible phosphorylation by PKCι. This could lead to false positives or missing PKCι phosphorylation altogether. Another way round the problem of creating a GST fusion protein would be to use another method to incorporate the Scribble and Patj DNA into a GST vector. One such method is to cut the vector and the DNA of Scribble or Patj with different restriction enzymes, so that the vector cannot self ligate (because the sticky ends are different) but will ligate to the Scribble or Patj DNA as they will be cut to complement the sticky ends of the vector. This would allow incorporation of the whole Scribble or Patj DNA sequence into the GST

vector. DMSO was used in the Scribble PCR to help break down secondary structures in GC rich DNA. The DMSO was not removed and may have been a factor in the Scribbles TOPO® not working, even though it was at a low concentration in the final reaction (1.67%). In future, the PCR product should be gel extracted to remove the DMSO in case it is affecting the TOPO®.

The results in figure 5.3 indicate that Pals-1 is not phosphorylated by PKCι in an *in vitro* kinase assay. However, due to the limitations with an *in vitro* method, the situation *in vivo* cannot be determined. For example, Pals-1 may need a binding partner to be recognised by PKCι. Pals-1 may also need a post-translational modification, which does not occur in bacteria, to be recognised and or phosphorylated by PKCι. It is impossible to prove that Pals-1 is not phosphorylated by PKCι, but this data suggests that it may not be the case and it is likely that as it is not phosphorylated *in vitro,* it is not phosphorylated *in vivo* either. This suggests that PKCι is not regulating polarity by phosphorylating and controlling the function of Pals-1.

The surprising result from this chapter was that Dlg increases the amount of PKCι phosphorylation (figure 5.4). Dlg is a MAGUK protein, but its kinase domain is inactive (Kistner et al., 1995). Therefore it must be PKCι autophosphorylation that is increased by Dlg. An assay to confirm that Dlg increases PKCι autophosphorylation *in vivo* would be to see if the amount of Dlg protein in a cell alters the amount of PKCι phosphorylation of its known targets such as Lgl or Par-1b. This could be achieved by overexpressing or knocking down Dlg.

Dlg recruitment to the leading edge of migrating astrocytes is controlled by the Par-PKCι/ζ complex, knock down of PKCζ or PKCζ inhibition prevents the recruitment of Dlg to the leading edge. However, Dlg knockdown does not alter PKCζ localisation (Etienne-Manneville et al., 2005). The Dlg recruitment to the leading edge could activate PKCι further at the leading edge and drive migration. Dlg mutants do have abnormal cell polarity in *Drosophila* (Bilder et al., 2000; Wodarz, 2000). Dlg localises to the sites of cell-cell contact in polarised cells, but has not been reported to directly colocalise with PKCι or PKCζ. However, Dlg may still activate PKCι by interacting with it transiently. Dlg may transiently localise with and activate PKCι during the establishment of polarity. Live cell imaging of Dlg and PKCι during the establishment of polarity would reveal if this occurs.

Dlg localises to the mitotic spindle in mitosis (Narayan et al., 2009) as does PKCι/ζ (chapter 3). It is possible then that one of the roles of Dlg at the mitotic spindle is to

activate PKCι/ζ by causing autophosphorylation. This would explain the increase in PKCι autophosphorylation seen in the kinase assay containing Dlg in this work and the increase in active phospho-PKCι/ζ seen in mitotic cells on the centrosomes and spindle (chapter 3). To test this, co localisation of Dlg with PKCι needs to be established at the mitotic spindle. If this co localisation occurs then a knock down of Dlg in mitotic cells needs to be performed to see a decrease in PKCι/ζ autophosphorylation.

The results in figure 5.5 indicate that, although there are predicted phosphorylation sites within LGN, phosphorylation of LGN by PKCι could not be detected using this assay. Due to the limitations with an *in vitro* method, the situation *in vivo* cannot be determined. For example, as with Pals-1, LGN may need a binding partner to be recognised by PKCι. LGN may also need a post-translational modification that does not occur in bacteria to be recognised and or phosphorylated by PKCι. However, Zheng and colleagues have very recently published data showing that LGN is apically excluded in MDCK cells, and that this exclusion is mediated by PKCι/ζ and that kinase activity of PKCι/ζ is important (Zheng et al., 2010). This indicates that PKCι/ζ either phosphorylates LGN directly or that it phosphorylates another protein that mediates the exclusion effect on LGN. Interestingly the authors do not show an *in vitro* kinase assay for PKCι/ζ and LGN. Further work will be required to elucidate the exact mechanism. As PKCι/ζ and LGN colocalise in HEK293 cells during mitosis (Yasumi et al., 2005), it will be interesting to see if this occurs in other polarised cell types, and whether this occurs during mitosis. LGN may still be phosphorylated by PKCι, but may only bind to PKCι in the complex with Par-6 and Lgl. Potentially this can be followed up with a kinase assay using more than just LGN and PKCι, but include Lgl and or Par-6 proteins.

The results in figure 5.6 show that phosphorylation of GSK3β by PKCι could not be detected in an *in vitro* kinase assay. It has been shown that PKCι/ζ activity causes the phosphorylation of GSK3β *in vivo*, however, direct phosphorylation has not been shown (Etienne-Manneville and Hall, 2003a). The authors of this paper make no mention of PKCι, and the inhibitors and the antibodies they use are not proven in the paper to only inhibit/detect PKCζ. This makes it possible that they are presenting results that are relevant to PKCζ and PKCι. Because of this it is unlikely that it is due to the use of PKCι in the kinase assay instead of PKCζ that is responsible for the lack of phosphorylation visualised. So there are three possibilities, either GSK3β is not phosphorylated by PKCι at all, that

GSK3β needs some sort of post translational modification or binding partner before it can be phosphorylated by PKCι or that PKCι is phosphorylating another kinase that goes on to phosphorylate GSK3β. This would explain the phosphorylation seen *in vivo*, but not in the *in vitro* kinase assay presented here. If it is a binding partner that is required, it may be bound to unphosphorylated GSK3β which could be immunoprecipitated from a cell lysate and the binding partner identified. If it is another kinase such as Par-1 that is phosphorylating GSK3β then an *in vitro* kinase assay with kinases that PKCι phosphorylates could be set up. If one is found, this can be knocked down *in vivo* to see if there is a decrease in GSK3β phosphorylation.

Chapter 6

The Hippo Pathway and PKCι

6.1 Introduction

6.1.1 The Hippo Pathway

The Hippo pathway controls proliferation and cell death in epithelial cells and is linked to the control of organ size and tumorigenesis. Activation of the Hippo pathway suppresses Yap and Taz, which are transcriptional co-activators. This results in repression of cell proliferation. As depicted in figure 6.1, the mammalian hippo pathway consists of Mst1/2 (*Drosophila* hippo) a Ste-20 family protein kinase, which interacts with Salvador, a scaffold protein (Callus et al., 2006) and phosphorylates Lats1/2 (*Drosophila* Warts), a serine threonine kinase (Chan et al., 2005). Lats1/2 then phosphorylates Yap (*Drosophila* Yorkie) and its paralog Taz (Hao et al., 2008; Lei et al., 2008; Zhao et al., 2007) sequestering Yap outside of the nucleus where it is unable to act as a transcriptional co-activator (Basu et al., 2003)

6.1.2 Mst1/2, Hippo and Salvador

Mst1/2 and Hippo are serine/threonine kinases. In *Drosophila* eye discs, mutation of Hippo causes tissue overgrowth (Harvey et al., 2003). The C-terminal portion of Hippo binds the N-terminal of Salvador, which aids the binding of Hippo to Warts and the phosphorylation of Warts. Hippo is required for cell cycle exit as Hippo mutant cells continue dividing, creating overgrowth. There are also elevated protein levels of Cyclin E. DIAP1 protein levels are also elevated in Hippo mutant cells. Overexpression of Hippo decreases DIAP1 protein levels. Hippo can phosphorylate DIAP1 *in vitro,* but it has not been shown if this occurs *in vivo* and causes DIAP1 degradation.

In mammals, MST1/2 binds to WW45 and phosphorylates Lats1/2 which then phosphorylates Yap, sequestering Yap out of the nucleus (Zeng and Hong, 2008). Yap is not phosphorylated by Lats1 in overexpression studies, unless Mst2 is also overexpressed (Oka et al., 2008). This indicates that Mst1/2 and Lats1/2 act in the same way in mammals as they do in *Drosophila.*

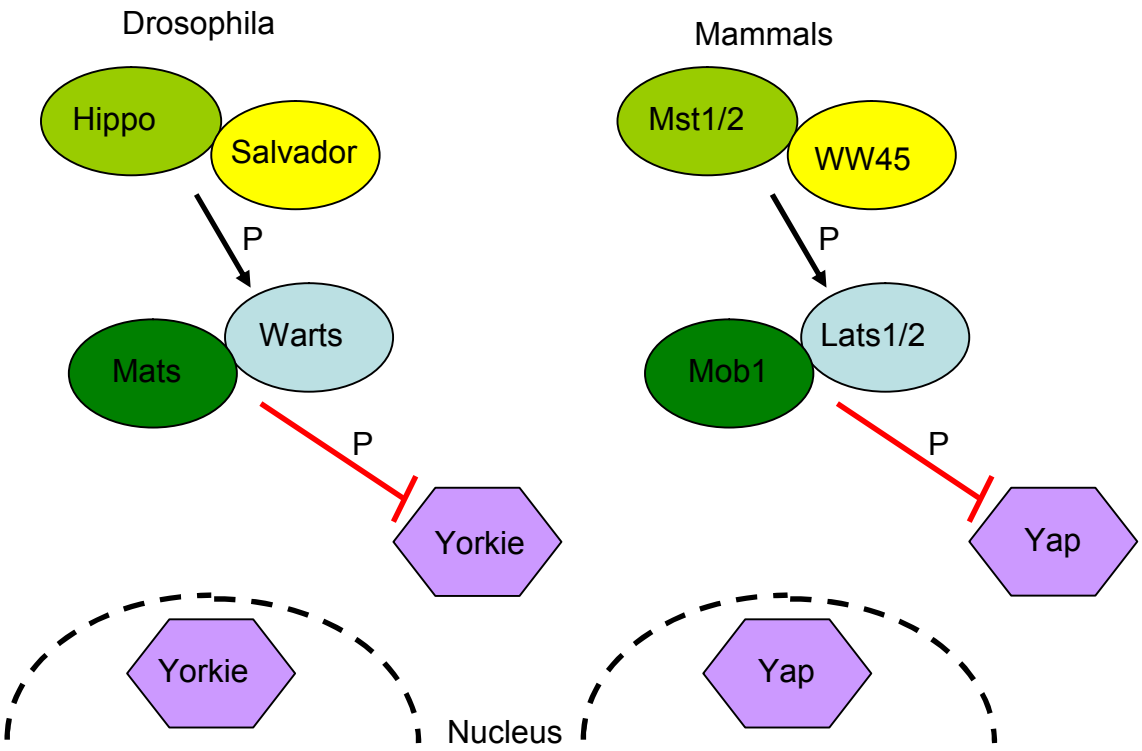

Figure 6.1 The *Drosophila* and Mammalian Hippo Pathways

A comparison of the *Drosophila* and mammalian Hippo pathways. Mst1/2 (Hippo) binds to WW45 (Salvador), which promotes the phosphorylation of Lats1/2 (Liu et al.) by Mst1/2. Lats1/2 interacts with Mob1 (Mats) and phosphorylates Yap (Yorkie) causing its retention in the cytoplasm, out of the nucleus.

6.1.3 Lats and Warts

Lats1 and Lats2 are the mammalian orthologues of *Drosophila* Warts (Hori et al., 2000). Lats1 and Lats2 interact with Yap in Hela cells (Hao et al., 2008; Zhang et al., 2008) and in Cos7 cells (Hao et al., 2008). Lats1 interacts with Yap via the WW domains of Yap and the PPXY motif in Lats1 (Oka et al., 2008). When Yap is overexpressed in MCF10 cells there is an increase in anchorage independent growth and cell migration; however, when Lats1 is co-expressed with Yap the phenotype is cancelled, indicating that Lats1 represses Yap (Zhang et al., 2008). Yap is phosphorylated by Lats1 and Lats2 *in vivo* in Cos7 cells. There are five Lats phosphorylation sites in Yap: S61, S109, S127, S164 and S397, two of which are conserved in *Drosophila* Yorkie, S109 and S127 (S111 and S168 in *Drosophila*). Lats1 phosphorylation of Yap sequesters it in the cytoplasm shown by a double transfection of Lats and Yap; however, Lats1 and Yap S5A (all five serines mutated) results in Yap nuclear accumulation. This indicates that Lats1 represses Yap via

phosphorylation (Hao et al., 2008). Lats binds to Mob1 which stimulates the kinase activity of Lats1/2 (Lai et al., 2005; Wei et al., 2007).

6.1.4 Yap and Yorkie

Yap was first characterised in 1995, Yap mRNA was found at high levels in the placenta, testis, ovary and small intestine and at lower levels elsewhere (Sudol et al., 1995). Yap regulation is important for the control of organ size. Yap contains two WW domains which bind proline rich sequences in the TEAD family of transcription factors. Activation of Yap in the liver of adult mice results in a four fold increase in liver size, and in the intestine, Yap overexpression results in an expansion of progenitor cells (Camargo et al., 2007). Yap activating mutations phenocopy the Mst1/2, Lats and Salvador loss-of-function mutations. The *Drosophila* homologue of Yap is Yorkie and Yap can functionally replace Yorkie in *Drosophila* (Huang et al., 2005). Yorkie co-immunoprecipitates from *Drosophila* S2 cells with Warts and the WW domains of Yorkie are required for this interaction. Warts phosphorylates Yorkie *in vitro* (Huang et al., 2005). Phosphorylation of Yorkie at serine 168 increases when Yorkie and Hippo, Salvador or Warts are overexpressed together in S2 cells. This phosphorylation causes Yorkie to bind 14-3-3 proteins and sequesters Yorkie in the cytoplasm, out of the nucleus. Conversely, loss of Hippo signalling causes Yorkie nuclear accumulation (Dong et al., 2007). Yorkie is phosphorylated by Warts *in vivo* and there appear to be multiple phospho-isoforms. A Yorkie mutant that has a serine to alanine mutation at serine 168 (S168A), which prevents the serine phosphorylation, cannot bind 14-3-3 proteins and accumulates in the nucleus; however there is still some cytoplasmically located Yorkie. This indicates that there might be another mechanism that either puts more Yorkie in the nucleus or sequesters it out of the nucleus. The Yorkie S168A mutant is hyperactivated, indicated by a severe overgrowth phenotype, which resembles the Hippo mutant (Oh and Irvine, 2008).

Another mode of Yorkie regulation is mediated via its WW domains. Yorkie binds Expanded at the apical domain of cells via the WW domains in Yorkie and the PPXY motif within Expanded. This binding does not require Yorkie phosphorylation. Yorkie binding to Expanded inhibits Yorkie, presumably by keeping it out of the nucleus (Badouel et al., 2009). If the Yorkie WW domains are mutated Yorkie no longer localises to the apical domain (Zhang et al., 2009). Yorkie also binds Hippo via its WW domain and the PPXY motif in Hippo, which also represses Yorkie activity (Oh et al., 2009), so Yorkie signalling can be attenuated by direct binding to members of the Hippo pathway as well as

phosphorylation by Warts. However, this direct binding regulation has yet to be shown for mammalian Yap.

6.1.5 Downstream of Yap and Yorkie

Downstream of Yorkie is a transcription factor called Scalloped (Goulev et al., 2008). Downstream of Yap is the TEAD family of transcription factors and targets of these include connective tissue growth factor (CTGF) (Zhao et al., 2008) DIAP1, CyclinE (Kango-Singh et al., 2002; Tapon et al., 2002) and Expanded (Badouel et al., 2009). CTGF promotes cell migration and proliferation in fibroblasts and is also involved in extracellular matrix remodelling (Moussad and Brigstock, 2000). DIAP1 is a caspase inhibitor and therefore prevents caspase-dependent cell death (Wang et al., 1999). Cyclin E is involved in the G1-S phase transition of the cell cycle (Ohtsubo et al., 1995). Anti-Cyclin E antibodies prevent fibroblasts going into S-phase when microinjected into them.

6.1.6 The Hippo Pathway and Cancer

Hippo pathway misregulation leads to tissue overgrowth and Yap is thought to be an oncogene. Overexpression of Yap in MCF10A breast cells induces EMT, anchorage independent growth and inhibition of apoptosis (Overholtzer et al., 2006). Therefore, Yap can transform MCF10A cells. High levels of Yap and nuclear accumulation of Yap have also been found in colonic adenocarcinoma, lung adenocarcinoma and ovarian serous cystadenocarcinoma (Steinhardt et al., 2008). There is also strong nuclear Yap staining in hepatocellular carcinoma (Zhao et al., 2007) and the presence of high levels of Yap correlate with a poor patient prognosis (Xu et al., 2009).

6.1.7 Upstream of the Hippo Pathway

Upstream of the Hippo pathway in *Drosophila*, there are multiple mechanisms of regulation. One protein upstream of the Hippo pathway is the transmembrane cadherin Fat, which binds to Dachsous, another transmembrane cadherin. These two proteins recruit each other to the membrane (Willecke et al., 2008). Phosphorylation of Fat and Dachsous by the kinases, Four-jointed and Discs overgrown regulates their binding (Feng and Irvine, 2009; Ishikawa et al., 2008). Fat and Dachsous signal through the unconventional myosin Dachs, which stabilises Warts (Cho et al., 2006) allowing Hippo pathway activation; however, how this stabilisation occurs is unknown. Fat and Dachsous are also regulated by Lowfat, which stabilises them (Mao et al., 2009), though again, how this stabilisation is

achieved is unknown. Another protein, Approximated, a palmitoyltransferase, also regulates Fat signalling by regulating the localisation and levels of Dachs (Matakatsu and Blair, 2008). High levels of Approximated lead to low levels of Dachs and therefore Hippo pathway suppression. A direct Hippo inhibitor is *Drosophila* RASSF (dRASSF). dRASSF binds directly to Hippo which prevents Hippo from binding to Salvador (Polesello et al., 2006). This prevents the activation of Warts and consequently represses the Hippo pathway.

Yorkie can also be directly inhibited by direct association with Expanded; this inhibition is possibly mediated by Expanded sequestering Yorkie out of the nucleus (Badouel et al., 2009). This sequestration would prevent Yorkie from acting as a transcriptional co-activator.

Another mode of Hippo regulation is through the Kibra-Expanded-Merlin complex. Expanded and the cytoskeletal protein, Merlin bind the WW-domain containing protein, Kibra at the apical membrane and this results in the core Hippo pathway components being localised to the apical membrane for activation (Baumgartner et al., 2010; Genevet et al., 2010; Yu et al., 2010). How the Kibra-Expanded-Merlin complex activates the core Hippo pathway components is unknown.

Crumbs also regulates the Hippo pathway by binding to Expanded and localising it to the apical membrane (Ling et al., 2010). This localisation would allow Expanded to bind Merlin and Kibra. Kibra is also phosphorylated by PKCζ (Buther et al., 2004), however, whether this phosphorylation has any effect on the binding of Kibra to Expanded and Merlin and therefore any effect on the Hippo pathway is unknown.

PKCι/ζ and Lgl also regulate the Hippo pathway. Lgl inhibits PKCι/ζ which activates the Hippo pathway. So if PKCι/ζ is not inhibited the Hippo pathway is inhibited by PKCι/ζ leading to Yorkie activation. PKCι/ζ inhibits the Hippo pathway by mislocalising Hippo and dRASSF, therefore preventing the interaction of Hippo with Salvador (Grzeschik et al., 2010). However, how this affect by PKCι/ζ is mediated is unknown. This links polarity complexes directly to Hippo pathway regulation

6.1.8 The Hippo Pathway and Polarity

In *Drosophila* it has also been shown that Warts mutant cells have larger apical domains (Justice et al., 1995). Two papers have been recently published that link polarity and the hippo pathway, both used *Drosophila* as a model organism. Genevet and

colleagues created a null Hippo mutant and showed that in imaginal discs there is an increase in the apical domain and an increase in the amount of PKCι protein present at the apical membrane (Genevet et al., 2009). They also showed that the adherens junctions are larger. The authors suggest that either Yorkie activates an apical determinant or that there maybe an imbalance between apical and basal endocytosis. Hamaratoglu and colleagues showed that in Hippo and Warts mutants, membrane levels of DaPKC, Patj and Crumbs are increased in the wing, antenna and eye imaginal discs (Hamaratoglu et al., 2009). The authors suggest that the Hippo pathway regulates the amount of apical complexes at the membrane.

On the basis of the polarity and Hippo pathway links and that PKCι is often upregulated in cancer, as is Yap; Yap became a possible target of PKCι. The following work was done in collaboration with Dr. Makoto Furutani-Seiki and Dr. Stefan Bagby (University of Bath). As this is a collaboration, Medaka Yap and Taz were used. The Yap and Taz only contain about first 250 amino acids, they are missing about 200 aminoacids from the C-terminal, which contains a PDZ motif and SH3 domain.

6.2 Results

6.2.1 PKCι Phosphorylates Yap and Taz

As the Hippo pathway appears to interact with polarity proteins it was hypothesised that PKCι may directly phosphorylate members of the Hippo pathway. Yap and Taz were scanned using Scansite which showed they have predicted PKCι phosphorylation sites and Figure 6.2a depicts the domains of the proteins with the predicted scansite phosphorylation sites in black and the Lats sites in red. The S397 is not shown as this is a small piece of Yap that does not contain this site. Purified Yap and Taz were kindly donated by Claire Webb and Stefan Bagby (University of Bath). The Coomassie stain of the purified proteins is shown in figure 6.2b. These proteins were put into a kinase assay with PKCι, run on an SDS-PAGE gel and visualised using autoradiography. Clear phosphorylation of Yap and Taz by PKCι can be seen in figure 6.2c; therefore, Yap and Taz are *in vitro* PKCι targets.

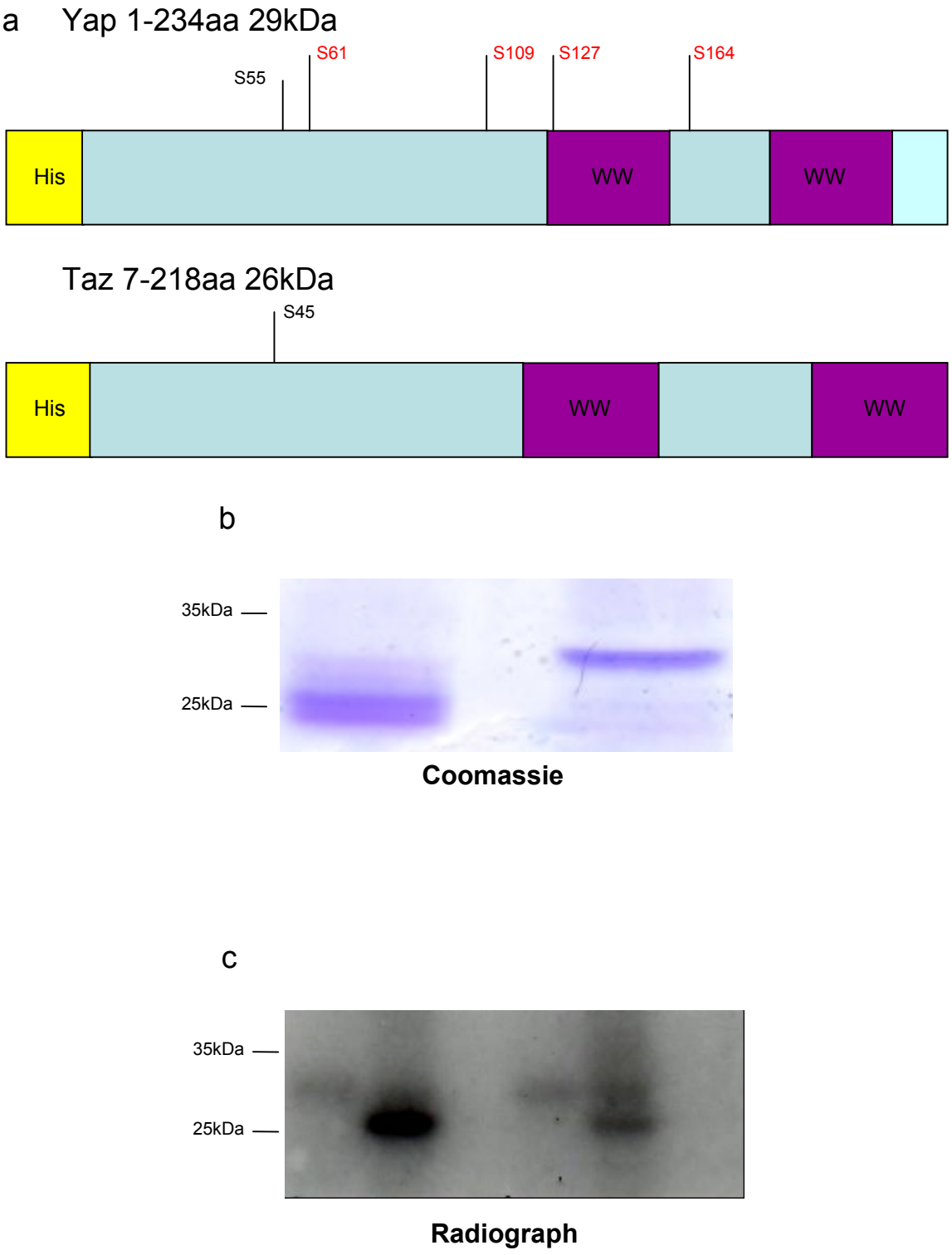

Figure 6.2 Yap and Taz are Phosphorylated by PKCι *in vitro*

(a) A schematic diagram of the domains of Yap and Taz tagged to His including the phosphorylation sites predicted by Scansite in black (S54 and S45 respectively) and the known Lats phosphorylation sites for Yap in red, **(b)** His column purified Taz and Yap, **(c)** The purified His-tagged Taz and Yap were used in a kinase assay with PKCι. Clear phosphorylation of Taz and Yap can be seen on the autoradiograph.

6.2.2 A Truncated Version of Yap and Taz, Missing the Potential PKCι Phosphorylation Sites Predicted by Scansite is Not Phosphorylated by PKCι

The predicted PKCι phosphorylation sites for Yap and Taz were at S54 and S45 respectively. Claire Webb and Stefan Bagby kindly donated purified Yap and Taz that was truncated so didn't contain the predicted PKCι phosphorylation sites; however, it does still contain the three of the five serines phosphorylated by Lats1.

The schematic diagrams for the truncated Yap and Taz are depicted in figure 6.3a. The truncated proteins were put into a kinase assay with PKCι, run on an SDS-PAGE gel and visualised by autoradiography. The truncated Yap and Taz proteins were not phosphorylated by PKCι in an *in vitro* kinase assay (figure 6.3b). This experiment was repeated three times and the same result was achieved each time, so it can be concluded that PKCι phosphorylates the N-terminal part of Yap and Taz. MBP was used as a positive control, to ensure the PKCι was functional. MBP was phosphorylated by PKCι (figure 6.3c) indicating that the *in vitro* kinase assay worked correctly.

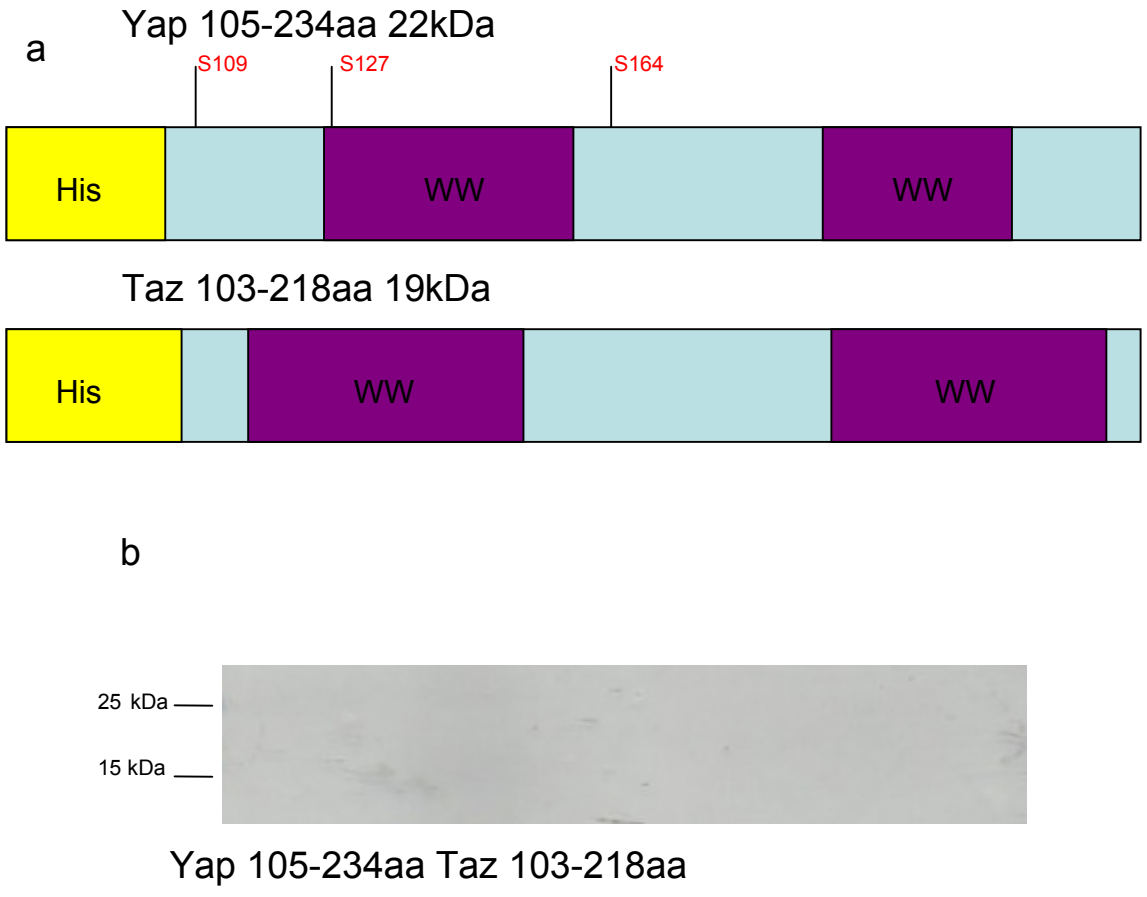

Figure 6.3 A Truncated Version of Yap and Taz, Missing the Potential PKCι Phosphorylation Sites Predicted by Scansite is not Phosphorylated by PKCι

(a) A schematic diagram of the domains of truncated Yap and Taz tagged to His which are missing the potential PKCι phosphorylation site predicted by Scansite, but still contain three of the Lats sites (in red), **(b)** The purified, truncated Yap and Taz were used in a kinase assay with PKCι. No phosphorylation could be visualised on the autoradiograph, **(c)** MBP was used as a positive control for the kinase assay; clear phosphorylation of MBP can be seen on the autoradiograph.

6.2.3 Mutated Yap and Taz are still Phosphorylated by PKCι

Plasmid DNA coding for Yap and Taz was kindly donated by Makoto Furutani-Seiki. To determine if Yap and Taz are phosphorylated on S54 and S45 respectively, they were mutated to alanines. The sequences surrounding the predicted phosphorylation sites are identical, so the same primers were used for both Yap and Taz. The sequences are depicted in figure 6.4.

Yap - VVPQSVPMRMRKLPDSFFKPPEPKSHSRQASTDAG

Taz - RQPSSVPMRMRKLPDSFFKPPEPRGHSRQASSDGG

Figure 6.4 Sequence Comparisons Between Taz and Yap
A sequence comparison of the amino acids surrounding the predicted serine phosphorylated by PKCι (in red). The amino acids either side of the predicted serine are almost identical although they differ more as you get further upstream or downstream of the serine.

The mutations were made using site directed mutagenesis and confirmed by sequencing. The schematics in figure 6.5a depict the domains of Yap and Taz with their mutations.

The Yap and Taz proteins were made in E.coli and purified. The mutant proteins along side the wild type were then put into a kinase assay with PKCι as before. The kinase assay products were then run on an SDS-PAGE gel and visualised using autoradiography. The top panels in figures 6.5b and c show the Coomassie stained gel and therefore the proteins in the kinase assay. The lower panels in figure 6.5b and c shows the autoradiograph. Yap and Taz S54A and S45A mutants are still phosphorylated by PKCι. This result indicates that this site is either not phosphorylated by PKCι or that it is and is one of multiple PKCι phosphorylation sites in Yap and Taz. It is likely that there are multiple sites as the phosphorylation of the mutants appeared to be less than that of the wild type protein. However, this has not been quantified.

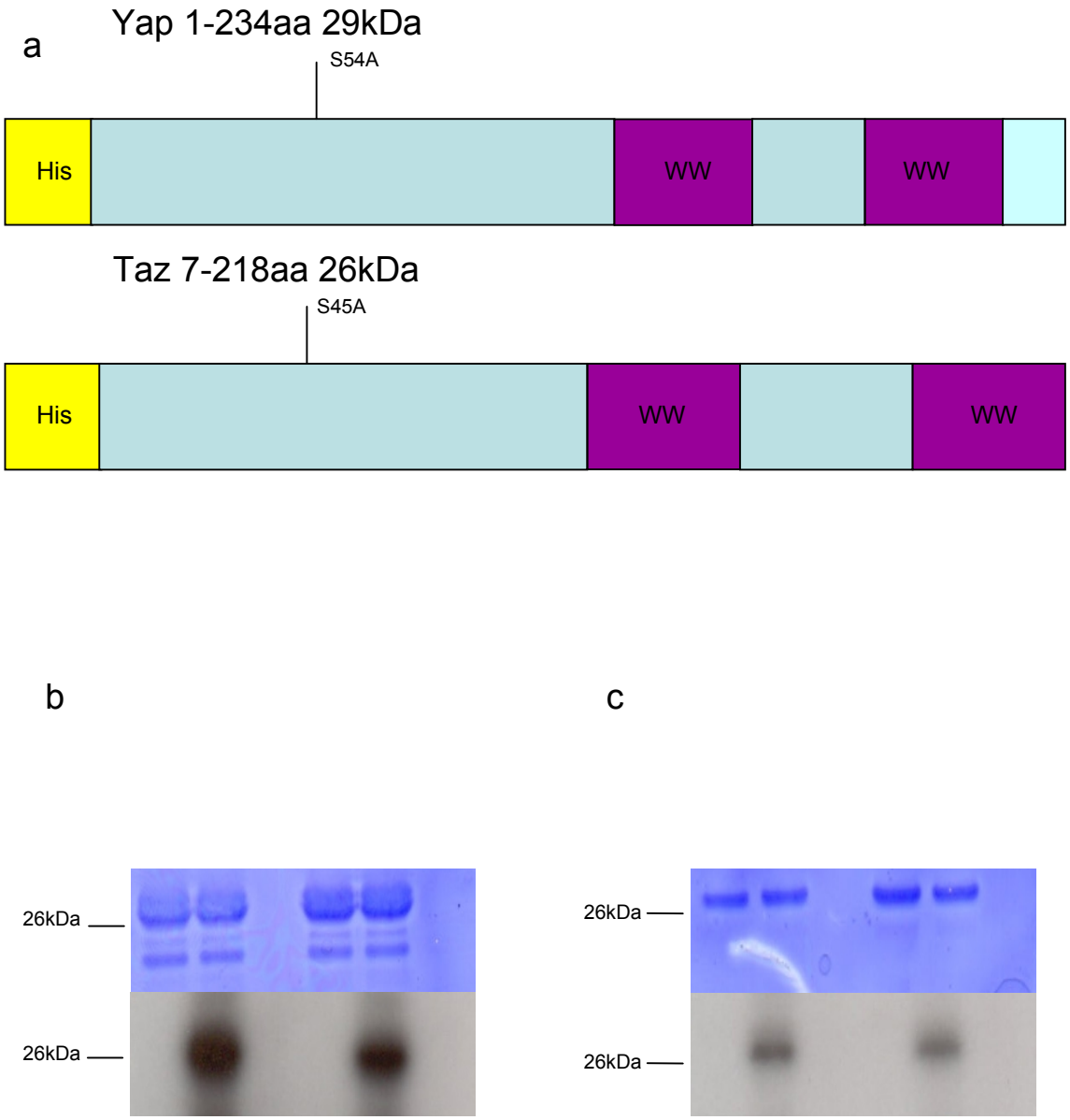

Figure 6.5 Yap and Taz, when Mutated at the Scansite Predicted Serine are still Phosphorylated by PKCι in an *in vitro* Kinase Assay

(a) A schematic of the domains of Taz and Yap tagged to His including the serine phosphorylation sites predicted by Scansite mutated to alanine, **(b)** The purified His-tagged S54A Yap was used in a kinase assay with PKCι. Clear phosphorylation of S54A Yap can be seen on the autoradiograph (lower panel). The purified S54A Yap protein can be seen on the Coomassie stained kinase assay SDS-PAGE gel (top panel), **(c)** The purified His-tagged S45A Taz was used in a kinase assay with PKCι. Clear phosphorylation of S45A Taz can be seen on the autoradiograph. The purified S45A Taz protein can be seen on the Coomassie stained kinase assay SDS-PAGE gel (top panel).

6.2.4 Overexpression of Yap and PKCι causes Nuclear Accumulation of Yap

The data shown in figures 6.2, 6.3 and 6.5 show that PKCι phosphorylates Yap and Taz. To begin to establish the functional relevance of this it was decided to overexpress human Yap and human constitutively active PKCι together in MDCK cells and see if there was any movement of Yap within the cell.

The consitutively active PKCι has an alanine to glutamate substitution at residue 120. this is within the pseudosubstrate domain and has been shown to be active using an invitro kinase assay (Spitaler et al., 2000). When Yap is overexpressed in MDCK cells alone it shows uniform cytoplasmic staining (figure 6.6a). However, when PKCι and Yap were overexpressed together in MDCK cells strong nuclear staining of Yap could be seen (figure 6.6b). Therefore, PKCι causes Yap nuclear translocation. The *in vitro* studies were carried out with Medaka Yap, however, in the expression studies Human Yap was used. The two proteins are similar and the predicted PKCι phosphorylation site is conserved.

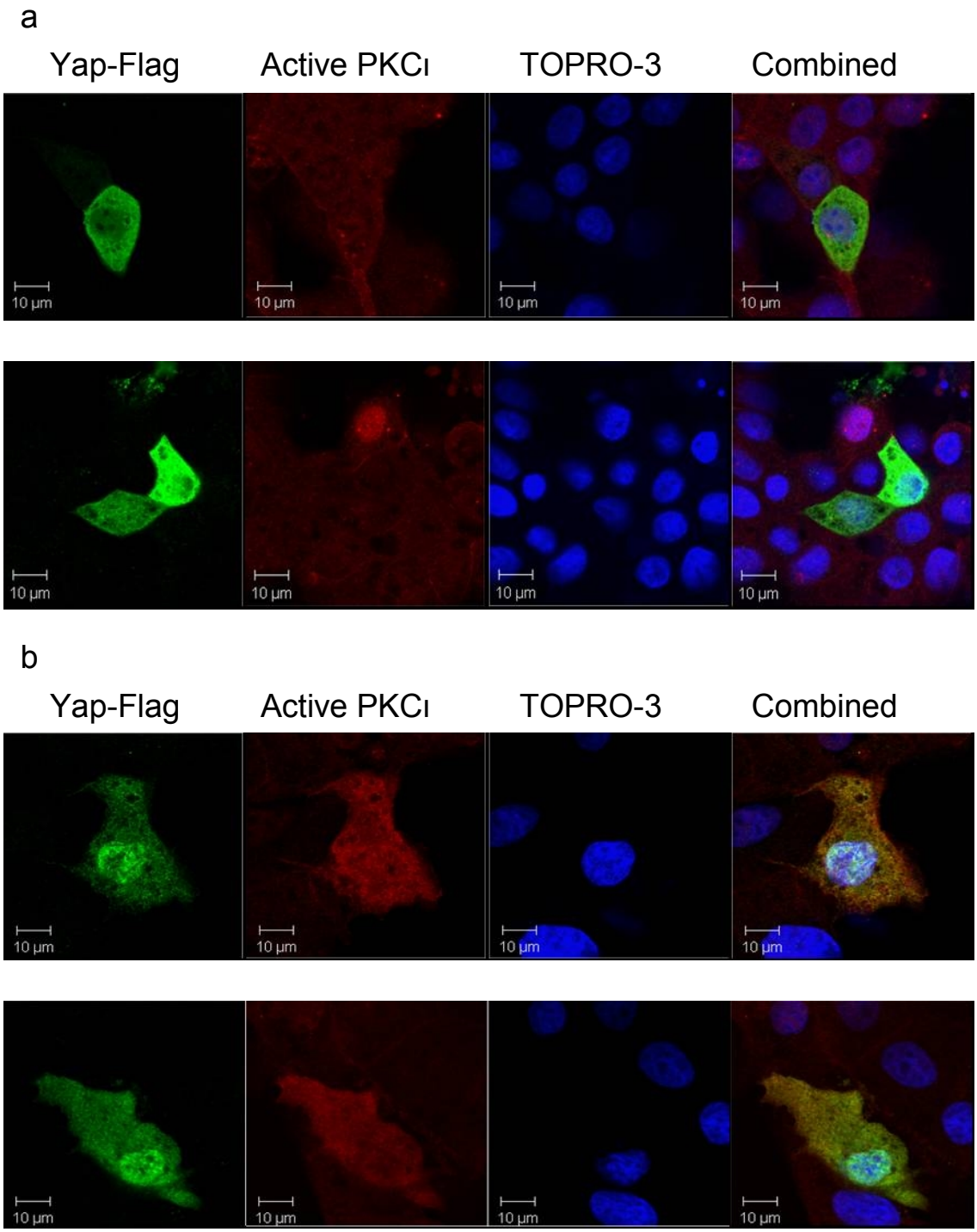

Figure 6.6 PKCι Causes Yap to Move into the Nucleus when they are Overexpressed in MDCK Cells

(a) When Flag tagged Yap is overexpressed in MDCK cells it shows uniform cytoplasmic staining, two representative images containing transfected cells are shown (upper and lower panels) **(b)** When Flag tagged Yap is overexpressed with PKCι in MDCK cells, there is clear nuclear accumulation of Yap, but not PKCι, two representative images containing transfected cells are shown. The antibody used can detect PKCι and PKCζ.

6.3 Discussion

Yap and Taz act at the end of the Hippo signalling pathway. The data presented here shows that PKCι phosphorylates Yap and Taz *in vitro* on the N-terminal part of the protein (figure 6.3) and PKCι can promote the nuclear localisation of Yap (figure 6.4).

It appears that S54 and S45 are not the only phosphorylation targets for Yap and Taz respectively. When these sites were mutated to alanine phosphorylation of Yap and Taz by PKCι still occurs (figure 6.4). Therefore, these serines may be a PKCι phosphorylation targets, but cannot be the only phosphorylation site. The slight reduction in phosphorylation of the mutant Yap and Taz is consistent with this idea. This needs to be investigated further. The Yap and Taz protein sequences will have to be examined manually using the PSSM for PKCι (Fujii et al., 2004). There are thirteen serines and two threonines in the N-terminal half of Yap and Taz. This will allow a screen of the sequence and will hopefully identify candidate serine or threonine PKCι phosphorylation sites that can be mutated to alanine and used in an *in vitro* kinase assay to identify the PKCι phosphorylation site(s). The C-terminal half of Yap and Taz also needs to be checked using the *in vitro* kinase assay for PKCι phosphorylation. This phosphorylation also needs to be investigated *in vivo*. Once the phosphorylation sites have been elucidated a phospho-specific antibody could be generated and applied to cells overexpressing Yap and PKCι to see if it is the phosphorylation that causes nuclear localisation. The phospho-specific antibody could also be used to look for endogenous Yap phosphorylation. If PKCι phosphorylation causes Yap to move into the nucleus then only phospho-Yap will be seen in the nucleus. Another use for this antibody could be to see whether knocking down PKCι/ζ stops the Yap phosphorylation, to show that PKCι/ζ is the only kinase that phosphorylates Yap on those site(s).

When PKCι and Yap are overexpressed together, a significant portion of the Yap protein relocalises to the nucleus (figure 6.5). The phosphorylation of Yap by PKCι is likely to be the signal for Yap to move into the nucleus. This will have to be proven once the site(s) of Yap phosphorylation by PKCι are found. These site(s) can be mutated to alanine and if when overexpressed with PKCι the serine-alanine mutant does not go into the nucleus, the PKCι phosphorylation is the signal. This can be achieved using a Yap antibody or tagging the mutated Yap and using an antibody against the Tag. It will also be interesting to see if PKCι overexpression has the same effect on endogenous Yap as it does

on overexpressed Yap. A PKCι/ζ inhibitor could also be used to test whether endogenous Yap becomes less phosphorylated or moves out of the nucleus upon PKCι/ζ inhibition.

The phosphorylation of Taz by PKCι also needs to be investigated as little is known about the targets or regulation of Taz. To see if the same effect of PKCι on Yap occurs with Taz, it will be interesting to overexpress Taz with PKCι and see if nuclear accumulation of Taz occurs. If it does, the same experiments described for Yap can be carried out.

As high nuclear levels of Yap are found in many cancers (Steinhardt et al., 2008; Zhao et al., 2007), as is PKCι (Eder et al., 2005; Kojima et al., 2008; Li et al., 2008; Patel et al., 2008; Regala et al., 2005b; Scotti et al., 2010; Takagawa et al., 2010; Wang et al., 2009; Yang et al., 2008; Zhang et al., 2006) and the overexpression phenotype of Yap is tissue overgrowth and transformation (Overholtzer et al., 2006), it is possible that one of the effects of PKCι overexpression in cancer is to cause Yap to move into the nucleus and act as a transcriptional co-activator leading to transformation and overgrowth. This theory can be tested by knocking down Yap in a PKCι high expression setting such as a cancer cell line with high PKCι levels, such as A549, and see if transformation and proliferation still occur.

In a normal non-cancerous setting, the Hippo signal may override the PKCι signal as PKCι is mainly localised to the apical junctions not the nucleus (chapter 3). This may prevent PKCι from binding to and phosphorylating Yap, and therefore giving it a nuclear signal. However, PKCι may also phosphorylate Yap in the cytoplasm. PKCι/ζ also regulates the Hippo pathway by mislocalising Hippo, so there are two modes of Hippo regulation by PKCι/ζ (see introduction and depicted in figure 6.6). The two complexes, Hippo and polarity, may negatively regulate each other as Hippo signalling suppresses the amount of apical complexes (Hamaratoglu et al., 2009) and PKCι suppresses the Hippo pathway by phosphorylating and activating Yap as well as regulating Hippo localisation. Although this interaction needs to be investigated further, it has potential to help explain the function of these two oncogenic pathways.

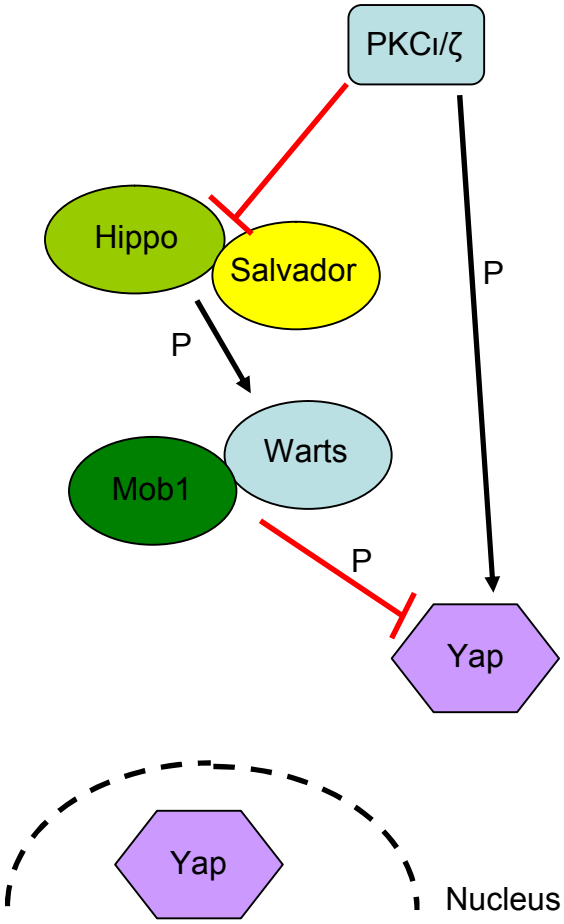

Figure 6.6 PKCι and the Hippo Pathway

PKCι inhibits the Hippo pathway by mislocalising Hippo, preventing the phosphorylation and activation of Warts. PKCι also directly phosphorylates Yap causing Yap nuclear accumulation.

Chapter 7

Final Summary and Future Directions

The aim of the work described here was to discover new substrates of PKCι with the aim of elucidating how PKCι functions in cancer.

Chapter 3 demonstrates the localisation of the atypical PKC proteins. Antibody staining revealed that both PKCι and PKCζ localise to the tight junctions. Further staining revealed that both isoforms also localise to the centrosomes during mitosis. The staining using the active phospho-PKC antibody indicated that PKCι/ζ was active at the centrosomes. Further work is required to determine which aPKC isoform is active at the centrosomes, or whether they are both active there.

To elucidate novel PKCι phosphorylation targets a kinase assay was developed (Chapter 4). Initially PKCι was overexpressed in *Xenopus* embryos with the known phosphorylation targets, Lgl and Par-1. These were then immunoprecipitated and subjected to a Western blot with pan phospho-serine and threonine antibodies. Unfortunately the antibodies did not recognise the phospho-Lgl or Phospho-Par-1. An *in vitro* kinase assay using commercially obtained PKCι, Lgl and Par-1b purified from *Xenopus* embryos and radiolabelled ATP was then tried. Par-1b phosphorylation could not be detected. The Lgl phosphorylation could be detected, but unfortunately PKCι immunoprecipitated with the Lgl, resulting in phosphorylation of Lgl, with and without the addition of PKCι to the kinase assay. Due to these difficulties it was decided to express the proteins in bacteria so that PKCι would not be immunoprecipitated with the candidate phosphorylation target. This was successfully achieved using GST-Par-1 and an *in vitro* kinase assay successfully carried out.

The establishment of the *in vitro* kinase assay allowed the testing of potential PKCι phosphorylation targets. As PKCι/ζ is a crucial regulator of cell polarity, possible polarity phosphorylation targets were tested using the *in vitro* kinase assay (Chapter 5). Patj and Scribbles were not successfully cloned into the GST vector and will require further work to be able to test these in a kinase assay. The cloning of Pals-1 and Dlg was successful and these were used in the kinase assay. Pals-1 displayed no detectable phosphorylation by PKCι, indicating that it is not a substrate of PKCι. Dlg also showed no detectable phosphorylation by PKCι, but interestingly increased the amount of PKCι

autophosphorylation. The phosphorylation cannot be Dlg phosphorylating PKCι as Dlg has no functional kinase domain. This indicates that Dlg, by binding to PKCι causes it to autophosphorylate and activate itself further. This result demonstrates a new method of PKCι activation and it will be interesting to see if this activation occurs *in vivo.* Dlg is found at the centrosomes, during metaphase, as is PKCι, so Dlg could cause the activation of PKCι at the centrosomes during mitosis. Testing this hypothesis will require further investigation, possibly by overexpression of Dlg in cultured cells, and seeing if the phosphorylation of PKCι substrates increases or if the autophosphorylation of PKCι itself increases. It will also be interesting to see if the Dlg induced autophosphorylation occurs during metaphase when PKCι is active at the centrosomes. The cells could be arrested in metaphase and then PKCι/ζ can be immunoprecipitated out and Western blotting used to see if Dlg is bound to PKCι during mitosis.

Yurt is another polarity protein that is regulated by phosphorylation in *Drosophila,* however, the kinase responsible is currently unknown. Yurt was not investigated in this project but future work could examine if Yurt is regulated by phosphorylation in mammalian cells and if this phosphorylation is carried out by PKCι. This can be achieved initially using the kinase assay described here with mammalian Yurt. If Yurt is phosphorylated by PKCι, further studies can be carried out to see if this phosphorylation occurs *in vivo* and the effects of the phosphorylation.

The staining in Chapter 3 also led to the testing of centrosomal proteins as potential PKCι phosphorylation targets (Chapter 5). Unfortunately, the two proteins tested, LGN and GSK3β displayed no detectable phosphorylation by PKCι, indicating that they are not direct phosphorylation substrates of PKCι. Further candidates will have to be tested to find the phosphorylation target(s) of PKCι at the centrosomes. One of these could be Rassf7, which localises to the centrosomes (Sherwood et al., 2008) and has predicted PKCι/ζ phosphorylation sites. Another centrosomal and spindle localised protein is the GEF Ect2 (Oceguera-Yanez et al., 2005), at the centrosomes, Ect2 activates Cdc42 by regulating the amount of GTP bound to it. Ect2 has been linked to the Par-PKC complex in NSCLC and has been shown to bind the complex (Justilien and Fields, 2009). In early mitosis Ect2 is phosphorylated by an unknown kinase, PKCι/ζ could phosphorylate Ect2, at the centrosomes, leading to Cdc42 activation and further PKCι/ζ activation, creating a positive

feedback loop. This needs to be investigated starting with the *in vitro* kinase assay described here.

The final chapter demonstrates that PKCι can phosphorylate and cause nuclear accumulation of the Hippo pathway members Yap and Taz. The site(s) phosphorylated by PKCι, remain unknown, but they are in the N-terminal half of the protein. The phosphorylation of Yap and Taz and the nuclear accumulation of Yap upon overexpression with PKCι is particularly exciting as it may help to explain the mechanism by which PKCι functions in tumorigenesis. PKCι is upregulated in cancer and this upregulation may cause Yap phosphorylation and nuclear entry. Overexpression of Yap causes tissue overgrowth, so the regulation of Yap by PKCι may explain how PKCι functions in cancer. It will be interesting to test it if is the phosphorylation by PKCι that causes Yap to go into the nucleus when they are overexpressed together. It will also be interesting to test whether PKCι phosphorylates Yap in a normal cell setting or just during growth.

A summary of the published phosphorylation substrates, substrates identified in this work and substrates that have been shown to not be phosphorylated *in vitro* including published data and data from this project by PKCι are listed in table 7.1.

Proteins Phosphorylated by PKCι/ζ	
Protein	Reference
Lgl	(Betschinger et al., 2003)
Par-1	(Hurov et al., 2004)
Par-3	(Nagai-Tamai et al., 2002)
Crumbs	(Sotillos et al., 2004)
X-GAP	(Hyodo-Miura et al., 2006)
p70 S6 Kinase	(Akimoto et al., 1998)
IKKβ	(Win and Acevedo-Duncan, 2008)
Numb	(Smith et al., 2007)
ZO-2	(Avila-Flores et al., 2001)
Nucleolin	(Zhou et al., 1997)
Ezrin	(Wald et al., 2008)
Miranda	(Atwood and Prehoda, 2009)
Bad	(Jin et al., 2005)
Src-3	(Garabedian and Logan, 2008; Yi et al., 2008)
IRS-1	(Weyrich et al., 2007)
Yap	This work
Taz	This work
Proteins Not Directly Phosphorylated by PKCι/ζ	
Par-6	(Lin et al., 2000)
GSK3β	This work
LGN	This work
Pals-1	This work
Dlg	This work

Table 7.1 A list of the known positive and negative phosphorylation substrates of PKCι

Overall these results provide an interesting platform for further research to elucidate the mechanisms of PKCι regulation and the mechanisms by which PKCι carries out its normal functions and promotes tumour growth

References

Akimoto, K., Mizuno, K., Osada, S., Hirai, S., Tanuma, S., Suzuki, K., Ohno, S., 1994. A new member of the third class in the protein kinase C family, PKC lambda, expressed dominantly in an undifferentiated mouse embryonal carcinoma cell line and also in many tissues and cells. J Biol Chem. 269**,** 12677-83.

Akimoto, K., Nakaya, M., Yamanaka, T., Tanaka, J., Matsuda, S., Weng, Q. P., Avruch, J., Ohno, S., 1998. Atypical protein kinase Clambda binds and regulates p70 S6 kinase. Biochem J. 335 (Pt 2)**,** 417-24.

Alieva, I. B., Uzbekov, R. E., 2008. The centrosome is a polyfunctional multiprotein cell complex. Biochemistry (Mosc). 73**,** 626-43.

Amanchy, R., Periaswamy, B., Mathivanan, S., Reddy, R., Tattikota, S. G., Pandey, A., 2007. A curated compendium of phosphorylation motifs. Nat Biotechnol. 25**,** 285-6.

Andersen, J. S., Wilkinson, C. J., Mayor, T., Mortensen, P., Nigg, E. A., Mann, M., 2003. Proteomic characterization of the human centrosome by protein correlation profiling. Nature. 426**,** 570-4.

Aono, S., Hirai, Y., 2008. Phosphorylation of claudin-4 is required for tight junction formation in a human keratinocyte cell line. Exp Cell Res. 314**,** 3326-39.

Atwood, S. X., Prehoda, K. E., 2009. aPKC phosphorylates Miranda to polarize fate determinants during neuroblast asymmetric cell division. Curr Biol. 19**,** 723-9.

Avila-Flores, A., Rendon-Huerta, E., Moreno, J., Islas, S., Betanzos, A., Robles-Flores, M., Gonzalez-Mariscal, L., 2001. Tight-junction protein zonula occludens 2 is a target of phosphorylation by protein kinase C. Biochem J. 360**,** 295-304.

Bachmann, A., Schneider, M., Theilenberg, E., Grawe, F., Knust, E., 2001. Drosophila Stardust is a partner of Crumbs in the control of epithelial cell polarity. Nature. 414**,** 638-43.

Badouel, C., Gardano, L., Amin, N., Garg, A., Rosenfeld, R., Le Bihan, T., McNeill, H., 2009. The FERM-domain protein Expanded regulates Hippo pathway activity via direct interactions with the transcriptional activator Yorkie. Dev Cell. 16**,** 411-20.

Balda, M. S., Matter, K., 1998. Tight junctions. J Cell Sci. 111 (Pt 5)**,** 541-7.

Balklava, Z., Pant, S., Fares, H., Grant, B. D., 2007. Genome-wide analysis identifies a general requirement for polarity proteins in endocytic traffic. Nat Cell Biol. 9**,** 1066-73.

Baluch, D. P., Capco, D. G., 2008. GSK3 beta mediates acentromeric spindle stabilization by activated PKC zeta. Dev Biol. 317**,** 46-58.

Bandyopadhyay, G., Standaert, M. L., Sajan, M. P., Kanoh, Y., Miura, A., Braun, U., Kruse, F., Leitges, M., Farese, R. V., 2004. Protein kinase C-lambda knockout in embryonic stem cells and adipocytes impairs insulin-stimulated glucose transport. Mol Endocrinol. 18**,** 373-83.

Basu, S., Totty, N. F., Irwin, M. S., Sudol, M., Downward, J., 2003. Akt phosphorylates the Yes-associated protein, YAP, to induce interaction with 14-3-3 and attenuation of p73-mediated apoptosis. Mol Cell. 11**,** 11-23.

Baumgartner, R., Poernbacher, I., Buser, N., Hafen, E., Stocker, H., 2010. The WW domain protein Kibra acts upstream of Hippo in Drosophila. Dev Cell. 18**,** 309-16.

Benton, R., St Johnston, D., 2003. Drosophila PAR-1 and 14-3-3 inhibit Bazooka/PAR-3 to establish complementary cortical domains in polarized cells. Cell. 115**,** 691-704.

Betschinger, J., Mechtler, K., Knoblich, J. A., 2003. The Par complex directs asymmetric cell division by phosphorylating the cytoskeletal protein Lgl. Nature. 422**,** 326-30.

Bhat, M. A., Izaddoost, S., Lu, Y., Cho, K. O., Choi, K. W., Bellen, H. J., 1999. Discs Lost, a novel multi-PDZ domain protein, establishes and maintains epithelial polarity. Cell. 96**,** 833-45.
Bilder, D., Li, M., Perrimon, N., 2000. Cooperative regulation of cell polarity and growth by Drosophila tumor suppressors. Science. 289**,** 113-6.
Blom, N., Gammeltoft, S., Brunak, S., 1999. Sequence and structure-based prediction of eukaryotic protein phosphorylation sites. J Mol Biol. 294**,** 1351-62.
Bobinnec, Y., Morin, X., Debec, A., 2006. Shaggy/GSK-3beta kinase localizes to the centrosome and to specialized cytoskeletal structures in Drosophila. Cell Motil Cytoskeleton. 63**,** 313-20.
Bossinger, O., Klebes, A., Segbert, C., Theres, C., Knust, E., 2001. Zonula adherens formation in Caenorhabditis elegans requires dlg-1, the homologue of the Drosophila gene discs large. Dev Biol. 230**,** 29-42.
Bowman, S. K., Neumuller, R. A., Novatchkova, M., Du, Q., Knoblich, J. A., 2006. The Drosophila NuMA Homolog Mud regulates spindle orientation in asymmetric cell division. Dev Cell. 10**,** 731-42.
Buther, K., Plaas, C., Barnekow, A., Kremerskothen, J., 2004. KIBRA is a novel substrate for protein kinase Czeta. Biochem Biophys Res Commun. 317**,** 703-7.
Cai, Y., Yu, F., Lin, S., Chia, W., Yang, X., 2003. Apical complex genes control mitotic spindle geometry and relative size of daughter cells in Drosophila neuroblast and pI asymmetric divisions. Cell. 112**,** 51-62.
Callus, B. A., Verhagen, A. M., Vaux, D. L., 2006. Association of mammalian sterile twenty kinases, Mst1 and Mst2, with hSalvador via C-terminal coiled-coil domains, leads to its stabilization and phosphorylation. FEBS J. 273**,** 4264-76.
Camargo, F. D., Gokhale, S., Johnnidis, J. B., Fu, D., Bell, G. W., Jaenisch, R., Brummelkamp, T. R., 2007. YAP1 increases organ size and expands undifferentiated progenitor cells. Curr Biol. 17**,** 2054-60.
Caruana, G., Bernstein, A., 2001. Craniofacial dysmorphogenesis including cleft palate in mice with an insertional mutation in the discs large gene. Mol Cell Biol. 21**,** 1475-83.
Chabu, C., Doe, C. Q., 2008. Dap160/intersectin binds and activates aPKC to regulate cell polarity and cell cycle progression. Development. 135**,** 2739-46.
Chalmers, A. D., Pambos, M., Mason, J., Lang, S., Wylie, C., Papalopulu, N., 2005. aPKC, Crumbs3 and Lgl2 control apicobasal polarity in early vertebrate development. Development. 132**,** 977-86.
Chalmers, A. D., Strauss, B., Papalopulu, N, 2003. Oriented cell divisions assymetrically segregate aPKC and generate cell fate diversity in the early Xenopus embryo. . Development. 2657-2668.
Chan, E. H., Nousiainen, M., Chalamalasetty, R. B., Schafer, A., Nigg, E. A., Sillje, H. H., 2005. The Ste20-like kinase Mst2 activates the human large tumor suppressor kinase Lats1. Oncogene. 24**,** 2076-86.
Chen, C. L., Hsieh, Y. T., Chen, H. C., 2007. Phosphorylation of adducin by protein kinase Cdelta promotes cell motility. J Cell Sci. 120**,** 1157-67.
Chen, X., Macara, I. G., 2005. Par-3 controls tight junction assembly through the Rac exchange factor Tiam1. Nat Cell Biol. 7**,** 262-9.
Chishti, A. H., Kim, A. C., Marfatia, S. M., Lutchman, M., Hanspal, M., Jindal, H., Liu, S. C., Low, P. S., Rouleau, G. A., Mohandas, N., Chasis, J. A., Conboy, J. G., Gascard, P., Takakuwa, Y., Huang, S. C., Benz, E. J., Jr., Bretscher, A., Fehon, R. G., Gusella, J. F., Ramesh, V., Solomon, F., Marchesi, V. T., Tsukita, S., Hoover,

K. B., et al., 1998. The FERM domain: a unique module involved in the linkage of cytoplasmic proteins to the membrane. Trends Biochem Sci. 23**,** 281-2.
Cho, E., Feng, Y., Rauskolb, C., Maitra, S., Fehon, R., Irvine, K. D., 2006. Delineation of a Fat tumor suppressor pathway. Nat Genet. 38**,** 1142-50.
Cohen, D., Brennwald, P. J., Rodriguez-Boulan, E., Musch, A., 2004. Mammalian PAR-1 determines epithelial lumen polarity by organizing the microtubule cytoskeleton. J Cell Biol. 164**,** 717-27.
Cohen, D., Musch, A., 2003. Apical surface formation in MDCK cells: regulation by the serine/threonine kinase EMK1. Methods. 30**,** 269-76.
Cohen, P., Knebel, A., 2006. KESTREL: a powerful method for identifying the physiological substrates of protein kinases. Biochem J. 393**,** 1-6.
Compton, D. A., 2000. Spindle assembly in animal cells. Annu Rev Biochem. 69**,** 95-114.
Costa, M. R., Wen, G., Lepier, A., Schroeder, T., Gotz, M., 2008. Par-complex proteins promote proliferative progenitor divisions in the developing mouse cerebral cortex. Development. 135**,** 11-22.
Cowan, C. R., Hyman, A. A., 2007. Acto-myosin reorganization and PAR polarity in C. elegans. Development. 134**,** 1035-43.
Cox, D. N., Lu, B., Sun, T. Q., Williams, L. T., Jan, Y. N., 2001. Drosophila par-1 is required for oocyte differentiation and microtubule organization. Curr Biol. 11**,** 75-87.
den Hollander, A. I., Ghiani, M., de Kok, Y. J., Wijnholds, J., Ballabio, A., Cremers, F. P., Broccoli, V., 2002. Isolation of Crb1, a mouse homologue of Drosophila crumbs, and analysis of its expression pattern in eye and brain. Mech Dev. 110**,** 203-7.
den Hollander, A. I., ten Brink, J. B., de Kok, Y. J., van Soest, S., van den Born, L. I., van Driel, M. A., van de Pol, D. J., Payne, A. M., Bhattacharya, S. S., Kellner, U., Hoyng, C. B., Westerveld, A., Brunner, H. G., Bleeker-Wagemakers, E. M., Deutman, A. F., Heckenlively, J. R., Cremers, F. P., Bergen, A. A., 1999. Mutations in a human homologue of Drosophila crumbs cause retinitis pigmentosa (RP12). Nat Genet. 23**,** 217-21.
Denning, M. F., 2007. Tightening the epidermal barrier with atypical PKCs. J Invest Dermatol. 127**,** 742-4.
Diaz-Meco, M. T., Lozano, J., Municio, M. M., Berra, E., Frutos, S., Sanz, L., Moscat, J., 1994. Evidence for the in vitro and in vivo interaction of Ras with protein kinase C zeta. J Biol Chem. 269**,** 31706-10.
Diaz-Meco, M. T., Municio, M. M., Frutos, S., Sanchez, P., Lozano, J., Sanz, L., Moscat, J., 1996a. The product of par-4, a gene induced during apoptosis, interacts selectively with the atypical isoforms of protein kinase C. Cell. 86**,** 777-86.
Diaz-Meco, M. T., Municio, M. M., Sanchez, P., Lozano, J., Moscat, J., 1996b. Lambda-interacting protein, a novel protein that specifically interacts with the zinc finger domain of the atypical protein kinase C isotype lambda/iota and stimulates its kinase activity in vitro and in vivo. Mol Cell Biol. 16**,** 105-14.
Diella, F., Gould, C. M., Chica, C., Via, A., Gibson, T. J., 2008. Phospho.ELM: a database of phosphorylation sites--update 2008. Nucleic Acids Res. 36**,** D240-4.
Doerflinger, H., Benton, R., Shulman, J. M., St Johnston, D., 2003. The role of PAR-1 in regulating the polarised microtubule cytoskeleton in the Drosophila follicular epithelium. Development. 130**,** 3965-75.
Dong, J., Feldmann, G., Huang, J., Wu, S., Zhang, N., Comerford, S. A., Gayyed, M. F., Anders, R. A., Maitra, A., Pan, D., 2007. Elucidation of a universal size-control mechanism in Drosophila and mammals. Cell. 130**,** 1120-33.

Dow, L. E., Brumby, A. M., Muratore, R., Coombe, M. L., Sedelies, K. A., Trapani, J. A., Russell, S. M., Richardson, H. E., Humbert, P. O., 2003. hScrib is a functional homologue of the Drosophila tumour suppressor Scribble. Oncogene. 22**,** 9225-30.
Dow, L. E., Humbert, P. O., 2007. Polarity regulators and the control of epithelial architecture, cell migration, and tumorigenesis. Int Rev Cytol. 262**,** 253-302.
Du, Q., Macara, I. G., 2004. Mammalian Pins is a conformational switch that links NuMA to heterotrimeric G proteins. Cell. 119**,** 503-16.
Du, Q., Stukenberg, P. T., Macara, I. G., 2001. A mammalian Partner of inscuteable binds NuMA and regulates mitotic spindle organization. Nat Cell Biol. 3**,** 1069-75.
Du, Q., Taylor, L., Compton, D. A., Macara, I. G., 2002. LGN blocks the ability of NuMA to bind and stabilize microtubules. A mechanism for mitotic spindle assembly regulation. Curr Biol. 12**,** 1928-33.
Ebnet, K., Suzuki, A., Ohno, S., Vestweber, D., 2004. Junctional adhesion molecules (JAMs): more molecules with dual functions? J Cell Sci. 117**,** 19-29.
Eckert, J. J., McCallum, A., Mears, A., Rumsby, M. G., Cameron, I. T., Fleming, T. P., 2005. Relative contribution of cell contact pattern, specific PKC isoforms and gap junctional communication in tight junction assembly in the mouse early embryo. Dev Biol. 288**,** 234-47.
Eder, A. M., Sui, X., Rosen, D. G., Nolden, L. K., Cheng, K. W., Lahad, J. P., Kango-Singh, M., Lu, K. H., Warneke, C. L., Atkinson, E. N., Bedrosian, I., Keyomarsi, K., Kuo, W. L., Gray, J. W., Yin, J. C., Liu, J., Halder, G., Mills, G. B., 2005. Atypical PKCiota contributes to poor prognosis through loss of apical-basal polarity and cyclin E overexpression in ovarian cancer. Proc Natl Acad Sci U S A. 102**,** 12519-24.
Elbert, M., Cohen, D., Musch, A., 2006. PAR1b promotes cell-cell adhesion and inhibits dishevelled-mediated transformation of Madin-Darby canine kidney cells. Mol Biol Cell. 17**,** 3345-55.
Etemad-Moghadam, B., Guo, S., Kemphues, K. J., 1995. Asymmetrically distributed PAR-3 protein contributes to cell polarity and spindle alignment in early C. elegans embryos. Cell. 83**,** 743-52.
Etienne-Manneville, S., Hall, A., 2003a. Cdc42 regulates GSK-3beta and adenomatous polyposis coli to control cell polarity. Nature. 421**,** 753-6.
Etienne-Manneville, S., Hall, A., 2003b. Cell polarity: Par6, aPKC and cytoskeletal crosstalk. Curr Opin Cell Biol. 15**,** 67-72.
Etienne-Manneville, S., Manneville, J. B., Nicholls, S., Ferenczi, M. A., Hall, A., 2005. Cdc42 and Par6-PKCzeta regulate the spatially localized association of Dlg1 and APC to control cell polarization. J Cell Biol. 170**,** 895-901.
Fan, S., Hurd, T. W., Liu, C. J., Straight, S. W., Weimbs, T., Hurd, E. A., Domino, S. E., Margolis, B., 2004. Polarity proteins control ciliogenesis via kinesin motor interactions. Curr Biol. 14**,** 1451-61.
Farese, R. V., Sajan, M. P., Yang, H., Li, P., Mastorides, S., Gower, W. R., Jr., Nimal, S., Choi, C. S., Kim, S., Shulman, G. I., Kahn, C. R., Braun, U., Leitges, M., 2007. Muscle-specific knockout of PKC-lambda impairs glucose transport and induces metabolic and diabetic syndromes. J Clin Invest. 117**,** 2289-301.
Farquhar, M. G., Palade, G. E., 1963. Junctional complexes in various epithelia. J Cell Biol. 17**,** 375-412.
Feng, Y., Irvine, K. D., 2009. Processing and phosphorylation of the Fat receptor. Proc Natl Acad Sci U S A. 106**,** 11989-94.

Fields, A. P., Frederick, L. A., Regala, R. P., 2007. Targeting the oncogenic protein kinase Ciota signalling pathway for the treatment of cancer. Biochem Soc Trans. 35**,** 996-1000.
Fields, A. P., Regala, R. P., 2007. Protein kinase C iota: human oncogene, prognostic marker and therapeutic target. Pharmacol Res. 55**,** 487-97.
Fujii, K., Zhu, G., Liu, Y., Hallam, J., Chen, L., Herrero, J., Shaw, S., 2004. Kinase peptide specificity: improved determination and relevance to protein phosphorylation. Proc Natl Acad Sci U S A. 101**,** 13744-9.
Fukunaga, R., Hunter, T., 1997. MNK1, a new MAP kinase-activated protein kinase, isolated by a novel expression screening method for identifying protein kinase substrates. Embo J. 16**,** 1921-33.
Fumoto, K., Hoogenraad, C. C., Kikuchi, A., 2006. GSK-3beta-regulated interaction of BICD with dynein is involved in microtubule anchorage at centrosome. Embo J. 25**,** 5670-82.
Garabedian, M. J., Logan, S. K., 2008. Atypical regulation of SRC-3. Trends Biochem Sci. 33**,** 301-4.
Genevet, A., Polesello, C., Blight, K., Robertson, F., Collinson, L. M., Pichaud, F., Tapon, N., 2009. The Hippo pathway regulates apical-domain size independently of its growth-control function. J Cell Sci. 122**,** 2360-70.
Genevet, A., Wehr, M. C., Brain, R., Thompson, B. J., Tapon, N., 2010. Kibra is a regulator of the Salvador/Warts/Hippo signaling network. Dev Cell. 18**,** 300-8.
Georgiou, M., Marinari, E., Burden, J., Baum, B., 2008. Cdc42, Par6, and aPKC regulate Arp2/3-mediated endocytosis to control local adherens junction stability. Curr Biol. 18**,** 1631-8.
Ghosh, S., Marquardt, T., Thaler, J. P., Carter, N., Andrews, S. E., Pfaff, S. L., Hunter, T., 2008. Instructive role of aPKCzeta subcellular localization in the assembly of adherens junctions in neural progenitors. Proc Natl Acad Sci U S A. 105**,** 335-40.
Goulev, Y., Fauny, J. D., Gonzalez-Marti, B., Flagiello, D., Silber, J., Zider, A., 2008. SCALLOPED interacts with YORKIE, the nuclear effector of the hippo tumor-suppressor pathway in Drosophila. Curr Biol. 18**,** 435-41.
Grawe, F., Wodarz, A., Lee, B., Knust, E., Skaer, H., 1996. The Drosophila genes crumbs and stardust are involved in the biogenesis of adherens junctions. Development. 122**,** 951-9.
Green, K. J., Jones, J. C., 1996. Desmosomes and hemidesmosomes: structure and function of molecular components. Faseb J. 10**,** 871-81.
Grifoni, D., Garoia, F., Bellosta, P., Parisi, F., De Biase, D., Collina, G., Strand, D., Cavicchi, S., Pession, A., 2007. aPKCzeta cortical loading is associated with Lgl cytoplasmic release and tumor growth in Drosophila and human epithelia. Oncogene. 26**,** 5960-5.
Grunicke, H. H., Spitaler, M., Mwanjewe, J., Schwaiger, W., Jenny, M., Ueberall, F., 2003. Regulation of cell survival by atypical protein kinase C isozymes. Adv Enzyme Regul. 43**,** 213-28.
Grzeschik, N. A., Parsons, L. M., Allott, M. L., Harvey, K. F., Richardson, H. E., 2010. Lgl, aPKC, and Crumbs regulate the Salvador/Warts/Hippo pathway through two distinct mechanisms. Curr Biol. 20**,** 573-81.
Guo, S., Kemphues, K. J., 1995. par-1, a gene required for establishing polarity in C. elegans embryos, encodes a putative Ser/Thr kinase that is asymmetrically distributed. Cell. 81**,** 611-20.

Gustafson, W. C., Ray, S., Jamieson, L., Thompson, E. A., Brasier, A. R., Fields, A. P., 2004. Bcr-Abl regulates protein kinase Ciota (PKCiota) transcription via an Elk1 site in the PKCiota promoter. J Biol Chem. 279**,** 9400-8.

Hamaratoglu, F., Gajewski, K., Sansores-Garcia, L., Morrison, C., Tao, C., Halder, G., 2009. The Hippo tumor-suppressor pathway regulates apical-domain size in parallel to tissue growth. J Cell Sci. 122**,** 2351-9.

Hao, Y., Chun, A., Cheung, K., Rashidi, B., Yang, X., 2008. Tumor suppressor LATS1 is a negative regulator of oncogene YAP. J Biol Chem. 283**,** 5496-509.

Harris, T. J., Peifer, M., 2005. The positioning and segregation of apical cues during epithelial polarity establishment in Drosophila. J Cell Biol. 170**,** 813-23.

Harvey, K. F., Pfleger, C. M., Hariharan, I. K., 2003. The Drosophila Mst ortholog, hippo, restricts growth and cell proliferation and promotes apoptosis. Cell. 114**,** 457-67.

Harwood, A. J., 2001. Regulation of GSK-3: a cellular multiprocessor. Cell. 105**,** 821-4.

Hashimoto, N., Kido, Y., Uchida, T., Matsuda, T., Suzuki, K., Inoue, H., Matsumoto, M., Ogawa, W., Maeda, S., Fujihara, H., Ueta, Y., Uchiyama, Y., Akimoto, K., Ohno, S., Noda, T., Kasuga, M., 2005. PKClambda regulates glucose-induced insulin secretion through modulation of gene expression in pancreatic beta cells. J Clin Invest. 115**,** 138-45.

Hernandez, A. I., Blace, N., Crary, J. F., Serrano, P. A., Leitges, M., Libien, J. M., Weinstein, G., Tcherapanov, A., Sacktor, T. C., 2003. Protein kinase M zeta synthesis from a brain mRNA encoding an independent protein kinase C zeta catalytic domain. Implications for the molecular mechanism of memory. J Biol Chem. 278**,** 40305-16.

Hirose, T., Izumi, Y., Nagashima, Y., Tamai-Nagai, Y., Kurihara, H., Sakai, T., Suzuki, Y., Yamanaka, T., Suzuki, A., Mizuno, K., Ohno, S., 2002. Involvement of ASIP/PAR-3 in the promotion of epithelial tight junction formation. J Cell Sci. 115**,** 2485-95.

Hirose, T., Karasawa, M., Sugitani, Y., Fujisawa, M., Akimoto, K., Ohno, S., Noda, T., 2006. PAR3 is essential for cyst-mediated epicardial development by establishing apical cortical domains. Development. 133**,** 1389-98.

Hong, Y., Stronach, B., Perrimon, N., Jan, L. Y., Jan, Y. N., 2001. Drosophila Stardust interacts with Crumbs to control polarity of epithelia but not neuroblasts. Nature. 414**,** 634-8.

Hori, T., Takaori-Kondo, A., Kamikubo, Y., Uchiyama, T., 2000. Molecular cloning of a novel human protein kinase, kpm, that is homologous to warts/lats, a Drosophila tumor suppressor. Oncogene. 19**,** 3101-9.

Horikoshi, Y., Suzuki, A., Yamanaka, T., Sasaki, K., Mizuno, K., Sawada, H., Yonemura, S., Ohno, S., 2009. Interaction between PAR-3 and the aPKC-PAR-6 complex is indispensable for apical domain development of epithelial cells. J Cell Sci. 122**,** 1595-606.

Horne-Badovinac, S., Lin, D., Waldron, S., Schwarz, M., Mbamalu, G., Pawson, T., Jan, Y., Stainier, D. Y., Abdelilah-Seyfried, S., 2001. Positional cloning of heart and soul reveals multiple roles for PKC lambda in zebrafish organogenesis. Curr Biol. 11**,** 1492-502.

Hsu, Y. C., Willoughby, J. J., Christensen, A. K., Jensen, A. M., 2006. Mosaic Eyes is a novel component of the Crumbs complex and negatively regulates photoreceptor apical size. Development. 133**,** 4849-59.

Huang, J., Wu, S., Barrera, J., Matthews, K., Pan, D., 2005. The Hippo signaling pathway coordinately regulates cell proliferation and apoptosis by inactivating Yorkie, the Drosophila Homolog of YAP. Cell. 122**,** 421-34.

Huang, L., Muthuswamy, S. K., 2010. Polarity protein alterations in carcinoma: a focus on emerging roles for polarity regulators. Curr Opin Genet Dev. 20**,** 41-50.
Hurd, T. W., Gao, L., Roh, M. H., Macara, I. G., Margolis, B., 2003. Direct interaction of two polarity complexes implicated in epithelial tight junction assembly. Nat Cell Biol. 5**,** 137-42.
Hurov, J. B., Watkins, J. L., Piwnica-Worms, H., 2004. Atypical PKC phosphorylates PAR-1 kinases to regulate localization and activity. Curr Biol. 14**,** 736-41.
Hutterer, A., Betschinger, J., Petronczki, M., Knoblich, J. A., 2004. Sequential roles of Cdc42, Par-6, aPKC, and Lgl in the establishment of epithelial polarity during Drosophila embryogenesis. Dev Cell. 6**,** 845-54.
Hyodo-Miura, J., Yamamoto, T. S., Hyodo, A. C., Iemura, S., Kusakabe, M., Nishida, E., Natsume, T., Ueno, N., 2006. XGAP, an ArfGAP, is required for polarized localization of PAR proteins and cell polarity in Xenopus gastrulation. Dev Cell. 11**,** 69-79.
Imai, F., Hirai, S., Akimoto, K., Koyama, H., Miyata, T., Ogawa, M., Noguchi, S., Sasaoka, T., Noda, T., Ohno, S., 2006. Inactivation of aPKClambda results in the loss of adherens junctions in neuroepithelial cells without affecting neurogenesis in mouse neocortex. Development. 133**,** 1735-44.
Ishidate, T., Matsumine, A., Toyoshima, K., Akiyama, T., 2000. The APC-hDLG complex negatively regulates cell cycle progression from the G0/G1 to S phase. Oncogene. 19**,** 365-72.
Ishiguro, H., Akimoto, K., Nagashima, Y., Kojima, Y., Sasaki, T., Ishiguro-Imagawa, Y., Nakaigawa, N., Ohno, S., Kubota, Y., Uemura, H., 2009. aPKClambda/iota promotes growth of prostate cancer cells in an autocrine manner through transcriptional activation of interleukin-6. Proc Natl Acad Sci U S A. 106**,** 16369-74.
Ishikawa, H. O., Takeuchi, H., Haltiwanger, R. S., Irvine, K. D., 2008. Four-jointed is a Golgi kinase that phosphorylates a subset of cadherin domains. Science. 321**,** 401-4.
Izumi, N., Fumoto, K., Izumi, S., Kikuchi, A., 2008. GSK-3beta regulates proper mitotic spindle formation in cooperation with a component of the gamma-tubulin ring complex, GCP5. J Biol Chem. 283**,** 12981-91.
Izumi, Y., Hirose, T., Tamai, Y., Hirai, S., Nagashima, Y., Fujimoto, T., Tabuse, Y., Kemphues, K. J., Ohno, S., 1998. An atypical PKC directly associates and colocalizes at the epithelial tight junction with ASIP, a mammalian homologue of Caenorhabditis elegans polarity protein PAR-3. J Cell Biol. 143**,** 95-106.
Jaken, S., Parker, P. J., 2000. Protein kinase C binding partners. Bioessays. 22**,** 245-54.
Jin, Z., Xin, M., Deng, X., 2005. Survival function of protein kinase C{iota} as a novel nitrosamine 4-(methylnitrosamino)-1-(3-pyridyl)-1-butanone-activated bad kinase. J Biol Chem. 280**,** 16045-52.
Joberty, G., Petersen, C., Gao, L., Macara, I. G., 2000. The cell-polarity protein Par6 links Par3 and atypical protein kinase C to Cdc42. Nat Cell Biol. 2**,** 531-9.
Johnson, S. A., Hunter, T., 2005. Kinomics: methods for deciphering the kinome. Nat Methods. 2**,** 17-25.
Justice, R. W., Zilian, O., Woods, D. F., Noll, M., Bryant, P. J., 1995. The Drosophila tumor suppressor gene warts encodes a homolog of human myotonic dystrophy kinase and is required for the control of cell shape and proliferation. Genes Dev. 9**,** 534-46.
Justilien, V., Fields, A. P., 2009. Ect2 links the PKCiota-Par6alpha complex to Rac1 activation and cellular transformation. Oncogene. 28**,** 3597-607.

Kamberov, E., Makarova, O., Roh, M., Liu, A., Karnak, D., Straight, S., Margolis, B., 2000. Molecular cloning and characterization of Pals, proteins associated with mLin-7. J Biol Chem. 275**,** 11425-31.
Kango-Singh, M., Nolo, R., Tao, C., Verstreken, P., Hiesinger, P. R., Bellen, H. J., Halder, G., 2002. Shar-pei mediates cell proliferation arrest during imaginal disc growth in Drosophila. Development. 129**,** 5719-30.
Karp, C. M., Tan, T. T., Mathew, R., Nelson, D., Mukherjee, C., Degenhardt, K., Karantza-Wadsworth, V., White, E., 2008. Role of the polarity determinant crumbs in suppressing mammalian epithelial tumor progression. Cancer Res. 68**,** 4105-15.
Kaushik, R., Yu, F., Chia, W., Yang, X., Bahri, S., 2003. Subcellular localization of LGN during mitosis: evidence for its cortical localization in mitotic cell culture systems and its requirement for normal cell cycle progression. Mol Biol Cell. 14**,** 3144-55.
Kim, L., Kimmel, A. R., 2006. GSK3 at the edge: regulation of developmental specification and cell polarization. Curr Drug Targets. 7**,** 1411-9.
Kim, M., Datta, A., Brakeman, P., Yu, W., Mostov, K. E., 2007. Polarity proteins PAR6 and aPKC regulate cell death through GSK-3beta in 3D epithelial morphogenesis. J Cell Sci. 120**,** 2309-17.
Kim, S., Gailite, I., Moussian, B., Luschnig, S., Goette, M., Fricke, K., Honemann-Capito, M., Grubmuller, H., Wodarz, A., 2009. Kinase-activity-independent functions of atypical protein kinase C in Drosophila. J Cell Sci. 122**,** 3759-71.
Kishimoto, A., Nishiyama, K., Nakanishi, H., Uratsuji, Y., Nomura, H., Takeyama, Y., Nishizuka, Y., 1985. Studies on the phosphorylation of myelin basic protein by protein kinase C and adenosine 3':5'-monophosphate-dependent protein kinase. J Biol Chem. 260**,** 12492-9.
Kistner, U., Garner, C. C., Linial, M., 1995. Nucleotide binding by the synapse associated protein SAP90. FEBS Lett. 359**,** 159-63.
Klezovitch, O., Fernandez, T. E., Tapscott, S. J., Vasioukhin, V., 2004. Loss of cell polarity causes severe brain dysplasia in Lgl1 knockout mice. Genes Dev. 18**,** 559-71.
Knebel, A., Morrice, N., Cohen, P., 2001. A novel method to identify protein kinase substrates: eEF2 kinase is phosphorylated and inhibited by SAPK4/p38delta. Embo J. 20**,** 4360-9.
Knoblich, J. A., 2008. Mechanisms of asymmetric stem cell division. Cell. 132**,** 583-97.
Koike, C., Nishida, A., Akimoto, K., Nakaya, M. A., Noda, T., Ohno, S., Furukawa, T., 2005. Function of atypical protein kinase C lambda in differentiating photoreceptors is required for proper lamination of mouse retina. J Neurosci. 25**,** 10290-8.
Kojima, Y., Akimoto, K., Nagashima, Y., Ishiguro, H., Shirai, S., Chishima, T., Ichikawa, Y., Ishikawa, T., Sasaki, T., Kubota, Y., Inayama, Y., Aoki, I., Ohno, S., Shimada, H., 2008. The overexpression and altered localization of the atypical protein kinase C lambda/iota in breast cancer correlates with the pathologic type of these tumors. Hum Pathol. 39**,** 824-31.
Kovac, J., Oster, H., Leitges, M., 2007. Expression of the atypical protein kinase C (aPKC) isoforms iota/lambda and zeta during mouse embryogenesis. Gene Expr Patterns. 7**,** 187-196.
Krahn, M. P., Klopfenstein, D. R., Fischer, N., Wodarz, A., 2010. Membrane targeting of Bazooka/PAR-3 is mediated by direct binding to phosphoinositide lipids. Curr Biol. 20**,** 636-42.
Krishnamurthy, K., Wang, G., Silva, J., Condie, B. G., Bieberich, E., 2007. Ceramide regulates atypical PKCzeta/lambda-mediated cell polarity in primitive ectoderm

cells. A novel function of sphingolipids in morphogenesis. J Biol Chem. 282**,** 3379-90.
Lai, Z. C., Wei, X., Shimizu, T., Ramos, E., Rohrbaugh, M., Nikolaidis, N., Ho, L. L., Li, Y., 2005. Control of cell proliferation and apoptosis by mob as tumor suppressor, mats. Cell. 120**,** 675-85.
Lamb, R. S., Ward, R. E., Schweizer, L., Fehon, R. G., 1998. Drosophila coracle, a member of the protein 4.1 superfamily, has essential structural functions in the septate junctions and developmental functions in embryonic and adult epithelial cells. Mol Biol Cell. 9**,** 3505-19.
Laprise, P., Beronja, S., Silva-Gagliardi, N. F., Pellikka, M., Jensen, A. M., McGlade, C. J., Tepass, U., 2006. The FERM protein Yurt is a negative regulatory component of the Crumbs complex that controls epithelial polarity and apical membrane size. Dev Cell. 11**,** 363-74.
Laprise, P., Lau, K. M., Harris, K. P., Silva-Gagliardi, N. F., Paul, S. M., Beronja, S., Beitel, G. J., McGlade, C. J., Tepass, U., 2009. Yurt, Coracle, Neurexin IV and the Na(+),K(+)-ATPase form a novel group of epithelial polarity proteins. Nature. 459**,** 1141-5.
Lee, C. Y., Robinson, K. J., Doe, C. Q., 2006. Lgl, Pins and aPKC regulate neuroblast self-renewal versus differentiation. Nature. 439**,** 594-8.
Lee, S. S., Weiss, R. S., Javier, R. T., 1997. Binding of human virus oncoproteins to hDlg/SAP97, a mammalian homolog of the Drosophila discs large tumor suppressor protein. Proc Natl Acad Sci U S A. 94**,** 6670-5.
Lehrich, R. W., Forrest, J. N., Jr., 1994. Protein kinase C zeta is associated with the mitotic apparatus in primary cell cultures of the shark rectal gland. J Biol Chem. 269**,** 32446-50.
Lei, Q. Y., Zhang, H., Zhao, B., Zha, Z. Y., Bai, F., Pei, X. H., Zhao, S., Xiong, Y., Guan, K. L., 2008. TAZ promotes cell proliferation and epithelial-mesenchymal transition and is inhibited by the hippo pathway. Mol Cell Biol. 28**,** 2426-36.
Leitges, M., Sanz, L., Martin, P., Duran, A., Braun, U., Garcia, J. F., Camacho, F., Diaz-Meco, M. T., Rennert, P. D., Moscat, J., 2001. Targeted disruption of the zetaPKC gene results in the impairment of the NF-kappaB pathway. Mol Cell. 8**,** 771-80.
Lemmers, C., Medina, E., Delgrossi, M. H., Michel, D., Arsanto, J. P., Le Bivic, A., 2002. hINADl/PATJ, a homolog of discs lost, interacts with crumbs and localizes to tight junctions in human epithelial cells. J Biol Chem. 277**,** 25408-15.
Lemmers, C., Michel, D., Lane-Guermonprez, L., Delgrossi, M. H., Medina, E., Arsanto, J. P., Le Bivic, A., 2004. CRB3 binds directly to Par6 and regulates the morphogenesis of the tight junctions in mammalian epithelial cells. Mol Biol Cell. 15**,** 1324-33.
Li, Q., Wang, J. M., Liu, C., Xiao, B. L., Lu, J. X., Zou, S. Q., 2008. Correlation of aPKC-iota and E-cadherin expression with invasion and prognosis of cholangiocarcinoma. Hepatobiliary Pancreat Dis Int. 7**,** 70-5.
Li, Y., Karnak, D., Demeler, B., Margolis, B., Lavie, A., 2004. Structural basis for L27 domain-mediated assembly of signaling and cell polarity complexes. Embo J. 23**,** 2723-33.
Lin, D., Edwards, A. S., Fawcett, J. P., Mbamalu, G., Scott, J. D., Pawson, T., 2000. A mammalian PAR-3-PAR-6 complex implicated in Cdc42/Rac1 and aPKC signalling and cell polarity. Nat Cell Biol. 2**,** 540-7.
Lin, D., Gish, G. D., Songyang, Z., Pawson, T., 1999. The carboxyl terminus of B class ephrins constitutes a PDZ domain binding motif. J Biol Chem. 274**,** 3726-33.

Ling, C., Zheng, Y., Yin, F., Yu, J., Huang, J., Hong, Y., Wu, S., Pan, D., 2010. The apical transmembrane protein Crumbs functions as a tumor suppressor that regulates Hippo signaling by binding to Expanded. Proc Natl Acad Sci U S A. 107**,** 10532-7.
Liu, J. W., Shen, J. J., Tanzillo-Swarts, A., Bhatia, B., Maldonado, C. M., Person, M. D., Lau, S. S., Tang, D. G., 2003. Annexin II expression is reduced or lost in prostate cancer cells and its re-expression inhibits prostate cancer cell migration. Oncogene. 22**,** 1475-85.
Liu, X. F., Xie, X., Miki, T., 2006. Inhibition of protein kinase C zeta blocks the attachment of stable microtubules to kinetochores leading to abnormal chromosome alignment. Cell Signal. 18**,** 2314-23.
Liu, Y., Wang, B., Wang, J., Wan, W., Sun, R., Zhao, Y., Zhang, N., 2009. Down-regulation of PKCzeta expression inhibits chemotaxis signal transduction in human lung cancer cells. Lung Cancer. 63**,** 210-8.
Liu, Y. F., Paz, K., Herschkovitz, A., Alt, A., Tennenbaum, T., Sampson, S. R., Ohba, M., Kuroki, T., LeRoith, D., Zick, Y., 2001. Insulin stimulates PKCzeta -mediated phosphorylation of insulin receptor substrate-1 (IRS-1). A self-attenuated mechanism to negatively regulate the function of IRS proteins. J Biol Chem. 276**,** 14459-65.
Lovestone, S., Hartley, C. L., Pearce, J., Anderton, B. H., 1996. Phosphorylation of tau by glycogen synthase kinase-3 beta in intact mammalian cells: the effects on the organization and stability of microtubules. Neuroscience. 73**,** 1145-57.
Lu, Y., Jamieson, L., Brasier, A. R., Fields, A. P., 2001. NF-kappaB/RelA transactivation is required for atypical protein kinase C iota-mediated cell survival. Oncogene. 20**,** 4777-92.
Lue, R. A., Marfatia, S. M., Branton, D., Chishti, A. H., 1994. Cloning and characterization of hdlg: the human homologue of the Drosophila discs large tumor suppressor binds to protein 4.1. Proc Natl Acad Sci U S A. 91**,** 9818-22.
Makarova, O., Roh, M. H., Liu, C. J., Laurinec, S., Margolis, B., 2003. Mammalian Crumbs3 is a small transmembrane protein linked to protein associated with Lin-7 (Pals1). Gene. 302**,** 21-9.
Mantovani, F., Massimi, P., Banks, L., 2001. Proteasome-mediated regulation of the hDlg tumour suppressor protein. J Cell Sci. 114**,** 4285-92.
Mao, Y., Kucuk, B., Irvine, K. D., 2009. Drosophila lowfat, a novel modulator of Fat signaling. Development. 136**,** 3223-33.
Martin-Belmonte, F., Gassama, A., Datta, A., Yu, W., Rescher, U., Gerke, V., Mostov, K., 2007. PTEN-mediated apical segregation of phosphoinositides controls epithelial morphogenesis through Cdc42. Cell. 128**,** 383-97.
Mashukova, A., Oriolo, A. S., Wald, F. A., Casanova, M. L., Kroger, C., Magin, T. M., Omary, M. B., Salas, P. J., 2009. Rescue of atypical protein kinase C in epithelia by the cytoskeleton and Hsp70 family chaperones. J Cell Sci. 122**,** 2491-503.
Massimi, P., Narayan, N., Cuenda, A., Banks, L., 2006. Phosphorylation of the discs large tumour suppressor protein controls its membrane localisation and enhances its susceptibility to HPV E6-induced degradation. Oncogene. 25**,** 4276-85.
Matakatsu, H., Blair, S. S., 2008. The DHHC palmitoyltransferase approximated regulates Fat signaling and Dachs localization and activity. Curr Biol. 18**,** 1390-5.
Matsumine, A., Ogai, A., Senda, T., Okumura, N., Satoh, K., Baeg, G. H., Kawahara, T., Kobayashi, S., Okada, M., Toyoshima, K., Akiyama, T., 1996. Binding of APC to the human homolog of the Drosophila discs large tumor suppressor protein. Science. 272**,** 1020-3.

Matsumoto, M., Ogawa, W., Akimoto, K., Inoue, H., Miyake, K., Furukawa, K., Hayashi, Y., Iguchi, H., Matsuki, Y., Hiramatsu, R., Shimano, H., Yamada, N., Ohno, S., Kasuga, M., Noda, T., 2003. PKClambda in liver mediates insulin-induced SREBP-1c expression and determines both hepatic lipid content and overall insulin sensitivity. J Clin Invest. 112**,** 935-44.

McLaughlin, M., Hale, R., Ellston, D., Gaudet, S., Lue, R. A., Viel, A., 2002. The distribution and function of alternatively spliced insertions in hDlg. J Biol Chem. 277**,** 6406-12.

Michel, D., Arsanto, J. P., Massey-Harroche, D., Beclin, C., Wijnholds, J., Le Bivic, A., 2005. PATJ connects and stabilizes apical and lateral components of tight junctions in human intestinal cells. J Cell Sci. 118**,** 4049-57.

Mitic, L. L., Anderson, J. M., 1998. Molecular architecture of tight junctions. Annu Rev Physiol. 60**,** 121-42.

Mochizuki, N., Cho, G., Wen, B., Insel, P. A., 1996. Identification and cDNA cloning of a novel human mosaic protein, LGN, based on interaction with G alpha i2. Gene. 181**,** 39-43.

Mori, D., Yamada, M., Mimori-Kiyosue, Y., Shirai, Y., Suzuki, A., Ohno, S., Saya, H., Wynshaw-Boris, A., Hirotsune, S., 2009. An essential role of the aPKC-Aurora A-NDEL1 pathway in neurite elongation by modulation of microtubule dynamics. Nat Cell Biol. 11**,** 1057-68.

Moussad, E. E., Brigstock, D. R., 2000. Connective tissue growth factor: what's in a name? Mol Genet Metab. 71**,** 276-92.

Muller, B. M., Kistner, U., Veh, R. W., Cases-Langhoff, C., Becker, B., Gundelfinger, E. D., Garner, C. C., 1995. Molecular characterization and spatial distribution of SAP97, a novel presynaptic protein homologous to SAP90 and the Drosophila discs-large tumor suppressor protein. J Neurosci. 15**,** 2354-66.

Muller, H. A., Wieschaus, E., 1996. armadillo, bazooka, and stardust are critical for early stages in formation of the zonula adherens and maintenance of the polarized blastoderm epithelium in Drosophila. J Cell Biol. 134**,** 149-63.

Murdoch, J. N., Henderson, D. J., Doudney, K., Gaston-Massuet, C., Phillips, H. M., Paternotte, C., Arkell, R., Stanier, P., Copp, A. J., 2003. Disruption of scribble (Scrb1) causes severe neural tube defects in the circletail mouse. Hum Mol Genet. 12**,** 87-98.

Murray, N. R., Jamieson, L., Yu, W., Zhang, J., Gokmen-Polar, Y., Sier, D., Anastasiadis, P., Gatalica, Z., Thompson, E. A., Fields, A. P., 2004. Protein kinase Ciota is required for Ras transformation and colon carcinogenesis in vivo. J Cell Biol. 164**,** 797-802.

Musch, A., Cohen, D., Yeaman, C., Nelson, W. J., Rodriguez-Boulan, E., Brennwald, P. J., 2002. Mammalian homolog of Drosophila tumor suppressor lethal (2) giant larvae interacts with basolateral exocytic machinery in Madin-Darby canine kidney cells. Mol Biol Cell. 13**,** 158-68.

Na, J., Zernicka-Goetz, M., 2006. Asymmetric positioning and organization of the meiotic spindle of mouse oocytes requires CDC42 function. Curr Biol. 16**,** 1249-54.

Nagafuchi, A., 2001. Molecular architecture of adherens junctions. Curr Opin Cell Biol. 13**,** 600-3.

Nagai-Tamai, Y., Mizuno, K., Hirose, T., Suzuki, A., Ohno, S., 2002. Regulated protein-protein interaction between aPKC and PAR-3 plays an essential role in the polarization of epithelial cells. Genes Cells. 7**,** 1161-71.

Nagasaka, K., Nakagawa, S., Yano, T., Takizawa, S., Matsumoto, Y., Tsuruga, T., Nakagawa, K., Minaguchi, T., Oda, K., Hiraike-Wada, O., Ooishi, H., Yasugi, T.,

Taketani, Y., 2006. Human homolog of Drosophila tumor suppressor Scribble negatively regulates cell-cycle progression from G1 to S phase by localizing at the basolateral membrane in epithelial cells. Cancer Sci. 97**,** 1217-25.
Nair, K. S., Mendez, A., Blumer, J. B., Rosenzweig, D. H., Slepak, V. Z., 2005. The presence of a Leu-Gly-Asn repeat-enriched protein (LGN), a putative binding partner of transducin, in ROD photoreceptors. Invest Ophthalmol Vis Sci. 46**,** 383-9.
Nakagawa, S., Huibregtse, J. M., 2000. Human scribble (Vartul) is targeted for ubiquitin-mediated degradation by the high-risk papillomavirus E6 proteins and the E6AP ubiquitin-protein ligase. Mol Cell Biol. 20**,** 8244-53.
Nakanishi, H., Exton, J. H., 1992. Purification and characterization of the zeta isoform of protein kinase C from bovine kidney. J Biol Chem. 267**,** 16347-54.
Nakaya, M., Fukui, A., Izumi, Y., Akimoto, K., Asashima, M., Ohno, S., 2000. Meiotic maturation induces animal-vegetal asymmetric distribution of aPKC and ASIP/PAR-3 in Xenopus oocytes. Development. 127**,** 5021-31.
Narayan, N., Massimi, P., Banks, L., 2009. CDK phosphorylation of the discs large tumour suppressor controls its localisation and stability. J Cell Sci. 122**,** 65-74.
Navarro, C., Nola, S., Audebert, S., Santoni, M. J., Arsanto, J. P., Ginestier, C., Marchetto, S., Jacquemier, J., Isnardon, D., Le Bivic, A., Birnbaum, D., Borg, J. P., 2005. Junctional recruitment of mammalian Scribble relies on E-cadherin engagement. Oncogene. 24**,** 4330-9.
Neri, L. M., Martelli, A. M., Borgatti, P., Colamussi, M. L., Marchisio, M., Capitani, S., 1999. Increase in nuclear phosphatidylinositol 3-kinase activity and phosphatidylinositol (3,4,5) trisphosphate synthesis precede PKC-zeta translocation to the nucleus of NGF-treated PC12 cells. Faseb J. 13**,** 2299-310.
Newton, A. C., 1995. Protein kinase C: structure, function, and regulation. J Biol Chem. 270**,** 28495-8.
Nigg, E. A., 2002. Centrosome aberrations: cause or consequence of cancer progression? Nat Rev Cancer. 2**,** 815-25.
Nishimura, T., Kaibuchi, K., 2007. Numb controls integrin endocytosis for directional cell migration with aPKC and PAR-3. Dev Cell. 13**,** 15-28.
Noda, Y., Takeya, R., Ohno, S., Naito, S., Ito, T., Sumimoto, H., 2001. Human homologues of the Caenorhabditis elegans cell polarity protein PAR6 as an adaptor that links the small GTPases Rac and Cdc42 to atypical protein kinase C. Genes Cells. 6**,** 107-19.
Nunbhakdi-Craig, V., Machleidt, T., Ogris, E., Bellotto, D., White, C. L., 3rd, Sontag, E., 2002. Protein phosphatase 2A associates with and regulates atypical PKC and the epithelial tight junction complex. J Cell Biol. 158**,** 967-78.
Obenauer, J. C., Cantley, L. C., Yaffe, M. B., 2003. Scansite 2.0: Proteome-wide prediction of cell signaling interactions using short sequence motifs. Nucleic Acids Res. 31**,** 3635-41.
Oceguera-Yanez, F., Kimura, K., Yasuda, S., Higashida, C., Kitamura, T., Hiraoka, Y., Haraguchi, T., Narumiya, S., 2005. Ect2 and MgcRacGAP regulate the activation and function of Cdc42 in mitosis. J Cell Biol. 168**,** 221-32.
Oh, H., Irvine, K. D., 2008. In vivo regulation of Yorkie phosphorylation and localization. Development. 135**,** 1081-8.
Oh, H., Reddy, B. V., Irvine, K. D., 2009. Phosphorylation-independent repression of Yorkie in Fat-Hippo signaling. Dev Biol. 335**,** 188-97.

Ohno, S., 2001. Intercellular junctions and cellular polarity: the PAR-aPKC complex, a conserved core cassette playing fundamental roles in cell polarity. Curr Opin Cell Biol. 13**,** 641-8.
Ohtsubo, M., Theodoras, A. M., Schumacher, J., Roberts, J. M., Pagano, M., 1995. Human cyclin E, a nuclear protein essential for the G1-to-S phase transition. Mol Cell Biol. 15**,** 2612-24.
Oka, T., Mazack, V., Sudol, M., 2008. Mst2 and Lats kinases regulate apoptotic function of Yes kinase-associated protein (YAP). J Biol Chem. 283**,** 27534-46.
Ono, Y., Fujii, T., Ogita, K., Kikkawa, U., Igarashi, K., Nishizuka, Y., 1989. Protein kinase C zeta subspecies from rat brain: its structure, expression, and properties. Proc Natl Acad Sci U S A. 86**,** 3099-103.
Osmani, N., Vitale, N., Borg, J. P., Etienne-Manneville, S., 2006. Scrib controls Cdc42 localization and activity to promote cell polarization during astrocyte migration. Curr Biol. 16**,** 2395-405.
Overholtzer, M., Zhang, J., Smolen, G. A., Muir, B., Li, W., Sgroi, D. C., Deng, C. X., Brugge, J. S., Haber, D. A., 2006. Transforming properties of YAP, a candidate oncogene on the chromosome 11q22 amplicon. Proc Natl Acad Sci U S A. 103**,** 12405-10.
Page Baluch, D., Koeneman, B. A., Hatch, K. R., McGaughey, R. W., Capco, D. G., 2004. PKC isotypes in post-activated and fertilized mouse eggs: association with the meiotic spindle. Dev Biol. 274**,** 45-55.
Pal, S., Claffey, K. P., Cohen, H. T., Mukhopadhyay, D., 1998. Activation of Sp1-mediated vascular permeability factor/vascular endothelial growth factor transcription requires specific interaction with protein kinase C zeta. J Biol Chem. 273**,** 26277-80.
Parkinson, S. J., Le Good, J. A., Whelan, R. D., Whitehead, P., Parker, P. J., 2004. Identification of PKCzetaII: an endogenous inhibitor of cell polarity. Embo J. 23**,** 77-88.
Patel, R., Win, H., Desai, S., Patel, K., Matthews, J. A., Acevedo-Duncan, M., 2008. Involvement of PKC-iota in glioma proliferation. Cell Prolif. 41**,** 122-35.
Pauken, C. M., Capco, D. G., 2000. The expression and stage-specific localization of protein kinase C isotypes during mouse preimplantation development. Dev Biol. 223**,** 411-21.
Pawson, T., Schlessingert, J., 1993. SH2 and SH3 domains. Curr Biol. 3**,** 434-42.
Peng, C. Y., Manning, L., Albertson, R., Doe, C. Q., 2000. The tumour-suppressor genes lgl and dlg regulate basal protein targeting in Drosophila neuroblasts. Nature. 408**,** 596-600.
Perander, M., Bjorkoy, G., Johansen, T., 2001. Nuclear import and export signals enable rapid nucleocytoplasmic shuttling of the atypical protein kinase C lambda. J Biol Chem. 276**,** 13015-24.
Petronczki, M., Knoblich, J. A., 2001. DmPAR-6 directs epithelial polarity and asymmetric cell division of neuroblasts in Drosophila. Nat Cell Biol. 3**,** 43-9.
Pinheiro, E. M., Montell, D. J., 2004. Requirement for Par-6 and Bazooka in Drosophila border cell migration. Development. 131**,** 5243-51.
Plant, P. J., Fawcett, J. P., Lin, D. C., Holdorf, A. D., Binns, K., Kulkarni, S., Pawson, T., 2003. A polarity complex of mPar-6 and atypical PKC binds, phosphorylates and regulates mammalian Lgl. Nat Cell Biol. 5**,** 301-8.
Plusa, B., Frankenberg, S., Chalmers, A., Hadjantonakis, A. K., Moore, C. A., Papalopulu, N., Papaioannou, V. E., Glover, D. M., Zernicka-Goetz, M., 2005. Downregulation

of Par3 and aPKC function directs cells towards the ICM in the preimplantation mouse embryo. J Cell Sci. 118**,** 505-15.
Plyte, S. E., Hughes, K., Nikolakaki, E., Pulverer, B. J., Woodgett, J. R., 1992. Glycogen synthase kinase-3: functions in oncogenesis and development. Biochim Biophys Acta. 1114**,** 147-62.
Polesello, C., Huelsmann, S., Brown, N. H., Tapon, N., 2006. The Drosophila RASSF homolog antagonizes the hippo pathway. Curr Biol. 16**,** 2459-65.
Ponting, C. P., Phillips, C., Davies, K. E., Blake, D. J., 1997. PDZ domains: targeting signalling molecules to sub-membranous sites. Bioessays. 19**,** 469-79.
Qin, Y., Capaldo, C., Gumbiner, B. M., Macara, I. G., 2005. The mammalian Scribble polarity protein regulates epithelial cell adhesion and migration through E-cadherin. J Cell Biol. 171**,** 1061-71.
Qin, Y., Meisen, W. H., Hao, Y., Macara, I. G., 2010. Tuba, a Cdc42 GEF, is required for polarized spindle orientation during epithelial cyst formation. J Cell Biol. 189**,** 661-9.
Qiu, R. G., Abo, A., Steven Martin, G., 2000. A human homolog of the C. elegans polarity determinant Par-6 links Rac and Cdc42 to PKCzeta signaling and cell transformation. Curr Biol. 10**,** 697-707.
Regad, T., Roth, M., Bredenkamp, N., Illing, N., Papalopulu, N., 2007. The neural progenitor-specifying activity of FoxG1 is antagonistically regulated by CKI and FGF. Nat Cell Biol. 9**,** 531-40.
Regala, R. P., Thompson, E. A., Fields, A. P., 2008. Atypical protein kinase C iota expression and aurothiomalate sensitivity in human lung cancer cells. Cancer Res. 68**,** 5888-95.
Regala, R. P., Weems, C., Jamieson, L., Copland, J. A., Thompson, E. A., Fields, A. P., 2005a. Atypical protein kinase Ciota plays a critical role in human lung cancer cell growth and tumorigenicity. J Biol Chem. 280**,** 31109-15.
Regala, R. P., Weems, C., Jamieson, L., Khoor, A., Edell, E. S., Lohse, C. M., Fields, A. P., 2005b. Atypical protein kinase C iota is an oncogene in human non-small cell lung cancer. Cancer Res. 65**,** 8905-11.
Rodriguez-Fraticelli, A. E., Vergarajauregui, S., Eastburn, D. J., Datta, A., Alonso, M. A., Mostov, K., Martin-Belmonte, F., 2010. The Cdc42 GEF Intersectin 2 controls mitotic spindle orientation to form the lumen during epithelial morphogenesis. J Cell Biol. 189**,** 725-38.
Rodriguez, E. M., Dunham, E. E., Martin, G. S., 2009. Atypical protein kinase C activity is required for extracellular matrix degradation and invasion by Src-transformed cells. J Cell Physiol. 221**,** 171-82.
Roh, M. H., Makarova, O., Liu, C. J., Shin, K., Lee, S., Laurinec, S., Goyal, M., Wiggins, R., Margolis, B., 2002. The Maguk protein, Pals1, functions as an adapter, linking mammalian homologues of Crumbs and Discs Lost. J Cell Biol. 157**,** 161-72.
Rolls, M. M., Albertson, R., Shih, H. P., Lee, C. Y., Doe, C. Q., 2003. Drosophila aPKC regulates cell polarity and cell proliferation in neuroblasts and epithelia. J Cell Biol. 163**,** 1089-98.
Sabherwal, N., Tsutsui, A., Hodge, S., Wei, J., Chalmers, A. D., Papalopulu, N., 2009. The apicobasal polarity kinase aPKC functions as a nuclear determinant and regulates cell proliferation and fate during Xenopus primary neurogenesis. Development. 136**,** 2767-77.
Schatten, H., 2008. The mammalian centrosome and its functional significance. Histochem Cell Biol. 129**,** 667-86.

Schimanski, C. C., Schmitz, G., Kashyap, A., Bosserhoff, A. K., Bataille, F., Schafer, S. C., Lehr, H. A., Berger, M. R., Galle, P. R., Strand, S., Strand, D., 2005. Reduced expression of Hugl-1, the human homologue of Drosophila tumour suppressor gene lgl, contributes to progression of colorectal cancer. Oncogene. 24**,** 3100-9.

Scotti, M. L., Bamlet, W. R., Smyrk, T. C., Fields, A. P., Murray, N. R., 2010. Protein kinase Ciota is required for pancreatic cancer cell transformed growth and tumorigenesis. Cancer Res. 70**,** 2064-74.

Selbie, L. A., Schmitz-Peiffer, C., Sheng, Y., Biden, T. J., 1993. Molecular cloning and characterization of PKC iota, an atypical isoform of protein kinase C derived from insulin-secreting cells. J Biol Chem. 268**,** 24296-302.

Shah, K., Shokat, K. M., 2002. A chemical genetic screen for direct v-Src substrates reveals ordered assembly of a retrograde signaling pathway. Chem Biol. 9**,** 35-47.

Sherwood, V., Manbodh, R., Sheppard, C., Chalmers, A. D., 2008. RASSF7 is a member of a new family of RAS association domain-containing proteins and is required for completing mitosis. Mol Biol Cell. 19**,** 1772-82.

Shi, S. H., Jan, L. Y., Jan, Y. N., 2003. Hippocampal neuronal polarity specified by spatially localized mPar3/mPar6 and PI 3-kinase activity. Cell. 112**,** 63-75.

Shin, K., Straight, S., Margolis, B., 2005. PATJ regulates tight junction formation and polarity in mammalian epithelial cells. J Cell Biol. 168**,** 705-11.

Shin, K., Wang, Q., Margolis, B., 2007. PATJ regulates directional migration of mammalian epithelial cells. EMBO Rep. 8**,** 158-64.

Smith, C. A., Lau, K. M., Rahmani, Z., Dho, S. E., Brothers, G., She, Y. M., Berry, D. M., Bonneil, E., Thibault, P., Schweisguth, F., Le Borgne, R., McGlade, C. J., 2007. aPKC-mediated phosphorylation regulates asymmetric membrane localization of the cell fate determinant Numb. Embo J. 26**,** 468-80.

Solecki, D. J., Model, L., Gaetz, J., Kapoor, T. M., Hatten, M. E., 2004. Par6alpha signaling controls glial-guided neuronal migration. Nat Neurosci. 7**,** 1195-203.

Soloff, R. S., Katayama, C., Lin, M. Y., Feramisco, J. R., Hedrick, S. M., 2004. Targeted deletion of protein kinase C lambda reveals a distribution of functions between the two atypical protein kinase C isoforms. J Immunol. 173**,** 3250-60.

Sotillos, S., Diaz-Meco, M. T., Caminero, E., Moscat, J., Campuzano, S., 2004. DaPKC-dependent phosphorylation of Crumbs is required for epithelial cell polarity in Drosophila. J Cell Biol. 166**,** 549-57.

Spitaler, M., Villunger, A., Grunicke, H., Uberall, F., 2000. Unique structural and functional properties of the ATP-binding domain of atypical protein kinase C-iota. J Biol Chem. 275**,** 33289-96.

St Johnston, D., Ahringer, J., 2010. Cell polarity in eggs and epithelia: parallels and diversity. Cell. 141**,** 757-74.

Stallings-Mann, M., Jamieson, L., Regala, R. P., Weems, C., Murray, N. R., Fields, A. P., 2006. A novel small-molecule inhibitor of protein kinase Ciota blocks transformed growth of non-small-cell lung cancer cells. Cancer Res. 66**,** 1767-74.

Steinhardt, A. A., Gayyed, M. F., Klein, A. P., Dong, J., Maitra, A., Pan, D., Montgomery, E. A., Anders, R. A., 2008. Expression of Yes-associated protein in common solid tumors. Hum Pathol. 39**,** 1582-9.

Storrs, C. H., Silverstein, S. J., 2007. PATJ, a tight junction-associated PDZ protein, is a novel degradation target of high-risk human papillomavirus E6 and the alternatively spliced isoform 18 E6. J Virol. 81**,** 4080-90.

Straight, S. W., Shin, K., Fogg, V. C., Fan, S., Liu, C. J., Roh, M., Margolis, B., 2004. Loss of PALS1 expression leads to tight junction and polarity defects. Mol Biol Cell. 15**,** 1981-90.

Sudol, M., Bork, P., Einbond, A., Kastury, K., Druck, T., Negrini, M., Huebner, K., Lehman, D., 1995. Characterization of the mammalian YAP (Yes-associated protein) gene and its role in defining a novel protein module, the WW domain. J Biol Chem. 270**,** 14733-41.

Sugiyama, Y., Akimoto, K., Robinson, M. L., Ohno, S., Quinlan, R. A., 2009. A cell polarity protein aPKClambda is required for eye lens formation and growth. Dev Biol. 336**,** 246-56.

Sun, R., Gao, P., Chen, L., Ma, D., Wang, J., Oppenheim, J. J., Zhang, N., 2005. Protein kinase C zeta is required for epidermal growth factor-induced chemotaxis of human breast cancer cells. Cancer Res. 65**,** 1433-41.

Sun, W., Qureshi, H. Y., Cafferty, P. W., Sobue, K., Agarwal-Mawal, A., Neufield, K. D., Paudel, H. K., 2002. Glycogen synthase kinase-3beta is complexed with tau protein in brain microtubules. J Biol Chem. 277**,** 11933-40.

Suzuki, A., Ishiyama, C., Hashiba, K., Shimizu, M., Ebnet, K., Ohno, S., 2002. aPKC kinase activity is required for the asymmetric differentiation of the premature junctional complex during epithelial cell polarization. J Cell Sci. 115**,** 3565-73.

Suzuki, A., Ohno, S., 2006. The PAR-aPKC system: lessons in polarity. J Cell Sci. 119**,** 979-87.

Suzuki, A., Yamanaka, T., Hirose, T., Manabe, N., Mizuno, K., Shimizu, M., Akimoto, K., Izumi, Y., Ohnishi, T., Ohno, S., 2001. Atypical protein kinase C is involved in the evolutionarily conserved par protein complex and plays a critical role in establishing epithelia-specific junctional structures. J Cell Biol. 152**,** 1183-96.

Takagawa, R., Akimoto, K., Ichikawa, Y., Akiyama, H., Kojima, Y., Ishiguro, H., Inayama, Y., Aoki, I., Kunisaki, C., Endo, I., Nagashima, Y., Ohno, S., 2010. High expression of atypical protein kinase C lambda/iota in gastric cancer as a prognostic factor for recurrence. Ann Surg Oncol. 17**,** 81-8.

Tanentzapf, G., Tepass, U., 2003. Interactions between the crumbs, lethal giant larvae and bazooka pathways in epithelial polarization. Nat Cell Biol. 5**,** 46-52.

Tapon, N., Harvey, K. F., Bell, D. W., Wahrer, D. C., Schiripo, T. A., Haber, D. A., Hariharan, I. K., 2002. salvador Promotes both cell cycle exit and apoptosis in Drosophila and is mutated in human cancer cell lines. Cell. 110**,** 467-78.

Tepass, U., 1996. Crumbs, a component of the apical membrane, is required for zonula adherens formation in primary epithelia of Drosophila. Dev Biol. 177**,** 217-25.

Tepass, U., Knust, E., 1993. Crumbs and stardust act in a genetic pathway that controls the organization of epithelia in Drosophila melanogaster. Dev Biol. 159**,** 311-26.

Thiery, J. P., 2002. Epithelial-mesenchymal transitions in tumour progression. Nat Rev Cancer. 2**,** 442-54.

Totong, R., Achilleos, A., Nance, J., 2007. PAR-6 is required for junction formation but not apicobasal polarization in C. elegans embryonic epithelial cells. Development. 134**,** 1259-68.

Traweger, A., Wiggin, G., Taylor, L., Tate, S. A., Metalnikov, P., Pawson, T., 2008. Protein phosphatase 1 regulates the phosphorylation state of the polarity scaffold Par-3. Proc Natl Acad Sci U S A. 105**,** 10402-7.

Wakefield, J. G., Stephens, D. J., Tavare, J. M., 2003. A role for glycogen synthase kinase-3 in mitotic spindle dynamics and chromosome alignment. J Cell Sci. 116**,** 637-46.

Wald, F. A., Oriolo, A. S., Mashukova, A., Fregien, N. L., Langshaw, A. H., Salas, P. J., 2008. Atypical protein kinase C (iota) activates ezrin in the apical domain of intestinal epithelial cells. J Cell Sci. 121**,** 644-54.

Wallingford, J. B., 2005. Vertebrate gastrulation: polarity genes control the matrix. Curr Biol. 15**,** R414-6.

Wang, J. M., Li, Q., Du, G. S., Lu, J. X., Zou, S. Q., 2009. Significance and expression of atypical protein kinase C-iota in human hepatocellular carcinoma. J Surg Res. 154**,** 143-9.
Wang, Q., Chen, X. W., Margolis, B., 2007. PALS1 regulates E-cadherin trafficking in mammalian epithelial cells. Mol Biol Cell. 18**,** 874-85.
Wang, Q., Hurd, T. W., Margolis, B., 2004. Tight junction protein Par6 interacts with an evolutionarily conserved region in the amino terminus of PALS1/stardust. J Biol Chem. 279**,** 30715-21.
Wang, S. L., Hawkins, C. J., Yoo, S. J., Muller, H. A., Hay, B. A., 1999. The Drosophila caspase inhibitor DIAP1 is essential for cell survival and is negatively regulated by HID. Cell. 98**,** 453-63.
Watts, J. L., Etemad-Moghadam, B., Guo, S., Boyd, L., Draper, B. W., Mello, C. C., Priess, J. R., Kemphues, K. J., 1996. par-6, a gene involved in the establishment of asymmetry in early C. elegans embryos, mediates the asymmetric localization of PAR-3. Development. 122**,** 3133-40.
Wei, X., Shimizu, T., Lai, Z. C., 2007. Mob as tumor suppressor is activated by Hippo kinase for growth inhibition in Drosophila. Embo J. 26**,** 1772-81.
Weyrich, P., Neuscheler, D., Melzer, M., Hennige, A. M., Haring, H. U., Lammers, R., 2007. The Par6alpha/aPKC complex regulates Akt1 activity by phosphorylating Thr34 in the PH-domain. Mol Cell Endocrinol. 268**,** 30-6.
White, W. O., Seibenhener, M. L., Wooten, M. W., 2002. Phosphorylation of tyrosine 256 facilitates nuclear import of atypical protein kinase C. J Cell Biochem. 85**,** 42-53.
Willecke, M., Hamaratoglu, F., Sansores-Garcia, L., Tao, C., Halder, G., 2008. Boundaries of Dachsous Cadherin activity modulate the Hippo signaling pathway to induce cell proliferation. Proc Natl Acad Sci U S A. 105**,** 14897-902.
Win, H. Y., Acevedo-Duncan, M., 2008. Atypical protein kinase C phosphorylates IKKalphabeta in transformed non-malignant and malignant prostate cell survival. Cancer Lett.
Win, H. Y., Acevedo-Duncan, M., 2009. Role of protein kinase C-iota in transformed non-malignant RWPE-1 cells and androgen-independent prostate carcinoma DU-145 cells. Cell Prolif. 42**,** 182-94.
Wissler, F., Labouesse, M., 2007. PARtners for endocytosis. Nat Cell Biol. 9**,** 1027-9.
Wodarz, A., 2000. Tumor suppressors: linking cell polarity and growth control. Curr Biol. 10**,** R624-6.
Wodarz, A., Hinz, U., Engelbert, M., Knust, E., 1995. Expression of crumbs confers apical character on plasma membrane domains of ectodermal epithelia of Drosophila. Cell. 82**,** 67-76.
Wodarz, A., Ramrath, A., Kuchinke, U., Knust, E., 1999. Bazooka provides an apical cue for Inscuteable localization in Drosophila neuroblasts. Nature. 402**,** 544-7.
Woods, D. F., Bryant, P. J., 1994. Tumor suppressor genes and signal transduction in Drosophila. Princess Takamatsu Symp. 24**,** 1-13.
Woods, D. F., Hough, C., Peel, D., Callaini, G., Bryant, P. J., 1996. Dlg protein is required for junction structure, cell polarity, and proliferation control in Drosophila epithelia. J Cell Biol. 134**,** 1469-82.
Xu, M. Z., Yao, T. J., Lee, N. P., Ng, I. O., Chan, Y. T., Zender, L., Lowe, S. W., Poon, R. T., Luk, J. M., 2009. Yes-associated protein is an independent prognostic marker in hepatocellular carcinoma. Cancer. 115**,** 4576-85.
Yamanaka, T., Horikoshi, Y., Sugiyama, Y., Ishiyama, C., Suzuki, A., Hirose, T., Iwamatsu, A., Shinohara, A., Ohno, S., 2003. Mammalian Lgl forms a protein

complex with PAR-6 and aPKC independently of PAR-3 to regulate epithelial cell polarity. Curr Biol. 13**,** 734-43.

Yamanaka, T., Horikoshi, Y., Suzuki, A., Sugiyama, Y., Kitamura, K., Maniwa, R., Nagai, Y., Yamashita, A., Hirose, T., Ishikawa, H., Ohno, S., 2001. PAR-6 regulates aPKC activity in a novel way and mediates cell-cell contact-induced formation of the epithelial junctional complex. Genes Cells. 6**,** 721-31.

Yang, Y. L., Chu, J. Y., Luo, M. L., Wu, Y. P., Zhang, Y., Feng, Y. B., Shi, Z. Z., Xu, X., Han, Y. L., Cai, Y., Dong, J. T., Zhan, Q. M., Wu, M., Wang, M. R., 2008. Amplification of PRKCI, located in 3q26, is associated with lymph node metastasis in esophageal squamous cell carcinoma. Genes Chromosomes Cancer. 47**,** 127-36.

Yasumi, M., Sakisaka, T., Hoshino, T., Kimura, T., Sakamoto, Y., Yamanaka, T., Ohno, S., Takai, Y., 2005. Direct binding of Lgl2 to LGN during mitosis and its requirement for normal cell division. J Biol Chem. 280**,** 6761-5.

Yi, P., Feng, Q., Amazit, L., Lonard, D. M., Tsai, S. Y., Tsai, M. J., O'Malley, B. W., 2008. Atypical protein kinase C regulates dual pathways for degradation of the oncogenic coactivator SRC-3/AIB1. Mol Cell. 29**,** 465-76.

Yu, F., Morin, X., Cai, Y., Yang, X., Chia, W., 2000. Analysis of partner of inscuteable, a novel player of Drosophila asymmetric divisions, reveals two distinct steps in inscuteable apical localization. Cell. 100**,** 399-409.

Yu, J., Zheng, Y., Dong, J., Klusza, S., Deng, W. M., Pan, D., 2010. Kibra functions as a tumor suppressor protein that regulates Hippo signaling in conjunction with Merlin and Expanded. Dev Cell. 18**,** 288-99.

Zeng, Q., Hong, W., 2008. The emerging role of the hippo pathway in cell contact inhibition, organ size control, and cancer development in mammals. Cancer Cell. 13**,** 188-92.

Zhan, L., Rosenberg, A., Bergami, K. C., Yu, M., Xuan, Z., Jaffe, A. B., Allred, C., Muthuswamy, S. K., 2008. Deregulation of scribble promotes mammary tumorigenesis and reveals a role for cell polarity in carcinoma. Cell. 135**,** 865-78.

Zhang, J., Smolen, G. A., Haber, D. A., 2008. Negative regulation of YAP by LATS1 underscores evolutionary conservation of the Drosophila Hippo pathway. Cancer Res. 68**,** 2789-94.

Zhang, L., Huang, J., Yang, N., Liang, S., Barchetti, A., Giannakakis, A., Cadungog, M. G., O'Brien-Jenkins, A., Massobrio, M., Roby, K. F., Katsaros, D., Gimotty, P., Butzow, R., Weber, B. L., Coukos, G., 2006. Integrative genomic analysis of protein kinase C (PKC) family identifies PKCiota as a biomarker and potential oncogene in ovarian carcinoma. Cancer Res. 66**,** 4627-35.

Zhang, X., Milton, C. C., Humbert, P. O., Harvey, K. F., 2009. Transcriptional output of the Salvador/warts/hippo pathway is controlled in distinct fashions in Drosophila melanogaster and mammalian cell lines. Cancer Res. 69**,** 6033-41.

Zhao, B., Wei, X., Li, W., Udan, R. S., Yang, Q., Kim, J., Xie, J., Ikenoue, T., Yu, J., Li, L., Zheng, P., Ye, K., Chinnaiyan, A., Halder, G., Lai, Z. C., Guan, K. L., 2007. Inactivation of YAP oncoprotein by the Hippo pathway is involved in cell contact inhibition and tissue growth control. Genes Dev. 21**,** 2747-61.

Zhao, B., Ye, X., Yu, J., Li, L., Li, W., Li, S., Lin, J. D., Wang, C. Y., Chinnaiyan, A. M., Lai, Z. C., Guan, K. L., 2008. TEAD mediates YAP-dependent gene induction and growth control. Genes Dev. 22**,** 1962-71.

Zheng, Z., Zhu, H., Wan, Q., Liu, J., Xiao, Z., Siderovski, D. P., Du, Q., 2010. LGN regulates mitotic spindle orientation during epithelial morphogenesis. J Cell Biol. 189**,** 275-88.

Zhou, G., Seibenhener, M. L., Wooten, M. W., 1997. Nucleolin is a protein kinase C-zeta substrate. Connection between cell surface signaling and nucleus in PC12 cells. J Biol Chem. 272**,** 31130-7.
Zieve, G. W., Turnbull, D., Mullins, J. M., McIntosh, J. R., 1980. Production of large numbers of mitotic mammalian cells by use of the reversible microtubule inhibitor nocodazole. Nocodazole accumulated mitotic cells. Exp Cell Res. 126**,** 397-405.